Role of Histone Deacetylase 9 in premature aging of the lung during chronic inflammation

Inaugural Dissertation

submitted to the

Faculty of Veterinary Medicine and

Medicine in partial fulfillment of the

requirements

for the **PhD-Degree** of the Faculties of Veterinary Medicine and

Medicine of the Justus Liebig University Giessen

by

Edibe AVCI

From *Ankara, Turkey*

Giessen, 2023

From the Max-Planck-Institute for Heart and Lung Research
Department of Lung Development and Remodeling

Chair: **Prof. Dr. Martin Diener**
Vice-chair /Co-supervisor: **Prof. Dr. Reinhard Dammann**
First reviewer/ Supervisor: **Prof. Dr. Soni Savai Pullamsetti**
Second reviewer: **Prof. Dr. Björn Schumacher**

Disputation date: **4th October 2023**

Dedicated to:

My precious parents Sükran and Semir Avci

Florebo quocumque ferar

TABLE OF CONTENTS

1. INTRODUCTION

1.1. Aging

Aging is a growing risk factor for the rapid increase in death for all age-related chronic lung diseases. Human society has today surpassed 617 million individuals over age 65, which is expected to be increased to 2 billion by 2050 on a global scale (Dzau et al., 2019, Schneider et al., 2021). This rapid transition leads to a heavy burden on the healthcare system from a socioeconomic perspective since elderly individuals are afflicted by a disproportioned increase in cardiovascular and pulmonary diseases as well as dementia and cancer. Eventually, these changes contribute to susceptibility to many aging-related diseases or even death. Thus, age-associated diseases are putting an increasing burden on global health care and require urgent attention.

Aging is characterized by progressive physiological changes in cells, tissues, and organs, that lead to increased death or a decline of biological tissue functions. The hallmarks of aging are telomere shortening upon cell division, genomic instability, epigenetic dysregulation, mitochondrial changes, cell senescence, signaling dysfunction of cell-cell communication as well as metabolic aberrations (Ito and Barnes et al., 2009, Lopez-Otin et al., 2013). Selectively restoration of one dysregulated pathway in an aging organism might positively improve other disrupted pathways as there is an inter-dependent relation among the organs. In this regard, understanding the impact of aging on the fitness of the organs is crucial.

Physiological changes occur with aging in all organ systems, including the lungs. Human lungs consist of various cell types that are exposed to different immunological, biological, mechanical, and chemical stress during their lifetime. A decline in the lung function of healthy individuals with advanced age leads to a severe immunological response to various infections and impairment of gas exchange. The resident cells of the lung cope with cumulative stress via stress response mechanisms (de Cabo and Mattson et al., 2019). However, aging is defined as a progressively decreased ability to respond to these stressors. Understanding why these response pathways become overwhelmed by aging will enlighten their involvement in age-related lung diseases.

1.2. Stress Responses In The Aged Lung

Throughout the years, human lungs are exposed to various environmental stimuli including allergens, pollutants, microparticles, cigarette smoke, aerosols, hyperoxia, radiation, injury, infectious pathogens, and pneumotoxic medications. Lung resident cells adapt themselves to

cope with these biological and chemical stress mediators. Here, the balance in maintaining homeostasis against stress response mechanisms is the key. While over-activation of these response pathways can lead to atypical cell activation, fibrotic scarring, and aberrant lung remodeling, under-activation can usher in the unsuccessful repair of the lungs. Notably, cell-type-specific stress responses vary with aging. For example, previous studies extensively studied alveolar epithelial type II cells (AT2) and how their response alters toward the accumulated stress factors during aging. However, how the other aged pulmonary cell-types respond to the exogenous environmental stimuli is not elucidated so far. In this section, we review the hallmarks of aging and how stress response mechanisms are involved in the ability of endo- and exogenous stressors.

The defined hallmarks of aging can be categorized into 9 sections (**Figure 1**)(Lopez-Otin et al., 2013).

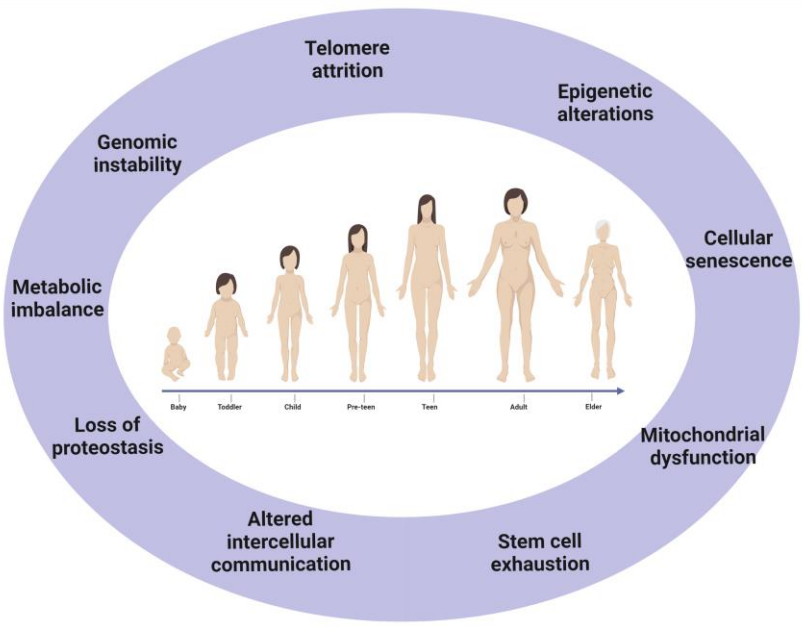

Figure 1.1: The schematic scheme shows the nine hallmarks of aging: genomic instability, telomere attrition, epigenetic alterations, stem cell exhaustion, loss of proteostasis, metabolic imbalance, mitochondrial dysfunction, cellular senescence, and altered intercellular communication. Adapted from *Lopez-Otin et al., 2013*.

1.2.1. Genomic Instability

The first common hallmark of aging is increased genetic damage accumulation throughout human life (Moskalev et al., 2013). All eukaryotes, including humans, have evolved a

packaging system so-called chromatin, where DNA is wrapped around four different histone dimers and constitutes nucleosome structure (Henikoff et al., 2015). Chromatin is a highly dynamic nuclear organization, responsible for DNA stability and gene expression. The studies have indicated that changes occurring in chromatin structure underlie the aging process (Feser et al., 2011). Specifically, changes in gene expression patterns are known to contribute to cell senescence and might explain the decline of tissue and organ functions in complex organisms (Van Deursen, 2014).

Genome instability as a definition refers to DNA alterations, from chromosomal rearrangements and chromosomal numeric changes due to deletions, insertions, and point mutations. DNA damage drives genomic instability and involves changes in nucleic acid structure, such as modified bases, cross-links, breaks, depyrimidination, and depurination DNA damage commits to organismal aging via impairment of transcription and induction of cellular senescence and apoptosis (Yousefzadeh et al., 2021)(**Figure 2**).

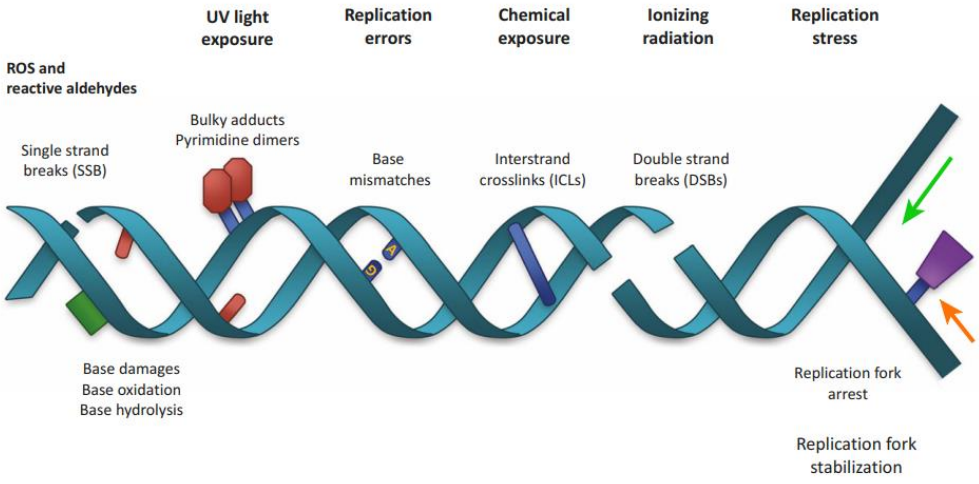

Figure 1.2: The schematic scheme shows different DNA lesions arising from intrinsic and extrinsic factors. Adapted from *Fakouri et al., 2018*.

Various premature aging disorders, such as Bloom and Werner syndromes, are the outcome of DNA damage accumulation (Burtner and Kennedy et al., 2010). DNA integrity is constantly under threat by biological and chemical agents (exogenous challenges), as well as reactive oxygen species (ROS), DNA replication errors, and random hydrolytic reactions (endogenous challenges) (Fakouri et al., 2019; Hoeijmakers, 2009). The genetic lesions caused by intrinsic or extrinsic threats are highly dynamic and diverse, which include telomere shortening, translocations, chromosomal deletions or insertions, point mutations, and gene structure

changes via virus integrations into the genome or transposons. To eliminate these lesions, organisms have advanced DNA repair mechanisms that deal with most of the damages fairly good (Lord and Ashworth, 2012).

There is also a specific genomic stability mechanism to maintain the length and function of telomeres and mitochondrial DNA (mtDNA) integrity (Blackburn et al., 2006; Kazak et al., 2012). In addition, damage in the nuclear architecture so-called laminopathies, can result in genomic instability and lead to premature aging diseases (Reddy and Comai, 2012).

Nuclear DNA

One of the oldest aging theories is somatic mutation theory which indicates the accumulation of somatic mutations within cells. Dosage-variant DNA Copy Number Variations (CNVs) and aneuploidies have also been linked to aging (Moskalev et al., 2013; Faggioli et al., Forsberg et al., 2012) as well as increased clonal mosaicism (Jacobs et al., 2012; Laurie et al., 2012). All these DNA changes might jeopardize the tissue and organ homeostasis unless the alteration is eliminated by apoptosis or senescence. This concept is highly relevant to maintain the function of stem cells for tissue renewal, where DNA damage might impact their competence and lead to stem cell exhaustion (Jossi et al., 2007).

Several studies describing the link between increased DNA damage and aging have shown that deficient DNA repair mechanisms accelerate aging in mouse models and lead to human syndromes, such as Seckel syndrome, xeroderma pigmentosum, Cockayne syndrome, and trichothiodystrophy (Gregg et al., 2012; Hoeijmakers, 2009; Murga et al., 2009). In the literature, transgenic mice overexpressing BubR1, a mitotic checkpoint factor, has been shown to extend lifespan by increasing the protection against cancer and aneuploidy (Baker et al., 2012). In another study, PARP (poly ADP ribose polymerase) activity, a suppressor of DNA damage, is reported to be increased in centenarians and correlates with longer lifespan over 13 species (Trucco et al., 1998; Grube and Bürkle, 1992). These studies provide evidence that artificial boosting of DNA repair mechanism might cause the delay of aging.

Mitochondrial DNA (mtDNA)

mtDNA is a potential target of age-related accumulated somatic mutations due to a lack of histone protection, efficient mtDNA repair mechanisms compared to nuclear DNA and the oxidative environment of the mitochondria (Linnane et al., 1989; Lopez-Otin et al., 2013). The role of mtDNA mutations in aging is controversial due to a phenomenon which is referred to as

heteroplasmy. Heteroplasmy is a condition where mutated mtDNA and wild-type mtDNA can coexist within the same cell (Just et al.,2015; Huang et al., 2011). Recent studies have indicated that the ratio of mutant to wild-type mtDNA is the key factor for disease development. This disease determinant ratio is called as Threshold Effect, where somatic mutations should reach 70-90% of heteroplasmy to cause a deleterious effect on mitochondria function (Rossignol et al., 2003). Previous studies showed that mtDNA copy number declined in the whole blood with age and a lower copy number of mtDNA was linked to poorer survival (Mengel-From et al., 2014; Lee et al., 2010). In another study, whole genome sequencing data from peripheral blood samples of two British cohorts comprising more than 1500 women demonstrated that high level of mutant mtDNA was accumulated in aged individuals than in younger women (Zhang et al., 2017). In addition, a recent study has found that there is a positive correlation between a high level of A3243G mtDNA mutation and reduced cardiovascular fitness and metabolism in elderly subjects. They also reported that a higher risk of stroke and dementia is observed in patients with a high mt DNA mutation burden (Tranah et al., 2018). Interestingly, most of the mtDNA mutations in aged cells occur due to replication errors in early life, rather than other damage factors including oxidative stress (**Figure 3**). The region of mtDNA most prone to genomic instability is D-Loop (Rothfuss et al., 2010). This region as the primary replication initiation site accrues DNA point mutations with aging among various tissues including the heart, muscle, skin, and brain (Jazin et al., 1996; Michikawa et al., 1999; Wang et al., 2001; Nekhaeva et al., 2002). 5 kb deletion of human mtDNA has been detected in the aging heart, muscle, and brain and is associated with mitochondrial disease (Cortopassi et al, 1990; Fayet et al., 2002). These accumulated mitochondrial defects might undergo clonal expansion, create mosaic phenotypes, and lead to respiratory chain dysfunction in tissue (Ameur et al., 2011). For instance, mutations or deletions in mtDNA with age may lead to the accumulation of ragged red fibers (RRF), muscle fibers affecting cytochrome c oxidase (respiratory complex IV)

activity, and causing sarcopenia (Fayet et al., 2002). In some cases, the origin of polyclonal expansion is thought to be raised from stem-cell aging (Oh et al. 2014; Chocron et al., 2019).

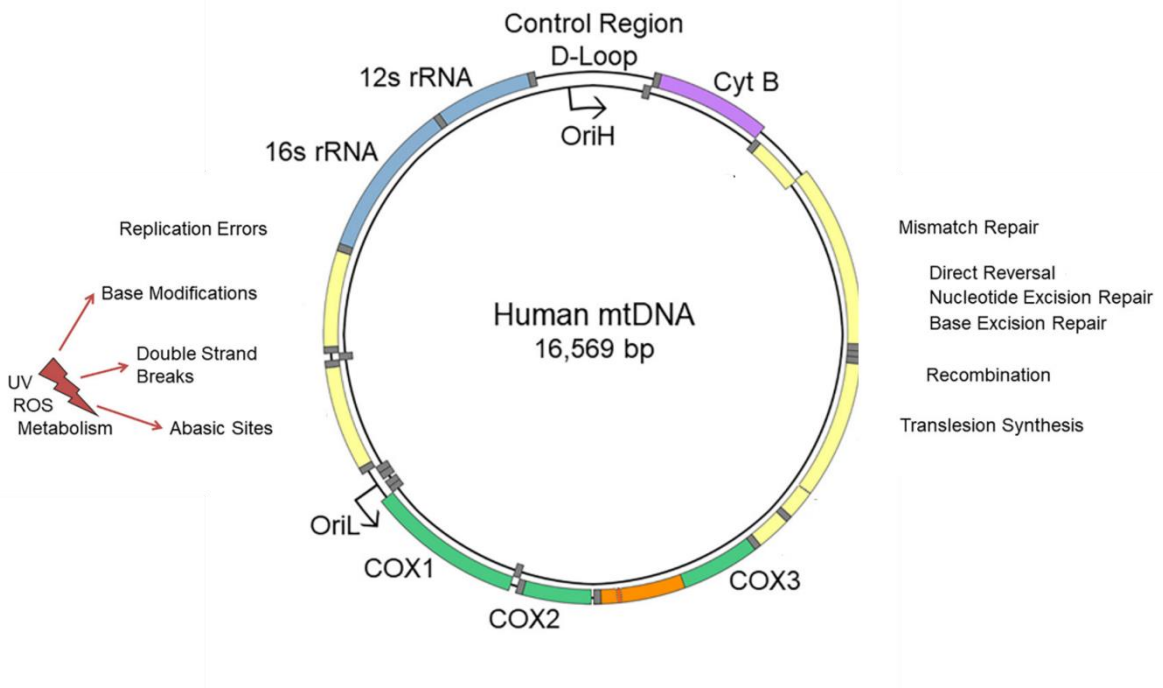

Figure 1.3: Various type of mtDNA damage factors within human cell. Adapted from *Chocrona et al., 2019.*

Nuclear Architecture

Genomic instability can lead to nuclear lamina defects. The nuclear lamina consists of nuclear lamins, providing a scaffold for tethering chromatin structure to maintain genomic stability (Dechat et al., 2008; Gonzalez-Suarez et al., 2009; Liu et al., 2005). Any mutation in genes coding nuclear components, alterations in nuclear shape and volume, changes in nuclear bodies, and aberrant chromatin regions directly affect the health of a cell. Even though it is still debated, these changes at the cellular level indicate aging.

During human aging, aberrant production of progerin, prelamin A isoform, has been detected. A previous study indicated that telomere dysfunction promotes progerin expression in human fibroblasts, suggesting that there is a link between telomere maintenance and production of progerin during normal aging (Scaffidi and Misteli, 2006; Ragnauth et al., 2010; Cao et al., 2011). In addition, lamin B1 expression declines during cell senescence, which is used as a biomarker of the process (Shimi et al., 2011; Freund et al., 2012).

Cellular and animal models used in the studies enabled the identification of stress pathways caused by aberrant nuclear lamina characteristics. These stress pathways are activation of tumor protein 53 (TP53), attenuation of adult stem cells, and somatotrophic axis dysfunction (Varela et al., 2005; Espada et al., 2008; Scaffidi and Misteli, 2008). In a mouse model of Hutchinson-Gilford syndrome (HGPS), a progeroid syndrome, decreasing prelamin A levels was shown to delay the onset of this premature aging disease by systemic injection of farnesyltransferase inhibitors and antisense oligonucleotides (Yang et al., 2006; Varela et al., 2008; Osorio et al., 2011). In another study, NF-κB signaling inhibition improves the lifespan of progeroid mice models as well as hormonal treatments to restore the somatotrophic axis (Osorio et al., 2011). A cell therapy approach, to correct nuclear lamina mutations in induced pluripotent stem cells (iPSCs) derived from HGPS patients has emerged (Liu et al., 2011). However, further studies are necessary to delay aging by reinforcement of the nuclear architecture.

1.2.2. Telomere Attrition

DNA damage accumulation during aging affects telomeres, which are chromosomal regions at the end of the linear DNA (Blackburn et al., 2006). Replicative DNA polymerase cannot replicate fully the terminal fragments of linear DNA, where is a need to have specialized DNA polymerase so-called telomerase. Most of the somatic cells do not produce telomerase and this leads to cumulative loss of telomere segments at the chromosome ends. Telomere attrition is the limitation in the proliferative capacity of some cell types *in vitro*, a phenomenon named as Hayflick limit or replicative senescence (Hayflick and Moorhead, 1961; Olovnikov, 1996). Here, there is another challenge regarding the shelterin, specialized nucleoprotein complex. Shelterin formation even in the presence of telomerase leads to perceiving telomeres as invisible DNA breaks escaping from DNA repair machinery (Palm and de Lange, 2008). Therefore, persistent type of accumulated DNA damage at telomeres causes detrimental effects within cells, such as apoptosis and senescence (Fumagalli et al., 2012; Hewitt et al., 2012; Rossiello et al., 2022).

Short telomere does not mean necessarily short lifespan among different species. For instance, humans have shorter telomeres than rodents but longer lifespan. Here, the most important key is the rate of telomere shortening and increase in short telomeres to predict the lifespan (Whittemore et al., 2019). Regardless of most of the long telomeres, the presence of a few critically short telomeres triggers DNA damage response (DDR), urges cellular senescence in vivo, and eventually determines cell fate, leading to organismal aging (Hemann et al., 2001). During aging, DDR marker levels and telomere-associated DDR foci (TAFs) are known to

increase in different tissues of mammalians. Mice display dysfunctional telomeres based on aging in both non-proliferating and proliferating tissues, despite the fact that they have long telomeres as well as ubiquitous telomerase expression (Hewitt et al., 2012; Birch et al., 2015; Farr et al., 2016; Anderson et al. 2019; Ogrodnik et al., 2019). For humans, most of the data based on telomere studies comes from the leukocytes. However, a recent study revealed that 21 out of 24 different tissues from 952 individuals showed telomere shortening dependent on aging (Demanelis et al., 2020). The most postulated hypothesis is that telomere dysfunction-activated tDDR (DDR at telomeres) leads to cellular senescence and facilitates tissue function loss during aging (Gorgoulis et al., 2019). Cellular senescence may take place during development, independently of telomere dysfunction (Di Micco et al., 2021). The contribution of telomere attrition-dependent or independent cellular senescence needs to be addressed regarding age-related diseases.

1.2.3. Epigenetic Alterations

Epigenetics is defined as reversible heritable mechanisms, affecting gene expression without direct modification in DNA sequences, but rather through chromatin modifications. Eukaryotic chromatin contains nucleosomes, structural subunits. Each nucleosome subunit is made up of a histone octamer, having two copies of histones H2A, H2B, H3, and H4, as well as histone variants, such as macroH2A, H3.3, and H2A.Z. The histone octamer is wrapped around 147 base pair-DNA (Luger, et al., 1997; Richmond et al. 2003). Histone fold domains of each histone cores serve as an interaction platform between histones and N-terminal histone tails. These histone tails can be exposed to post-translation modifications, including histone acetylation, methylation, phosphorylation, and ubiquitination and eventually affect gene expression (Torres et al. 2015).

1.2.3.1.Epigenetic Changes in Aging

1.2.3.1.1. Histone modifications

Depending on the histone residue sites and modification types (methylation, phosphorylation, and ubiquitination, etc.), these histone modifications may promote or suppress transcriptional activity. Histone methylation is associated with both activating and repressing gene expression and thus an important player in the aging process. Previous studies displayed that H3K9, H3K27, and H4K20 methylation represses transcription, while H3K4, H3K36, and H3K79 promote transcription levels (Greer et al., 2012). It is not fully clear whether histone-modifying enzymes can impact the aging process via purely epigenetic modifications or by protein-protein

interaction altering metabolism or signaling pathways outside of the nucleus. For instance, histone demethylases were shown to modulate lifespan through insulin/IGF1 signaling pathway (Jin et al., 2011). The role of histone methylation on aging in mice and humans is not studied broadly. However, in the invertebrate *Caenorhabditis elegans* (*C. elegans*), the trimethylation of lysine 4 residue of histone H3 (H3K4me3) was negatively correlated to longevity. Loss of H3K4me3 methyltransferase *set2*, *wdr5,* and *ash2* increased survival, while the loss of H3K4 demethylase *rbr2* oppositely affected the survival (Greer et al., 2010). The loss of *Lid*, an ortholog of *rbr2* in *Drosophila*, showed decreased lifespan as well (Li et al., 2010). In yeast, H3K4me3 levels were reduced during aging, and its loss is associated with the initiation of aging-related genes (Cruz et al., 2018). H3K27me3 (trimethylation on lysine 27 residue of histone H3) was shown to be declined in *C. elegans* during aging through affecting transcription with Ubiquitously Transcribed TPR on X1 (UTX1) demethylase. The depletion of UTX1, increasing H3K27me3 levels, increased lifespan (Jin et al., 2011). Surprisingly, H3K27me3 levels during aging increased in quiescent mouse muscle stem cells (Liu et al., 2013). Moreover, decreased level of SUV39H, H3K9me3 methyltransferase, was observed during aging in both, human and murine hematopoietic stem cells (Djeghloul et al., 2016).

Apart from H3 modifications, H4K20me3 (the trimethylation of lysine 20 residue on histone 4) has been shown to be associated with aging. Liver and kidney samples collected from 10, 30, 300, and 450-day-old rats showed increased levels of H4K20me3 in animals older than 30 days (Sarg et al., 2002). Moreover, senescent IMR90 cells, primary human fibroblasts, accumulated high levels of H4K20me3 (Nelson et al., 2016).

As an anti-aging factor, both ADP-ribosyl transferases and sirtuin family of NAD-dependent protein deacetylases have been studied frequently. There are several studies in mammals, showing that some of the seven sirtuins may delay aging in mice (Sebastian et al., 2012; Houtkooper et al., 2012). Transgenic overexpression of SIRT1 was shown to improve healthy aging but not extend lifespan (Herranz et al., 2010). In another study, SIRT6 provided proof of its pro-longevity role by regulating genomic stability and glucose metabolism via histone H3K9 deacetylation on NF-κB promoter region (Kawahara et al., 2009; Zhong et al., 2010; Kanfi et al., 2010). In addition, SIRT6-deficient mice exhibit fast aging, while SIRT6-overexpressed transgenic mice displayed an extended lifespan than control animals by reducing serum IGF-1 levels (Mostoslavsky et al., 2006; Kanfi et al., 2012). This finding was supported in another study related to rats. Sirt6-overexpressed rats showed repressed apoptosis along with senescence (Chen et al., 2018). Moreover, the depletion of SIRT6 in human fibroblasts in vitro

displayed abnormal telomere length, which is similar to the observed situation in a premature aging syndrome so-called Werner syndrome (Michishita et al., 2008). Interestingly, SIRT7, augmenting H4K12ac (acetylation) via HAT1 regulation, was reported to be a regulator of aging. The loss of SIRT7 resulted in an aging phenotype in mice (Liu et al., 2020). Besides, H4K16ac is to regulate telomere silencing and maintains chromosome stability. The supplementation of SIRT7 prevents the event, where SIRT1 deacetylases H4K16. Senescence phenotype and defects in DNA repair mechanism were linked to lower acetylation activity in mice (Krishnan et al., 2011; Xu et al., 2016; Krishnan and Chow et al., 2011). As an early indicator of DNA damage response, histone variant H2AX and its phosphorylation site on serine 139 residue (γH2AX) are linked to aging. The positive relationship between a high abundance of γH2AX and PD-L1 expression was observed in lung squamous cell carcinoma (Osoegawa et al., 2018).

Lastly, histone ubiquitination is another hallmark of aging. This is a post-translational modification, where ubiquitin is transferred to H2A and H2B, histone core members. The ubiquitination of H2A is linked to the reduction of gene expression, while H2B ubiquitination promotes transcription (Maleszewska eta l., 2016). H2A ubiquitination dependent on aging was discovered first in *Drosophila*, and later confirmed as evolutionarily conserved in humans as well (Yang et al., 2019). The inhibition of the monoubiquitination of H2Bub1 (Histone H2B monoubiquitylation) exhibits reduced senescent phenotype in human glioma cells (Gao et al., 2011).

1.2.3.1.2. DNA methylation

'DNA methylation and aging' association is a complex concept to investigate. However, early studies mentioned global hypomethylation during aging. The following analyses described hypermethylated loci, including Polycomb genes and numerous tumor suppressor genes, in aging (Maegawa et al., 2010). DNA methylation along with histone modifications in cells obtained from patients and mice models of premature aging syndromes displayed the recapitulated pattern in normal aging (Shumaker et al., 2006; Osorio et al., 2010). Two large-scale studies remarkably contributed to enlightening the relationship between aging and DNA methylation patterns. The researchers identified 353 (Horvath et al., 2013) and 71 (Horvath et al., 2015) cytosine-phospho-guanine (CpG) dinucleotides- rich sites, that were differentially methylated during aging in different human tissues. They described these CpG sites as valid age predictors and described the term 'epigenetic clock'. In another comparative study, the epigenetic clock was determined as the most accurate readout among the all other age predictors

(Jylhävä et al. 2017). Nevertheless, further studies are needed to address the relationship between altered DNA methylation patterns and aging.

1.2.3.1.3. ATP-dependent chromatin Remodeling

The chromatin structure is highly compact, and it must be accessible to be remodeled to initiate the cellular process. ATP-dependent chromatin remodeling complexes facilitate this remodeling process and lead to altered transcription activity. These remodelers contain ATPase subunit, which is highly conserved and belongs to super-family II helicase-related proteins (Liu et al.,2012). There are four major categories of these remodelers based on their ATPase-flanking domain: ISWI (imitation switch), CHD (chromodomain helicase DNA-binding), INO80 and SWI/SNF (switch/sucrose non-fermentable) (Clapier et al., 2009).

Recent data displayed that BRG1 (SMARCA4) and BRM (SMARCA2), SWI/SNF complex subunits, are involved in telomere maintenance. BRG1 was discovered to be negatively correlated with human telomerase reverse transcriptase (hTERT) in human cervical cancer cells. The authors discovered elevated hTERT transcription status when BRG1 was knock-down (Wu et al., 2014). In another study, BRM was identified as a required component for the transcription of TRF1 and TRF2, the telomere-binding proteins responsible for telomere maintenance (Wu et al., 2020). Another remodeler INO80 was found essential for telomere maintenance in mice and its deletion caused defects in cell proliferation and activation of p21 resulting in cellular senescence (Min et al., 2013).

1.2.3.1.4. Transcriptional alterations

Transcriptional noise increases during aging and eventually leads to aberrant maturation and production of various mRNAs (Bahar et al., 2006; Nicholas et al., 2010; Harries et al., 2011). Microarray-based studies among several species from young and old tissues confirmed that genes related-inflammatory, mitochondrial, and lysosomal pathways showed transcriptional changes during aging (de Magalhaes et al., 2009). These age-related transcriptional alterations affect miRNAs (microRNAs) that influence stem cell behavior and lifespan (Ugalde et al., 2011; Boulias and Horvitz, 2012; Toledano et al., 2012). In the aging field regarding miRNAs and their functions to discover, *C.elegans* is the most used model organism. One of the studies showed that *C. elegans* requires miRNA lin-4 expression to regulate lin-14, a transcription factor during both development and aging. The study discovered that overexpression of miRNA lin-4 extended lifespan along with the interference of lin-14 activity (Boehm et al., 2005). In addition, the silencing of mir-125, a homolog of lin-4 in *Drosophila* reduced lifespan as well

(Chawla et al., 2016). Nevertheless, the role of this miRNA remains unclear in humans during aging. A very recent study identified 127 differentially expressed miRNAs from whole blood samples of 5000 individuals in an age-dependent manner (Huan et al., 2018).

1.2.4. Loss of proteostasis

Impaired protein homeostasis is associated with aging and age-related diseases (Powers et al., 2009). Proteostasis is a quality control mechanism of a cell to maintain the stability and functionality of its proteome. Mentioned quality control mechanisms consist of protein synthesis, folding, trafficking, and degradation by proteasome or lysosome (Balch et al., 2008; Mizushima et al., 2008; Koga et al., 2011; Hartl et al., 2011). Altered proteotoxic stress response increases by aging through molecular chaperones to maintain protein folding (Calderwood et al., 2009). Moreover, the functions of the ubiquitin-proteasome system (UPS) and autophagy-lysosome systems decline with age (Rubinsztein et al., 2011).

The lungs face many perturbations throughout life, resulting in aberrant post-translational modifications, disturbed protein-protein interactions, and protein misfolding. In a very recent study, proteomic analysis of AT2 cells obtained from young and old mice displayed a proteostasis network collapse in the aging lung. In addition, the importance of the co-chaperone adaptive response (CARE) network was highlighted to handle misfolded proteins (Loguercio et al., 2019).

Besides failed chaperone network, altered protein degradation mechanisms such as autophagy in the aged lung were identified either (Schneider and Sanchez, 2016). Autophagy is a self-degradative process where the organelles and intracellular macromolecule cargos are carried to lysosomes to be degraded in stress response. Chaperone-mediated autophagy and macroautophagy in various tissue types were reported to be declined with age in progressive fibrotic lung diseases. For instance, the suppression of macroautophagy in alveolar epithelial cells was shown to stabilize p62 and transactivate EMT transcription factor Snail2, resulting in epithelial-to-mesenchymal transition (EMT) (Hill et al., 2019). Remarkably, age mice exposed to bleomycin exhibit reduced autophagic activity compared to younger mice (Sosulski et al., 2015). A few pulmonary diseases are owing to protein misfolding as a consequence of primary genetic mutations. For instance, pulmonary fibrosis, a disease manifesting later in life around age 60-70, is linked to the mutations in surfactant protein C gene (SFTPC) and promoter region of MUC5B (Mucin 5B) gene (Lawson et al., 2004; Seibold et al., 2011). This suggests that age-related failed proteostasis drives the pathogenesis of the disease due to mutations causing

misfolded proteins (Balch et al., 2014). While younger organisms have a functional proteolytic response, older organisms might have burdened their capacity due to the gradual loss of the proteostasis network in aging. The decline in chaperone-mediated autophagy and macroautophagy with age might result in the overwhelmed system and being defeated by the disease. This is supported by the study showing that restoring UPS and autophagy response in alpha-1 antitrypsin deficiency exhibit therapeutic effects (Lomas, 2018). However, further studies are needed to address the underlying mechanisms of burdened and lost proteostasis in aging.

1.2.5. Mitochondrial dysfunction

Changes in the lipid structure of the mitochondrial membrane, increase in mtDNA mutations, destabilization of the electron transport chain (ETC) and elevated oxidation of mitochondria occur with age (Haas, 2019). Remarkably, approximately 50% of total mitochondria mass in the lung comes from AT2 cells that are prone to loss of cristae, mitochondrial enlargement, and dysfunctional respiratory capacity with age (Massaro et al., 1975; Bueno et al., 2015). In addition, mitochondrial dysfunction of senescent epithelial cells in the lung was observed due to disruption in mTOR/PGC-1a/b axis (Summer et al., 2019).

The regulation of mitochondria biogenesis and degradation is normally under tight control. However, these processes decreased with age. AMPK signaling pathway, SIRT1 regulation, activation of NRF-2 through its coactivator, and PGC-1a are part of mitochondrial biogenesis, all are attenuated with age. Notably, telomere-deficient mice showed the repression of PGC-1a and PGC-1b in a p53-mediated manner, leading to mitochondrial biogenesis reduction (Sahin and DePinho, 2012). In a complementary study in old mice, the reduction of mitochondrial biogenesis was partially restored by telomere activation (Bernardes de Jesus et al., 2012). A recent study revealed the contribution of telomerase-mediated mitochondrial dysfunction in response to pulmonary innate immunity. Short telomeres having Terc null mice demonstrated severe lung inflammation and increased mortality rate due to pneumonia (Kang et al., 2018). Telomere attrition explicitly in AMs results in reduced ETC activity, decreased ATP levels, and elevated ROS due to distorted PGC-1a/ERRa transcriptional activity. This leads to NLRP3 inflammasome activation and severe innate immunity response, which is similar to the pro-inflammatory condition observed in healthy aging. Strikingly, idiopathic pulmonary fibrosis (IPF) patients harbor telomerase mutations, yet how aging drives the disease pathogenesis and the contribution of mitochondrial impairment are unclear (Calado and Young, 2009).

Mitophagy in age-related lung diseases is a crucial quality control mechanism (Cloonan and Choi, 2016). Mitophagy is a process where damaged mitochondria are degraded to prevent deleterious effects on cellular homeostasis under stress (Chen at al., 2020). Interestingly, AT2 cells isolated from IPF patients demonstrated increased accumulation of impaired mitochondria and decreased expression of PINK1, a serine/threonine kinase recruiting ubiquitin ligase E3 (Bueno et al., 2015). Depletion of PINK1 in AT2 cells resulted in increased pro-fibrotic factors, TGF-b1 (transforming growth factor b1), and TGF-b2, along with mitochondrial depolarization. In addition, PINK-1 deficient mice were shown to be prone to develop lung fibrosis at a young age even. Even when older wild-type mice were exposed to bleomycin, the animals malfunctioned to induce mitophagy and resulted in dysfunctional ETC activity (Liu et al., 2011; Sosulski et al., 2015). Failure of mitophagy is not a hallmark for only lung fibrosis but also COPD (chronic obstructive pulmonary disease). In contrast, upregulations of mitophagy and PINK1 were observed in COPD (Mizumura et al., 2014). Consequently, molecular drivers of age-related lung diseases might differ from each other during aging.

1.2.6. Deregulated Nutrient-sensing

Impaired metabolic function occurs with aging and is defined by deregulated nutrient sensing, altered signaling pathways, and energy disproportion. Even though the lung is not characterized as an organ involved in providing energy to the whole body, AT2 cells are known to have metabolic activity and can adapt rapidly to changes in the presence of oxygen. Under normal conditions, alveolar epithelium inhabits in an environment with 100 mmHg-O2 levels, higher than any other organs in the body (Schumacker, 2011). When AT2 cells face acute or chronic hypoxic stress stimuli, they preserve ATP to maintain energetic homeostasis under limited O2 levels (Lottes et al., 2014). AMPK, mTOR, and HIF2a signaling pathways, mediating hypoxic response, are imbalanced with aging. The question here is how the cells residing in the lung rewire their metabolic status during aging and whether metabolic modulation might therapeutically elevate age-associated lung diseases.

Sirtuins, nicotinamide adenine dinucleotide (NAD)+ -dependent protein deacetylases family, are involved in age-related lung diseases. Mammalian sirtuins shuttle among different compartments including cytoplasm (SIRT2), mitochondria (SIRT3-5), and nucleus (SIRT1 and SIRT6-SIRT7) and they act as metabolic sensors by modifying their substrates post-translationally to regulate downstream response (Haigis and Sinclair, 2010). For instance, SIRT1 was found to be decreased in COPD patients, and *in vivo* animal model, SIRT1 genetic ablation leads to reduced lung function, airspace enlargement, and impaired exercise capacity

due to lack of deacetylation of FOXO3 (Yao et al., 2012). SIRT1 restoration genetically and pharmacologically is shown to decline premature cell senescence in cigarette smoke-induced emphysema-bearing lungs via targeting SIRT1/FOXO3 axis (Yuan et al., 2015). In another study, FOXO3A activation was inhibited by aberrant EGFR (epidermal growth factor receptor) signaling in COPD airways while IL-8 (interleukin-8) signaling was enhanced (Ganesan et al, 2013).

SIRT3 deacetylation via its substrates is known to be involved with mitochondria-related processes such as fatty acid β-oxidation, TCA (tricarboxylic acid) cycle, and ETC (Yang et al., 2016). SIRT3 expression decreases in aged mice along with fibrotic areas of human lungs and IPF mice models. In the aged lung, SIRT3 ablation resulted in the inactivation of SOD2 and TCA-related enzymes through increased acetylation, which eventually results in impaired mitochondrial function (Sosulski et al., 2017).

Single-cell transcriptomic studies from young and old mice lungs revealed AT2-specific alterations of lipid regulators such as Srebf2, a sterol-response element binding protein (SREBP), important for surfactant production and lipogenesis, and Insig1, insulin-induced gene-1 as a negative regulator of SREBPs transcriptional function. In corroboration, genetically ablated Insig1/2 mice models displayed SREBP activation constitutively, leading to neutral lipid accumulation in AT2 cells and eventually lung inflammation based on lipotoxicity (Plantier et al., 2012). Lipid metabolism and its tight control in AT2 cells are crucial since they are essential in pulmonary surfactant production. In this aspect, the reason for the disturbance of lipid-mediated regulatory pathways with aging is an open field to discover further.

1.2.7. Stem Cell Exhaustion

Stem cell exhaustion is one of the driving factors of age-related diseases due to repetitive injuries (Signer et al., 2013 and Behrens et al., 2014). Constitutive asymmetric cell division and differentiation of stem cells in high-turnover organs are fundamental to maintaining homeostasis. However, the capacity of stem cell niches to meet expectations of supply-demand to stem cells is overburdened with aging (Ganuza et al., 2012 and Richardson et al., 2014). The lung is considered a slow-turnover organ (Stripp et al.,2008). This notion might apply to altered demand: supply ratio of lung stem cells and their impaired function with age. In the lung, airways are characterized as where the stem cell pool inhabits. Among these cells, airway basal cells are well-identified for their differentiation and self-renewal capacity (Hogan et al., 2014 and Rock et al., 2012). In addition, Clara cells (club cells) are described as progenitor cells since

they have the ability to differentiate into basal cells upon injury (Kotton et al., 2014 and Rawlins et al., 2014). When it comes to distal lung, AT2 cells emerge as progenitor cells based on accumulated data. During the development and injury repair processes, AT2 cells give rise to AT1 (alveolar type I cells) cells (Barkauskas et al., 2013). Additional distal stem cell populations are characterized such as integrin $\alpha6/\beta4^{+}$ and surfactant protein-alveolar epithelial cells (Hogan et al., 2014; Rock et al., 2012; Kotton et al., 2014). Similar to other cell types, stem cells exhibit hallmarks of aging due to accumulated environmental stress stimuli within the lung and possess decreased regenerative capacity (Issa et al., 2014). Circulating progenitor cells besides the local population within the lung have been involved with COPD. For instance, DNA damage and cellular senescence were observed in endothelial progenitor cells of COPD patients, leading to dysfunction of lung repair (Paschalaki et al., 2013). Along the same lines, mesenchymal stromal cells (MSCs) have been shown to have reduced regenerative capacity in a murine post-pneumectomy model (Paxson et al., 2013). In another study, bone marrow-derived MSCs have been associated with reduced anti-inflammatory capacity with aging (Bustos et al., 2014).

1.2.8. Altered Intercellular Communication

Aging involves also altered intercellular communication such as inflammaging, immunosenescence, and endocrine/neuroendocrine dysregulations (López-Otín C et al., 2013). Neurohormonal changes appear strongly as inflammatory response increases by aging while immune reactions against malignant cells or pathogens decline along with extracellular environment changes. Altogether affects the functionality of all tissues and creates an overburdened stress response.

Inflammaging is defined as a pro-inflammatory phenotype resulting from tissue damage, failure of pathogen clearance effectively and expansion of senescent cells secreting pro-inflammatory cytokines, increased NF-κB signaling pathway response, or impaired autophagy mechanism (Salminen et al., 2012). Paralleling inflammaging, adaptive immune system response declines and aging phenotype might be exhibited due to malignant cell transformation and increased infectious agents at the systemic level. Recognizing the senescent cells is one of the functions of the immune system. However, this ability declines with aging and results in the accumulation of hyperploid cells (Deeks, 2011; Davoli and de Lange, 2011; Huna et al., 2011). In particular, changes in the innate and adaptive immune responses are well-described for chronic obstructive diseases and emphysema formation. While environmental challenges such as smoke-exposed damaged cells and smoke components are sensed by innate immunity, adaptive immunity starts

to trigger aberrant responses to acute infections (Brusselle et al., 2011). Age-dependent changes occurred in the immune system are referred to as immunosenescence, responsible for the development of COPD (Meyer et al., 2010).

1.2.9. Cellular Senescence

Cellular senescence is characterized by cellular and transcriptional alterations, cell cycle arrest, and specific secretory phenotype, leading to modulation of tissue environment via auto-/paracrine stimuli. Human lung cells exhibit replicative senescence after serial passages in vitro cultures and this was the first hint that senescent cell accumulation occurred in the lung. It is also known that cigarette smoke exposure, oxidative stress, radiation, chemotherapy, and organismal aging might serve as triggers to initiate cellular senescence (Childs et al., 2015). Despite replicative senescence, these cells are metabolically active and secrete many different agents into the microenvironment, referred to as senescence-associated secretory phenotype (SASP). An increase in the inflammatory response, extracellular matrix remodeling, and excessive release of growth factors due to senescence lead to abnormal tissue repair. To avoid the transformation of damaged cells into malignant forms, an unalterable state of cell cycle arrest was considered as a protective mechanism but it is now accepted that the contribution of senescent cells cannot be ruled out when it comes to the development of age-related diseases such as pulmonary fibrosis and COPD as well as cancer. Thus, selectively eliminating senescent cells and targeting SASP phenotype might be a therapeutic approach to restore the health of aged lungs. Addressing this aspect, senolytic drug treatment has emerged as an effective prevention and therapeutic approach by depleting senescent cells (van Deursen, 2019). In early murine studies, young mice showed aging characteristics such as airspace enlargement and lung structure disruption when the mice were challenged with premature cell senescence inducer (Kurozumi et al., 1994). Major senescence markers including p21, p53, p16Ink4a as cell cycle blockers are upregulated in damaged lung resident cells. Aged human lungs as well as aged wild type mice showed increased SASP phenotype compared to young counterparts in alveolar and vascular compartments. It is also shown that senescent markers colocalize with ECM proteins, indicating an association of cellular senescence and lung remodeling with aging (Calhoun et al., 2016). Given this association for pulmonary diseases, β-galactosidase, p21, and p16 expressions were elevated in epithelial cells and fibroblasts isolated from IPF patients and a strong correlation between p16 expression and disease severity has been found (Schafer et al., 2017). In the same study, eliminating the senescent cells was shown to rejuvenate the status of pulmonary fibrosis (Schafer et al., 2017). However, cell-specific SASP phenotype responses

have been observed. For instance, while conditional media (CM) collected from senescent bronchiolar epithelial cells did not trigger a fibrotic response, CM from murine senescent fibroblasts exhibited elevated levels of pro-inflammatory and pro-fibrotic factors. Senolytic drugs selectively eliminate senescent cells to block SASP factor release, leading to deleterious effects in the tissue environment. One of the first small molecule combinations (dasatinib and quercetin (D+Q)) as senolytic was employed to deplete senescent cells successfully based on the inhibition of survival transcriptional programs (Zhu et al., 2015). After this treatment in aged mice, it is shown that survival rate and physical activity increased due to the ablation of senescent cells (Xu et al., 2018). On the other hand, early intervention of D+Q treatment by depletion of senescent cells exhibits alleviation of reduced lung function in bleomycin-challenged animals (Schafer et al., 2017).

Recently, chimeric antigen receptor (CAR) T cells have been engineered to target a surface protein associated with senescence in $Kras^{G12D}$ $p53^{-/-}$ mice. These mice showed extended survival upon treatment, leading to T-cell infiltration and decreased senescent cancer cells (Amor et al., 2020). Thus, the use of senolytic agents will elucidate the underlying mechanisms of cellular senescence and its contribution to the development of pulmonary diseases with aging.

1.3. Age-associated pulmonary diseases (COPD and IPF)

Aging is one of the major factors for age-associated diseases including IPF and COPD. During aging, the respiratory system undergoes major changes, which have an interesting resemblance to young patients suffering from lung diseases (Mercado et al., 2015). It is known that the development and progression of pulmonary diseases are severely affected by exposure to environmental stimuli, cigarette smoke, and various air pollutants. However, it is still unclear why the manifestation of the diseases takes decades and how age-associated changes contribute to and promote pathophysiology.

The signature of an aged lung is a decrease in the number of bronchioles as well as an increase in bronchiole diameter. Aging leads to alveolar enlargement and increased airspace size dependent on the loss of alveolar compartments of the lungs (Fain et al., 2005). Lungs lose elasticity by aging and become stiffer due to reconditioned expressions of ECM proteins (Godin et al., 2016). Scaffold proteins such as lamin α3 and α4 were shown to exhibit altered gene expressions in aged rodent lungs compared to young counterparts. Thus, ECM aberrant expression in the lung may promote age-associated phenotypes.

During aging, the FEV1/FVC (forced expiratory volume in 1 second/ forced vital capacity) ratio along with elevation of functional residual capacity are observed (Garcia-Rio et al., 2004). A decline in FVC itself is a strong indicator of mortality in the population (Lee et al., 2010). Genome-wide association studies (GWAS) revealed that there are specific variations at certain loci, affecting FEV1/FVC, FEV1, and FVC measurements (Loth et al., 2014). However, it remains unclear how these specific genetic variants incline to lung aging-related phenotypes.

COPD is accepted as an age-associated disease that develops mainly from cigarette smoke exposure. However, only a small proportion of COPD patients (only 10-15% of them) are categorized as smokers. This clearly highlights that there are various effectors including epigenetic or posttranslational mechanisms, which increase the risk to the predisposition of COPD for certain individuals. Some of the aging hallmarks overlap with molecular features of COPD. These include telomere attrition, genomic instability, cellular senescence, and loss of proteostasis (Mercado et al., 2015). In this context, cigarette smoke exposure may prompt basal level modulations that take place during aging. In the previous studies, *Klotho* (β-glucuronidase)-deficient mice manifested early development of emphysema and short lifespan along with alveolar destruction, decreased elasticity, and enlargement of alveolar space (Ishii et al., 2008).

Strikingly, low FEV1 is a clinical indicator of premature lung aging and can be used to predict COPD diagnosis at a later age. For instance, individuals with low FEV1 at the age above 40 years showed a 3 times higher risk to be diagnosed with COPD (Lange et al., 2015).

Telomere attrition is one of the mechanisms responsible for premature aging and the development of COPD. A study from smokers with COPD exhibited that the telomere length of circulating leukocytes is a biomarker of COPD development (Cordoba-Lanus et al., 2017). The telomerase null mice develop emphysema after exposure to cigarette smoke. Germline deletion of the telomerase RNA component also resulted in emphysema formation, suggesting that telomere length is a marker of COPD susceptibility. In addition, some studies showed that patients with severe COPD harbor detrimental mutations in TERT, the telomerase gene (Stanley et al., 2015). Lungs acquired from COPD patients possess high levels of SASP secretome as well as more senescent cells (Woldhuis et al., 2020). However, it is still open debate whether aging itself is the sole contributor to trigger cell senescence via cigarette smoke exposure (Rashid et al., 2018). Premature senescence directly affects progenitor cells within the COPD lung, resulting in stem cell exhaustion. Thus, this fits with the notion that COPD is caused by

the inability to regenerate connective and epithelial tissues, consequently inducing aberrant lung remodeling.

There are conflicting studies about whether exposure to cigarette smoke disrupts or triggers autophagy response within cells. Chen et al. showed an upregulation of autophagy in the lung of COPD patients, while another study has demonstrated impaired autophagic response, leading to accumulated poly-ubiquitinated proteins and autophagic vacuoles (Vij et al., 2018). A recent study uncovered the suppressed activity of TFEB, a transcriptional factor of lysosomal biogenesis and autophagy, in COPD animal models (Bodas et al., 2017).

Changes such as aberrant lysine acetylation, altered microRNA expression as well as DNA methylation patterns have been associated with aging and COPD pathogenesis (Schamberger et al., 2014). Due to cigarette smoke exposure, the epigenomic landscape has been affected, thus COPD epigenome might be targeted for a therapeutic approach. If COPD is accepted as a representative of increased lung aging, targeting declined functions with aging might be beneficial for COPD.

IPF is a severe, chronic, fibrotic interstitial lung disease with less than 3 year-survival after the diagnosis. The disease is characterized by aberrant interstitial remodeling, distorted tissue structure, declined lung function as well as irreversible scarring. While cigarette smoke exposure is the major factor in COPD pathogenesis, in contrast, aging is the biggest risk factor for IPF than any other genetic or environmental stimuli (Ley et al., 2012). Several aging-related mechanisms have been linked to IPF so far (Gulati and Thannickal, 2019). Metabolic rewiring and myofibroblast differentiation are stimulated by various biochemical mediators, leading to tissue remodeling, fibrotic scar formation, and ECM accumulation eventually (Lederer and Martinez, 2018). The cells with aging are prone to dysfunctional repair response and tissue scarring due to a lack of wound healing and failed resolution of fibrotic processes. The changes during aging clearly affect the predisposition to lung fibrosis at an older age, yet the mechanisms behind still remain unclear. Recent studies have focused on the changes in the aged lung such as cellular senescence telomere attrition and impaired mitochondrial functions and their response to repetitive epithelium injury. Nintedanib and pirfenidone are FDA- approved drugs for IPF treatment, but targeting altered pathways within aged cells may be a promising approach for the disease.

IPF is a telomere-related disease with a high risk. Genetic defects in telomerase components and telomere-regulatory genes have been identified as contributing factors of aging in

pulmonary fibrosis (Snetselaar et al., 2015; Vulliamy et al., 2001). Armanios et al. showed that almost 15% of familial and 25% of sporadic IPF patients have significant telomere shortening. hTERT and hTR germline mutations are the main cause of familial IPF, however, the idiopathic form of the disease represents short telomerase as well in the lung and peripheral blood (Alder et al., 2008). These findings highlight telomere attrition in the development of IPF.

Telomere shortening affects the renewal capacity of lung resident cells by triggering cellular senescence. For instance, AT2 cells having telomere dysfunction in aged TRF-1 – deficient mice contribute to ECM remodeling due to senescent cell accumulation along with collagen deposition (Naikawadi et al., 2016). On the other hand, IPF human lungs harbor an increased number of senescent fibroblast and epithelial cells (Schafer et al., 2017). Importantly, senescent fibroblasts were shown to release pro-fibrotic factors, a response that has been abrogated by treatment with senolytic drug *in vivo* abrogated fibrotic deposition (Schafer et al., 2017). Bleomycin-challenged animal models exhibit the accumulation of senescent myofibroblasts by inducing the molecular signature of cellular senescence (Waters et al.,2018). Treatment to ablate senescent cells improves lung function in pulmonary diseases but here, senescent fibroblasts allow the resistance towards oxidative stress-induced apoptotic response via increased NOX4 expression. That is why senolytic drugs look promising in IPF treatment (Hecker et al., 2014).

AT2 cells require a solid ER machinery to cope with the demand of protein synthesis, folding, and release of surfactants. Almost 5% of IPF patients clinically exhibit mutations in MUC5B (mucin 5B), SFTPC, and SFTPA2 (surfactant-associated proteins A) genes, being associated with age-related proteostasis failure (Romero and Summer, 2017). For instance, SFTPC mutations lead to ER stress, activated unfolded protein response (UPR), and upregulated autophagic response. In both familial and sporadic IPF patients, mutant SFTPC expression was observed in AT2 cells harboring aberrant UPR and ER stress (Lawson et al., 2008). In another study, ER stress-related mediators including XBP-1, CHOP, ATF4, and ATF6 were found to be elevated in IPF patients (Korfei et al., 2008). A compound called 4-PBA (4-phenyl butyric acid) was shown to diminish ER stress and myofibroblast differentiation in a bleomycin-challenged animal model (Plate et al., 2016). Thus, age-related proteostasis failure is an open field to investigate in IPF.

The deleterious response of autophagy, as well as mitophagy in IPF, is another interesting aspect in light of aging. Suppression of ATG5 gene expression in human bronchial epithelial cells along with fibroblasts resulted in reduced senescence and blocks myofibroblast

transdifferentiation (Araya et al., 2013). Atg4b-depleted animal models showed dysfunctional autophagy with elevated pro-inflammatory response and dysregulated ECM remodeling with collagen deposition (Cabrera et al.,2015). mTOR inhibitor, rapamycin, accelerates autophagic response and extends the lifespan of model organisms (Lamming et al., 2013). The therapeutic efficacy of omipalisib (a PI3K/mTOR Inhibitor) was evaluated in preclinical models and patients, giving promising results (Lukey et al., 2019). Therefore, developing new strategies and therapeutic approaches for IPF in the aging context holds the potential to ameliorate the disease severity.

1.4. Pulmonary inflammaging

Inflammaging is a term, defined as a hallmark of aging, gradually leading to an overburdened inflammatory state and dysfunctional immune response. Individuals with advanced age exhibit elevated levels of circulating and tissue pro-inflammatory cytokines such as IL-1β, IL-6 and TNF-α (Franceschi et al., 2000).This chronic sterile inflammatory phenotype has been associated with human diseases including COPD (John-Schuster et al., 2016).

Abnormal activation of the innate immune system with age results in inflammaging and within the tissue, a gradual increase of the senescent cells contributes to this pro-inflammatory manifestation through SASP secretome. Dysregulated clearance and accumulation of the senescent cells stimulate the production of pro-inflammatory mediators by activating NLRP3 inflammasome and lead to release them into the circulation, eventually reaching the distal sites of the organism (Basisty et al., 2020). Impaired pulmonary innate immunity with age creates a tendency to a failure in protecting the mucosal surface of the lungs from pathogens. The aging innate immune system lost the ability to recognize the signals through toll-like receptors (TLRs), chemotaxis, and phagocytosis responses even though it enhances the release of pro-inflammatory cytokines (Shaw et al., 2013). As an example of TLR signaling defects of age-related immunosenescence, monocytes isolated from elder individuals showed decreased transcription of TLRs 1-9 (Renshaw et al., 2002). Reduced TLR expression occurs by the reduced levels of MyD88, an adaptor molecule in older rodents (Chelvarajan et al., 2007). Other innate immunity processes such as ROS production against pathogens, phagocytosis of the microbes, and migration of the neutrophils, and dendritic cells to the infection area are severely affected by age (Boe et al., 2017). Aged dendritic cells were shown to have impaired antigen-presenting response, aberrant phagocytosis, and cytokine production as well as migration to the lymph nodes (Agrawal et al., 2007; Zhao et al., 2011). This aberrant innate immune response leads to less robust stimulation of adaptive immune cells in the lung (Panda et al., 2010).

Alveolar epithelial cells isolated from aged mice were also shown to produce elevated levels of chemokines such as CXCL1/2, eventually resulting in excessive neutrophil migration to the lungs infected with influenza. This excessive neutrophil accumulation was the culprit of the high rate of mortality in these mice (Kulkarni et al., 2019). In another study, upon *S. Pneumoniae* infection, aged macrophages exhibit NLRP3 inflammasome activity, decreased cytokine production along with reduced NF-kB expression (Cho et al., 2018). Altogether, these studies point out that pulmonary innate immune response upon aging is severely affected against invading pathogens. Restoring this impaired immune function is critical for infectious and sterile inflammatory conditions in the lungs.

Besides innate immunity, adaptive immunity response with aging undergoes many changes such as suppression of lymphopoiesis, reduced production of naive T cells and increased number of regulatory T cells, declined B cell activation, and affected antibody production (Nikolich-Zugich, 2018). Advanced age impacts the function of hematopoietic stem cells (HSCs) which are very important for the production of naive T and B cells. Older mice show a decline in the number of HSC population with reduced ROS activity when compared to younger mice, indicating that there is a loss of HSC renewal capacity at the end (Jang and Sharkis, 2007). In another aspect, B cell differentiation is as well known to be reduced in aged rodents. Based on the loss of IL-7 expression from stromal cells and E47 expression by pre-B cells, RAG2 as a driver of B cell receptor (BCR) recombination is drastically affected. This eventually leads to limited BCR diversity in elderly mice (Van der Put et al., 2004; Labrie et al., 2004).

Similarly, T cells with advanced age become hypo-responsive, and naive T cell generation declined due to restricted T cell receptor (TCR) diversity. Loss of TCR diversity induces the failure in the ability to recognize the microbe antigens and cancer cells (Griffith et al., 2012; Wang et al., 2020). Naive $CD4^+$ T cells isolated from aged animals showed less Bim (pro-apoptotic molecule) expression, leading to reduced IL-2 production, proliferation capacity, and antibody responses based on $CD4^+$ T cells (Tsukamoto et al., 2009). T cells from aged mice undergo metabolic changes that have an impact on the functionality and activation of these cells. Aged $CD4^+$ T cells bearing CD39 with increased expression of ATPase led to mitochondrial dysregulation and apoptosis (Fang et al., 2016). In addition, these aged CD4+ T cells exhibit decreased oxygen consumption (Ron-Harel et al., 2016).

Similarly, B cell population exhibits dysregulated functionality with aging. Henry et al. showed elderly individuals demonstrate less frequency of *de novo* somatic mutations in immunoglobulin variable genes, affecting antibody titers and the protective response. Reduced

expression of Blimp1, an effector of B cell differentiation into plasma cells, also partly impacts defective antibody production (Frasca et al., 2017). In another study, expansion of B cell-repressive T follicular regulatory cells (T_{FR}) has discovered in aged mice and this incidence happens through increased levels of PD-1 expression. Finally, these cells have been shown as phenotypically different than those in young mice (Sage et al., 2015). Altogether, these findings point out that age-related alterations restrict B cell maturation and function, which leads to malfunctioning humoral immunity. Even though these changes are investigated regarding innate and adaptive immunity, it is still an open area how aged immunity landscape can drive the chronic age-related lung diseases.

1.5 Histone deacetylase alterations in cellular senescence and aging

The modulation of chromatin structure and gene expression in a cell is influenced by the histone acetylation signature. This process is regulated by the activities of histone acetyltransferases (HATs) and histone deacetylases (HDACs). HATs promote open chromatin structure and increased gene expression by acetylating lysine amino acid on histone tails. Conversely, HDACs remove acetyl groups from histone tails, causing the histones to wrap the DNA more tightly, resulting in decreased gene expression and transcriptional repression (Yang et al., 2008; Park et al., 2020). In this chapter, we discuss only HDACs in the aging-associated pulmonary diseases.

In human, 18 HDACs exist, which are classified into five groups based on their sequence homology and phylogenetic origin: (i) class I, (ii) class IIa, (iii) class IIb, (iv) class III, or sirtuins and, (v) class IV HDACs, which are dependent on zinc. Class I HDACs (HDAC1, 2, 3, and 8) contain a deacetylase domain and are predominantly located in the nucleus. Class II HDACs (HDAC4, 5, 6, 7, 9, and 10) have tissue-specific expression and can shuffle between the cytoplasm and nucleus based on regulatory signal. Members of class II HDACs are further divided into two subclasses: (i) class IIa consists of HDAC4, 5, 7, and 9, while class IIb comprises HDAC6 and 10. Class IIa HDACs possess a C-terminal catalytic domain and a significant N-terminal regulatory domain that is crucial for protein-protein interactions and play a vital role for the recruitment of several co-factors. In addition, class III HDACs, or sirtuins (including sirtuins 1 to 7), and class IV (HDAC11) show some level of enzymatic activity (Yang et al., 2008; Park et al., 2020; Haberland et al., 2009).

HDACs have a broad range of functions, including the deacetylation of chromatin proteins, leading to changes in gene transcription regulation, as well as various non-histone proteins,

which can impact their function, localization, and interactions with other proteins (Minucci et al., 2006; Kim et al., 2016). In addition to their effects on protein acetylation, HDACs have also been shown to influence the expression of numerous genes through a variety of mechanisms. They can form co-repressor complexes with nuclear receptors, even in the absence of a ligand, and interact directly with transcription factors such as p53, HIF1α, GATA2, E2f, NF-κB, Hsp90, and Stat3 (Kim et al., 2016; Ropero et al., 2007; Singh et al., 2010). HDACs can also bind to multiprotein co-repressor complexes such as N-CoR, mSin3, and SMRT, which can interact with other epigenetic gene modifiers, including histone methyltransferases, DNA methyltransferases, and methyl-CpG-binding proteins (Milazzo et al., 2020).

HDACs are closely associated with various tumorigenic features such as proliferation, metastasis, differentiation, and apoptosis-resistance phenotype of cells, and the abnormal expression or activity of HDACs is often linked to human cancers and poor prognosis. The potential of HDAC inhibition as an anti-aging strategy has been proposed in the literature. Roman et al. (2017) showed that aged fibroblasts exhibit slightly higher levels of reactive oxygen species (ROS) and a decreased expression of the antioxidant enzyme EC-SOD, which cannot be restored by treating them with a DNA methyltransferase inhibitor 5-aza-dC. The repression of EC-SOD expression in aged fibroblasts was associated with the deacetylation of histone H3 and histone H4 at the gene promoter. In this study, treating aged lung fibroblasts with inhibitors of HDAC class 1 and class 2 restored the expression of EC-SOD to the level seen in young fibroblasts. However, some studies suggest that HDAC downregulation can also contribute to the aging process. For example, Di Giorgi et al. (2021), Place et al. (2005), and Han et al. (2016) have shown that HDAC1 and HDAC4 were downregulated in senescent fibroblasts. In a recent study by Warnon et al. (2021), downregulation of HDAC2 and HDAC7 was reported to induce a senescence response in dermal fibroblasts. Overall, the role of HDACs in cellular senescence and aging is still widely unexplored field, specifically for the pulmonary diseases. Therefore, there is a necessity to identify the underlying molecular mechanisms that contribute to susceptibility to cellular senescence and pulmonary aging. In this study, we mainly focused on HDAC9, HDAC class IIa member, to hinder the knowledge gap between the contribution of an epigenetic player and development of pulmonary aging phenotype.

2. AIMS OF THE STUDY

Age-associated lung diseases are a growing public health burden in Europe and worldwide. The increase in the prevalence of chronic lung diseases at older ages suggests an age-associated loss of lung-intrinsic defense and regenerative mechanisms. However, the determinants of susceptibility to chronic lung diseases remain elusive, and preventive as well as curative strategies are poor. Accumulating clinical and experimental evidence demonstrates that transgenerational as well as perinatal factors determine lung structure and function throughout life and are critical in setting the susceptibility to chronic lung diseases. Conversely, environmental factors are known to contribute significantly to the development and course of chronic lung diseases. The molecular mechanisms that determine susceptibility to environmental factors and the interplay between the transgenerational/perinatal and environmental exposome that cause lung aging and ultimately chronic lung diseases are not yet understood and preventive or therapeutic measures are lacking.

I hypothesize that epigenetic mechanisms i.e. HDAC9 deficiency drives cellular senescence and premature lung aging via the modulation of pro-inflammatory lipid mediators. I investigated the above hypothesis by addressing the following aims:

1. Characterization of HDAC9 deficient mice at two different age groups (young versus advanced age) as a mouse model of accelerated cellular senescence
2. Investigation of inflammatory lung phenotype in advanced age as a consequence of accelerated senescence in HDAC9-deficient mice and to test whether HDAC9 deficiency alters the phenotypic switches of immune cells (M1 and M2-like macrophages derived from BM) and their immunometabolic responses as internal organ communication beyond the lung
3. Identification of which cell populations are dominantly affected by HDAC9 deficiency and contribute to lung inflammation in advanced age
4. Elucidation of chromatin changes along with the down-stream gene targets and related pathways
5. Identification of metabolic pathways (specifically choline and oxylipin metabolites) playing role in senescence phenotype

All these above-mentioned aims were completed using isolated AT2 cells, BMDMs, and lung samples from young and advanced-age HDAC9 knockout mice, co-culture models for AT2

cells and macrophages, and high throughput techniques such as ATAC-Seq, RNA-Seq, and metabolic screening.

3. MATERIAL AND METHODS

3.1 Approval for animal studies

All animal experiments using HDAC9^{tm1Eno} and littermate WTs were approved by the *Regierungspräsidium Darmstadt*, under the approval number B2-1170.

3.2 Mice

3.2.1 C57BL/6J wild type mice

Mus musculus C57BL/6J wild-type mice were kindly provided by Prof. Dr. Eric Olson and used as littermate controls. For aging studies, a batch of different age groups of C57BL/6J wild-type mice were purchased from The Jackson Laboratory.

3.2.2 HDAC9 ^{tm1Eno} mice (HDAC9 KO)

The HDAC9^{tm1Eno} null/knock out (KO) mice (MGI: 2387834) were kindly provided by Prof. Dr. Eric Olson. The mice were generated by replacing most of exon 4 and all of exon 5 via a cassette containing lacZ and neo inserted by homologous recombination. The deleted region encompassing the MEF2 binding domain affected MEF2-interacting transcriptional repressor (MITR) splice form. A combination of RT-PCR and sequence analysis of HDAC9 KO mice displayed an aberrant transcript in which the inserted cassette was excised leading to splicing of exon 3 to exon 6. This alternative splicing pattern introduced two stop codons downstream of exon 3, therefore, prohibiting normal protein translation.

3.3 Genotyping of HDAC9 KO animals

All instructions indicated down below were followed for genotyping.

Lysis of tail fragments

- Add 200 µl of peqlab tail lysis buffer with Proteinase K (1 µl/100 µl tail lysis buffer)
- Keep overnight at 55°C with shaking (600rpm). Next day, increase temp to 85°C for 45min with shaking (600rpm).
- Cool down the lysates (4°C)
- Centrifuge at max. speed for 15min

Purification of DNA

- Directly use 2 µl of lysate for genotyping

PCR protocol

(a) name and sequence of primers

- 1st primer:
  5'7 NKOup A 5' GCA ATT GAC TAT GCG GCT CTG G 3'
- 2nd primer:
  3'7 NKOlow B 5' CAG CAC TAT AGA ACA GCC ACA G 3'
- 3rd primer:
  5'Neo C 5' GGC ATG CTG GGG ATG CGG TG 3'

(b) PCR mix

4 µl	H_2O
1 µl	1st primer [10µM]
2 µl	2nd primer [10µM]
1 µl	3rd primer [10µM]
10 µl	ImmoMix™ Red

➔ **18 µl master mix + 2 µl DNA**

(c) PCR settings

95 °C	10 minutes	
95 °C	30 sec	35x
67 °C	30 sec	
72 °C	30 sec	
72 °C	5 minutes	
4 °C	hold	

- **Program:** PCR-machine biometra

(d) PCR products

genotype		**PCR product**
WT	+/+	only 1 band (500 bp)
HZ	+/-	2 bands

KO	-/-	only 1band (300 bp)

Sample picture:

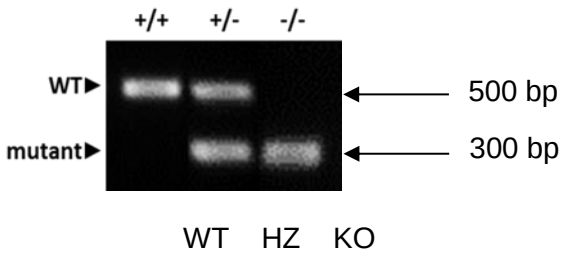

3.4 Defined age groups for the experimental set-ups

2 age groups were employed based on the publication (Zhang et al., 2002) for the experimental set-up. The age range per group is displayed in **Figure 3.1**.

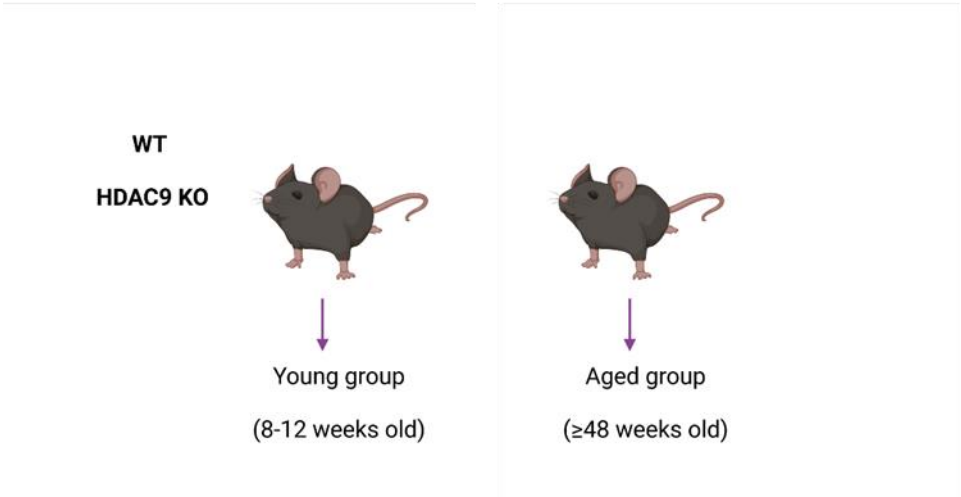

Figure 3.1: Schematic description of defined age groups. Generated by BioRender.

3.5 Mouse Alveolar Type II Cell isolation and culturing

Primary mouse AT2 cells were isolated using a modified isolation protocol from Sun *et al*. (27). The thoracic cavity was opened, and the lungs were perfused with cold Hank´s Balanced Salt Solution (HBSS) (Thermo Fisher Scientific, USA, #14175-046) from the right ventricle. The inferior vena cava was cut, and the lungs were continuously perfused with HBSS. A

tracheotomy was performed, and lungs were instilled with a 37 °C preheated 1 mL of dispase (Corning Incorporated, USA, #354235) and 0.5 mL of low melting point agar (Sigma-Aldrich, Germany, #A9414) using a blunt needle G24 (CML SUPPLY, USA, #901-21-050). After waiting for 3 min until the agarose solidified, the lungs were removed and incubated in 2 ml of pre-warmed dispase at room temperature for 45 min. The lungs were transferred to gentleMACS tubes (Miltenyi Biotec, Germany, #130-093-237) containing 7 ml of DMEM medium (Gibco, Germany, #61965-025), 10 mM HEPES, 1% P/S (Thermo Fisher Scientific, USA, #15140122) and 0.01% DNase (Merck KGaA, Germany, #260913). The lungs were dissociated with gentleMACS Octo Dissociator with Heaters (Miltenyi Biotech, Germany, #130-096-427) by using the `mouse lung 02.01` program for 10 seconds and `mouse lung 01.01` program for 30 seconds, the cell suspension was incubated for 10 min at room temperature on a shaker. The cell suspension was filtered in series through a 100 µm filter (Greiner Bio-One GmbH, Germany, #542000), a 40 µm filter (Greiner Bio-One GmbH,Germany, #542040), and a 20 µm nylon filter (Merck, Germany, #NY2004700) after washing the filters with DMEM/HEPES medium+DNAse combination as indicated above. The filtered cell suspension was centrifuged at 1000 rpm for 10 min at 4 °C. The pellet was resuspended in a DMEM medium containing 10% fetal bovine serum (FCS) (Gibco, Germany, #21885-026) and 1% P/S. The cells were stained with trypan blue solution (Thermo Fisher Scientific, USA, #15250061) and living cells were counted using a Neubauer chamber. The cells were centrifuged at 1000 rpm for 10 min at 4 °C, were resuspended in DMEM without FCS, and incubated with a cocktail of biotinylated anti-CD45 (0.9 µl per million cells) [BD (Becton Dickinson, #553078)], biotinylated anti-CD16/32 (0.7 µl per million cells) [BD (Becton Dickinson, #553143)] and biotinylated anti-CD31 (0.4 µlper million cells) [BD (Becton Dickinson, #553371)] for 30 min at 37 °C in a shaking water bath. The pre-washed Dynabeads™ biotin binder (2.4 µl per million cells) (Thermo Fisher Scientific, USA, #11047) was added to the cell suspension and incubated for 30 min at roomtemperature, which the mouse AT2 cells were negatively selected. The cell suspension containing antibodies was placed into a magnetic separator (Thermo Fisher Scientific, USA, #123.01) for 15 min at room temperature. CD31 and CD45 depleted cells were centrifuged at 1000 rpm for 10 min. The AT2 cells were collected and i) resuspended in DMEM containing 10% FCS and 1% P/S, and seeded on a 6-well plate inserted with a 24 mm Transwell® with 0.4 µm pore polyester membrane insert (Corning Incorporated, USA, #3450) in an air-liquid interface culture system (**Figure 3.2**); or ii) resuspended in protein lysis buffer for protein expression study; or iii) resuspended in TRIzol™ (Invitrogen, USA, #15596018) for RNA expression study.

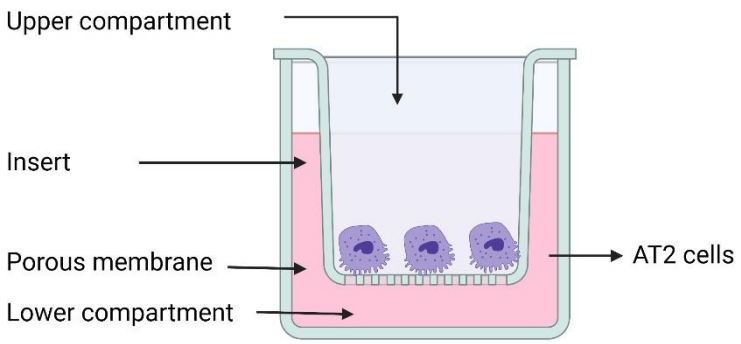

Figure 3.2: Air liquid interface culture system of AEII cells. Generated by BioRender.

3.6 MH-S cells

MH-S cell line (American Type Culture Collection, USA) is immortalized mouse alveolar macrophage cell line. These cells were cultured in RPMI-1640 Medium (Gibco, 21875034). To make the complete growth medium, 2-mercaptoethanol to a final concentration of 0.05 mM was added to basal media with 10 % FCS and 1% P/S. When the cells reached 80-90% of confluence, they were subcultured and split in a ratio of 1:3 depending on the density needed for the following experiments. For the cross-talk studies, alveolar macrophages were cultured for 24 hours with the media of isolated AT2 cells from HDAC9 KO mice.

3.7 Isolation and generation of mouse bone-marrow-derived macrophages

Bone marrow from the femur and tibia of HDAC9 KO mice and matching aged control WT mice were isolated. Bone marrows were flushed out with RPMI medium supplemented with 1% P/S and filtered through a 100 µm filter. The centrifugation then was performed at 1600 x g for 5 min at 20 °C and erythrocytes were depleted by red blood cell lysis buffer (Invitrogen, Germany, 00-4333-57). After second centrifugation at 1600 x g for 5 min at 20 °C, the cell pellet was cultured in RPMI medium supplemented with 10% FCS, and 1% P/S in the presence of 20 ng/mL recombinant murine macrophage stimulating factor (rmM-CSF, R&D Systems). Media of the cells was changed every 3 days for 7 days to allow differentiation and maturation of macrophages. Sequentially, M1 macrophages were polarized by 100 ng/mL Lipopolysaccharide (LPS, Sigma-Aldrich) and 100U/mL Interferon-γ (rmIfnγ,R&D Systems) were used to polarize M0 macrophages into M1 macrophages and 20 ng/mL rmIL4 (R&D

Systems) was used for M2 macrophage polarization for 24 hours. Polarized murine macrophages were harvested for RNA and protein isolation.

3.8 Total RNA isolation

Total RNA was isolated from mouse AT2 cells, BM-derived monocytes/macrophages and MH-S cells using the miRNeasy® Mini kit (Qiagen, Germany, #217004). The media of the cells cultured in 6 well plates was removed from each well and washed with 1 mL of sterile DPBS. The cells were scraped in 700 µl of TRIzol™ reagent after incubation at room temperature for 10 min. The lysates were transferred into the sterilized 1.5 ml tubes and 140 µl of chloroform was added. The tubes were vortexed vigorously and samples were incubated at RT for 3 min. The samples were then centrifuged at 12000 x g for 15 min at 4ºC. The upper aqueousphase was carefully transferred into the fresh 1.5ml tubes. 525 µl of 100% ethanol was added and mixed thoroughly by pipetting. 700 µl of the sample was pipetted into an RNeasy® Mini column in a 2 ml collection tube provided by the kit. The collection tube containing the sample was centrifuged at 12000 x g for 15 s at room temperature. After discarding the flow-through, 700 µl of Buffer RWT was added to the RNeasy Mini column and centrifuged for 15 s at 12000 x g. 500 µl of Buffer RPE was pipetted onto the RNeasy Mini column and centrifuged for 15 s at 12000 x g. As a second wash step, 500 µl of Buffer RPE was added to the RNeasy Mini column and centrifuged for 2 min at 12000 x g at room temperature. The pellet was dried under the chemical hood and as a final step, total RNA from cells was resuspended in 14 µl of nuclease-free water, which was pre-warmed at 60ºC for 15 min. The concentration and purity of RNA samples were analyzed by using a Nanodrop2000 spectrophotometer.

3.9 Gene expression analysis

The cDNA from the isolated RNA samples was synthesized using the high capacity cDNA synthesis kit according to the manufacturer's instructions. 1000 ng of RNA from MH-S cells, 250 ng of mouse AT2 cells and 250 ng of BM-derived monocytes/macrophages were used to synthesize cDNA and made the volume up to 10µl by nuclease-free water. RT master mix was prepared on ice and the RNA template of each sample was combined with 10 µl of RT master mix. RT master mix composition is shown in **Table 1** and thermal cycler conditions described in **Table 2** were followed. The synthesized cDNA was diluted 1:2 or 1:4 dependent on the samples before performing qPCR.

Table 1: Reaction mixture for cDNA synthesis

Component	Volume
Nuclease-free water	3.7 µL
10X RT Buffer	2.0 µL
25XdNTP Mix	0.8 µL
10XRT Random Primers	2.0 µL
Reverse Transcriptase	1.0 µL
Rnase Inhibitor	0.5 µL
Total	10.0 µL

Table 2: Thermal cycler conditions

Settings	Step 1	Step 2	Step 3	Step 4
Temperature	25°C	37°C	85°C	4°C
Time	10 min	120 min	5 min	-

Real time Quantitative Polymerase chain reaction (RT-qPCR)

Real Time-qPCR reaction mix was prepared by using Applied Biosystems™ PowerUp™ SYBR™ Green Master Mix as shown in **Table 3**.

Table 3: Reaction conditions for RT-qPCR program

Component	Volume (µL)
Applied Biosystems™ PowerUp™ SYBR™ Green Master Mix	5
Forward primer (10 mM)	0.2 5
Reverse primer (10 mM)	0.2 5
Nuclease-free water	3.5
cDNA template	1
Total	10

All primers were designed using the NCBI tool Primer-BLAST and Primer3Plus bioinformatic tools. Standard PCR guidelines were followed: (i) the amplicon length is approximately 50–200 bp; (ii) the primer length is 18–24 nucleotides, and free from internal secondary structure; (iii) primer pairs should have approximately 50% GC content as well as compatible melting temperatures. The only exception is the primers used for telomere length measurement. All primers

used are listed in **Table 4** (*Mus musculus* and *Homo sapiens* primers) with their sequence information and the corresponding annealing temperatures.

Table 4: *Mus musculus* primers used for RT-qPCR

Gene	Primer Sequence (5'-3')		Annealing	Species
Hprt	FP	GCTGACCTGCTGGATTACAT	58	Mouse
	RP	TTGGGGCTGTACTGCTTAAC		
Tnfα	FP	CATCTTCTCAAAATTCGAGTGACAA	60	Mouse
	RP	TGGGAGTAGACAAGGTACAACCC		
Il10	FP	ACATACTGCTAACCGACTCCT	58	Mouse
	RP	AAATCGATGACAGCGCCTC		
Il1b	FP	TGCCACCTTTTGACAGTGATG	59	Mouse
	RP	TGCTGCGAGATTTGAAGCTG		
iNOS	FP	ACTACTACCAGATCGAGCCC	58	Mouse
	RP	GCTAGTGCTTCAGACTTCCC		
Il6	FP	ACAGCCACTCACCTCTTCAG	60	Mouse
	RP	CCATCTTTTTCAGCCATCTTT		
Timp1	FP	AGGTGGTCTCGTTGATTTCT	58	Mouse
	RP	GTAAGGCCTGTAGCTGTGCC		
Mmp3	FP	GCTGAGGACTTTCCAGGTGTTG	60	Mouse
	RP	GGTCAGTTTTTTGGCATTTGGGTC		
Mmp12	FP	CTCCCATGAACGAGAGCGAA	60	Mouse
	RP	AGTTGAGGTGTCCAGTTGCC		
Mmp9	FP	ATCCAGTTTGGTGTCGCGGAGC	61	Mouse
	RP	GAAGGGGAAGACGCACAGCT		
Tgfβ	FP	GTGTGGAGCAACATGTGTGGAAC TCTA	60	Mouse
	RP	GTGCAATGCAGACGAAGCAGA		
Hdac9	FP	TGGAACACTGTTGAAGGTAGTCTG	60	Mouse
	RP	GATAACCACAACATTTCAACTTAACAA		
Cdkn1a	FP	AATGGAGACAGAGACCCCAGAT	61	Mouse
	RP	TCAAAGTTCCACCGTTCTCGG		
Cdkn2a	FP	GTCGCAGGTTCTTGGTCACT	61	Mouse
	RP	TCTGCACCGTAGTTGAGCAG		
Il1a	FP	TCAAGATGGCCAAAGTTCCT	60	Mouse
	RP	TGCAAGTCTCATGAAGTGAGC		

TEL	FP	CGGTTTGTTTGGGTTTGGGTTTGGGTTTGGGTTTGGGTT	63	Human
	RP	GGCTTGCCTTACCCTTACCCTTACCCTTACCCTTACCCT		
36B4	FP	CAGCAAGTGGGAAGGTGTAATCC	63	Human
	RP	CCCATTCTATCATCAACGGGTACAA		

In non-skirted 96-well PCR plate, 9 µl of the master mix and 1 µl of cDNA template were pipetted into each well and centrifuged at 3000 rpm for 2 min. The reaction was run in Applied Biosystems Step One Real-time PCR machine, following the conditions as shown in **Table 5**.

Table 5: Cycling conditions of PCR

Step	**Reaction**		**Temperature**	Time
1	Initial Denaturation	95 °C 45×	5 min	1
2	Denaturation		95 °C	2
3	Annealing		59 °C	3
4	Extension		72 °C	72 °C
5	Final Extension		72 °C	5 min
6	Melting CurveAnalysis			30min
7	Storage		4 °C	∞

Final data was analyzed by normalizing to the expression of housekeeping gene hypoxanthine phosphoribosyltransferase1 (*HPRT*) for mouse samples. And the level of mRNA expression was displayed as ΔCt values (Ct value of the housekeeping gene – Ct value of the gene of interest).

3.10 Protein Isolation

Mouse AT2, mouse BMDM, and MH-S cells were seeded in 6-well plates. After completion of the specific time point of the intended treatment, the medium was removed and washed each well with 2 mL of DPBS. RIPA buffer having protease-phosphatase inhibitor cocktail (PPi) was used to lysis the cells for 10 min at 4 ºC and isolate total protein. After transferring the content to the sterile 1.5 ml tubes, the centrifugation was performed at14800 rpm for 20 min at 4 ºC and the supernatants were transferred into new 1.5ml tubes. The supernatants were either stored at -80 ºC or taken for protein quantification directly. To measure total protein concentration, the samples were diluted in a range from 1:10 to 1:50 in RIPA buffer with PPi cocktail dependent on sample type. Bovine serum albumin (BSA) (Thermo Fisher Scientific, USA, # 11733046, P/N 55213) was prepared at different concentrations (0.125, 0.25, 0.50, 1, and 2 mg/mL) as protein standard. 5µl of pre-diluted samples and standards were added into 96-well microplates.

The reaction mixture was prepared by pipetting 20 µl of reagent S to 1ml of reagent A provided by the kit. 25 µl from this mixture was added to each well including standards and blank wells. After adding 200µl of the reagent B, the plate was incubated for 15 min at RT and then measured the absorbance at 750 nm via the ELISA plate reader (Infinite® 200 PRO, Germany, #M200PRO). The standard curve and the protein concentrations were provided using the Tecan software. The normalization of the protein samples was performed according to the least concentrated protein sample. The normalized proteins were then denatured at 95ºC for 5 min after mixing with the 5X gel loading buffer (4:1 ratio). The denatured samples were either stored at -20 ºC or taken directly for the western blotting.

3.11 Electrophesis and Western Blotting

The protein samples were loaded on a 10% sodium dodecyl sulphate (SDS) polyacrylamyde gel (PAGE) and resolved at 75 mV for the first 30 min and 100 mV until reaching the end of the resolving gel. The proteins were then transferred to a nitrocellulose membrane or polyvinylidene fluoride (PVDF) membrane, based on the recommended membrane type from antibody companies. The PVDF was activated by methanol for 1 min before the blotting sandwich was prepared. The blotting sandwich was developed as displayed in **Figure 3.3**.

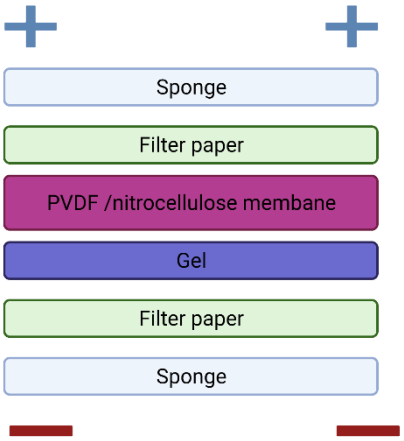

Figure 3.3: The blotting sandwich preparation in western blotting. Generated by BioRender.

The blotting process of the samples was performed at 100 V for 1 hr. Afterward, the membrane was incubated for 1 hr at RT in 5% non-fat dry milk or 5% BSA according to recommended blocking buffer of the antibody companies. For probing process, the membrane was incubated overnight with the primary antibody of interest diluted in the blocking buffer on a rotating shaker. After 3 times-washing for 15 min with 1X TBST buffer on the shaker at RT, the

membrane was incubated with secondary antibody conjugated to HRP (horseradish peroxidase) for 1 hr at RT. Protein-antibody conjugates were detected using chemiluminescence system. The exposure timings were based on the signal intensity of the samples. The buffer and gel preparations were displayed in **Table 6**. The primary antibody dilutions were listed in **Table 7**.

Table 6: Buffers used for SDS-PAGE & immunoblotting & gels

Buffer	Composition
10x SDS PAGE running buffer (pH 8)	35mM SDS 250mM Tris 0.86M glycine
Blotting buffer	25mM Tris 192mM glycine20% methanol
Washing buffer	1x PBS 0.2 % Tween 20

Stacking Gel	Resolving Gels (10%, 7,5 % and 15% gels)
5% Rotiphorese® Gel 30 (37,5:1)	10% Rotiphorese® Gel 30 (37,5:1)
125 mM Tris-Cl, pH=6.8	375 mM Tris-Cl, pH=8.8
0.05% SDS	0.10 % SDS
0.05% Ammonium persulfate	0.05 % Ammonium persulfate
0.065% TEMED	0.10 % TEMED

Table 7: Antibodies applied to Western Blotting

Antibodies	Company	Cat. No.	Source	Dilution
HDAC9	Introgen	sc-32940	Rabbit	1:100
HDAC9	Abcam	Ab9992	Goat	10 µg/mL (1:50)
HDAC9	R&D	150503	Mouse	1:100
GAPDH	Thermo	MA5-15738	Mouse	1:5000
COX1	Cell signaling	4841	Rabbit	1:1000
Annexin a1	Cell signaling	3299	Rabbit	1:1000
cPLA2	Cell signaling	D175	Rabbit	1:500
pERK	Santa Cruz	sc-7383	Mouse	1:1000

3.12 Flow Cytometry

Total lungs from HDAC9 KO and littermate WTs were transferred to gentleMACS tubes (Miltenyi Biotec, Germany, #130-093-237) containing DMEM medium(Gibco, Germany, #61965-025) and 1% P/S (Thermo Fisher Scientific, USA, #15140122). The lungs were dissociated with gentleMACS Octo Dissociator with Heaters (Miltenyi Biotech, Germany, #130-096-427) by using the `mouse lung 02.01` program for 10 seconds and `mouse lung 01.01` program for 30 seconds. The cell suspension was resuspended in PBS and filtered through 100-µm and 40-µm cell strainers (BD Biosciences). After blocking the cell suspension with blocking reagent FcγR diluted with 0.5% PBS-BSA for 15 min, the mouse single cells were stained with the following fluorochrome-conjugated antibodies as shown in **Table 8**.

Table 8: Antibodies used for flow cytometry from whole lung samples

Marker	Dye	< 5E6 pro 100µl	Provider
CD16/32	none	2	Biolegend
CD3	PE-CF594	1,5	BD
CD4	BV711	1	BD
CD8	BV650	0,5	eBioscience
CD11b	BV605	0,5	eBioscience
CD11c	BV711	1,5	BD
CD19	APC-H7	1	BD
CD31	PE-Cy7	0,1	Miltenyi
CD34	FITC	1	Miltenyi
CD44	AlexaFluor700	1	eBioscience
CD45	VioBlue	2	Biolegend
CD49f	PE-CF594	0,1	Miltenyi
CD90.2	PE	1	BD
CD117	APC-eFluor780	0,5	BD
CD140	PE	2	Biolegend
CD146	AlexaFluor488	1	Biolegend
CD324	AlexaFluor 647	1	eBioscience
CD326	BV711	0,5	eBioscience
GITR	FITC	1	BD
SiglecH	FITC	1	Biolegend
F4/80	PE-Cy7	1	Biolegend
γδ TCR	APC	1	eBioscience
HLA-DR (MHC II)	APC	0,5	Miltenyi
Ly-6C	PerCP-Cy5.5	1	BD
Ly-6G	APC-Cy7	1,5	Biolegend
NK1.1	BV510	1,5	BD

All antibodies were diluted to the optimal concentrations. Data was analyzed using LSR II/Fortessa flow cytometer and the gating strategy was implemented using fluorescence minus one control (FMO). In addition, isotype control was used to eliminate the background surface staining. For single-color compensation to create multicolor compensation matrices, Comp-Beads (BD Biosciences) were used. Instrument calibration was checked daily using Cytometer Setup and Tracking beads (BD Biosciences). The cell viability was assessed using 7-aminoactinomycin D (7-AAD) (BD Biosciences).

3.13 Cell proliferation Assay

50000 of primary AT2 cells and 15000 of MHS cells were seeded in 96-well plates for 24 hr. MHS cells were treated with conditional media of primary AT2 cells isolated from HDAC9 KO animals for 24 hr or 48 hr. The following day, the cell proliferation rate was assessed by ELISA BrdU kit (Roche). According to the manufacturer's protocol, the cells were incubated in the BrdU labeling solution for 2 hr. After removing the media, the cells were fixed for 30mins at RT using 200µl of FixDenat solution for each well. After the fixation, the cells were incubated for 3 hr in anti-BrdU-POD at RT, the wells were washed three times using wash buffer. The plate was incubated with 100µl of HRP -substrate solution until the color develops. The plates were measured spectrophotometrically at 370 nm with reference at 492nm using the ELISA plate reader (Tecan Infinite M200 PRO).

3.14 Cell death detection assay

The cell death experiments were performed using *in situ* cell death assay kit (Cell Death Detection ELISAPLUS, Roche Applied Science) based on the quantitative sandwich-enzyme-immunoassay principle, which utilizes antibody against cytoplasmic histone and nicked DNA. 50000 of primary AT2 cells and 15000 of MHS cells were seeded in 96-well plates for 24 hr. MHS cells were treated with conditional media of primary AT2 cells isolated from HDAC9 KO animals for 24 hr or 48 hr. The following day, the cells were centrifuged at 200 g for 10 min. After the centrifugation, the medium was removed and 200µl of 1x lysis buffer was added to each well and incubated in anti-histone antibody coated plates for 30 min at RT. Sequentially, immobilized histone/nicked DNA were detected by peroxidase-conjugated antibody and a color was developed using an ABTS (2, 2'-azino-bis (3-ethylbenzothiazoline-6-sulphonic acid) substrate. The read at 405 nm with reference measurement at 490nm was performed using Tecan Infinite M200 PRO reader.

3.15 Transfection with siRNA

MH-S and BM-derived monocytes were transfected with siRNA using Hiperfect Transfection Reagent (371707, Qiagen, Hilden, Germany) in OPTI-MEM serum-free medium (Gibco, Thermo Fischer, 31985062). Mouse HDAC9 siRNA, and all-star negative siRNA as non-silencing control were obtained from Qiagen (Qiagen, Hilden, Germany) (**Table 9**). The cells were transfected with siRNAs for 6 h in a serum-free medium according to the protocol provided by the manufacturer. After 6 h, serum-free media was changed to serum-containing medium for 24 hr or 48 hr based on RNA or protein expression studies, respectively.

Table 9: siRNA details

Gene	Product	GeneGlobal ID
mHDAC9	Ms_HDAC9_Flexitube_pool	SI02743377 SI02718380 SI02695259 SI02674700

3.16 Senescence β-Galactosidase Staining

AT2 cell isolation from aged and young of HDAC9 KO and their matching age-littermate WT controls was performed as described previously. 50000 cells of primary AT2 cells were seeded into 8-well chamber system (Nunc™ Lab-Tek™ II CC2™ Chamber Slide System, Thermo Fischer, 154739). After seeding for 24 hr, the cells were fixed and senescence was assessed using the Senescence β-Galactosidase Staining kit (Cell Signaling, 9860, Germany) according to the manufacturer`s instructions.

3.17 Quantitative lung histomorphometric analysis

Lung tissues from HDAC9 KO and WT animals were dissected and fixed with 4% paraformaldehyde (PFA) overnight at 4 °C. The following day, the lungs were placed into PBS, dehydrated, and then embedded in paraffin blocks. Paraffin sections from each sample were cut in 3 μm of thickness. The following section preparation, radial alveolar count, and mean linear intercept analysis were performed as described by previously (Hirani D. et al, 2022).

3.18 Haematoxylin & Eosin staining (H&E staining)

Lung tissues from HDAC9 KO and WT animals were dissected and fixed with 4% paraformaldehyde (PFA) overnight at 4 °C. The following day, the lungs were placed into PBS, dehydrated, and then embedded in paraffin blocks. Paraffin sections from each sample were cut

in 3 µm of thickness. Tissue sections were deparaffinized by heating for 1 hr at 60 °C and the slides were then passed through three times of xylol in total 30 min. The sections were immersed into different concentrations of ethanol (99%, 96%, and 70% respectively). Afterward, the slides were stained with Mayer's hematoxylin (AppliChem) for 20 min, and then incubated with Eosin Y (AppliChem). After washing three times, the slides were finally mounted with Pertex (Medite GmbH). Lastly, sections were scanned with Nanozoomer (2.0HT digital slide scanner C9600).

3.19 Immunocytochemistry (ICC)

AT2 cells were seeded into 8-well chamber system (50000/well). After 24 hr of seeding, the cells were washed with PBS for 5 min and fixed with acetone: methanol mixture (1:1) for 30 min at 4ºC. The fixed cells were washed three times with sterile PBS. The cells were then incubated in blocking reagent in combination of 5% BSA, 5% goat serum and 0.1% Triton X100 in PBS for 1hr at RT. The cells were incubated in the primary antibody diluted in the blocking reagent during overnight at 4 ºC. The primary antibody informations were displayed in **Table 10**. After the overnight incubation, the cells are washed in PBS tree times for 5 min and then incubated in the secondary antibody diluted in the blocking reagent for 1 hr at RT (anti rabbit IgG-AlexaFluor®488, AlexaFluor®555 and AlexaFluor®594, Invitrogen). Finally, the nucleus of the cells was stained using DAPI diluted in PBS (1:1000) for 10 min. The cells were then mounted using Dako fluorescent mounting medium. The images were acquired using the Zeiss LSM700 confocal microscope with the Zen black software.

Table 10: Antibodies employed for ICC

Antibodies	Company	Cat. No.	Source	Dilution
cPLA2	Abcam	Ab9992	Goat	10 µg/mL (1:50)
HDAC9	Introgen	sc-32940	Rabbit	1:100
HDAC9	Abcam	Ab9992	Goat	10 µg/mL (1:50)
HDAC9	R&D	150503	Mouse	1:100
HDAC9	Introgen	sc-32940	Rabbit	1:100
Surfactant C	Merck	AB3786	Rabit	1:150
E-cadherin	Santa Cruz	sc-8426	Mouse	1:200
p21	Abcam	ab188224	Mouse	1:250
Vimentin	Abcam	ab137321	Rabbit	1:250

3.20 Immunofluorescence staining (IFC)

Lung tissues from HDAC9 KO and WT animals were dissected and fixed with 4% paraformaldehyde (PFA) overnight at 4 °C. The following day, the lungs were placed into PBS, dehydrated, and then embedded in paraffin blocks. Paraffin sections from each sample were cut in 3 µm of thickness. Tissue sections were deparaffinized by heating for 1 hr at 60 °C and the slides were then passed through three times of xylol in total 30 min. The sections were immersed into different concentrations of ethanol (99%, 96%, and 70% respectively). The tissue sections were cooked in 10mM citrate buffer (10 mM Sodium citrate, 0.05% Tween 20, pH 6.0) for the antigen retrieval during 20 min. After cooling the sections at RT for 10 min, the sections were blocked in 5% BSA diluted in PBS for 1 hour at RT. The sections were then incubated with primary antibody during overnight at 4°C. The primary antibody informations were displayed in **Table 11**. Following primary antibody incubation, the slides were incubated with secondary antibody (anti rabbit IgG-AlexaFluor®488, AlexaFluor®555 and AlexaFluor®594, Invitrogen) at a dilution of 1:1000, counterstained with DAPI diluted in PBS (1:1000) for 10 min. The cells were then mounted using Dako fluorescent mounting medium. The images were acquired using the Zeiss LSM700 confocal microscope with the Zen black software.

Table 11: Antibodies employed for IFC

Antibodies	Company	Cat No.	Host	Dilution
CD3	Santa Cruz	sc-32940	Rabbit	1:100
CD19	Abcam	Ab9992	Goat	10 µg/mL (1:50)
Cytokeratin	DAKO	Z0622	Rabbit	1:250
CD45	Novusbio	NB100-417	Rabbit	1:1000
Iba-1	Antibodies	A104332	Rabbit	1:500

3.21 Immunohistochemistry (IHC)

Mouse lungs were submerged in 4% (w/v) paraformaldehyde for paraffin embedding. Immunohistochemical stainings were performed for the sections with 3 µm-thickness according to the manufacturer's protocol (Histostain Plus Kit, Zymed Laboratories, Invitrogen). Antigen retrieval was performed in 10 mM sodium citrate pH 6.0 in a pressure cooker. Proteinase K solution was used at room temperature after applying a blocking step with 10% BSA solution for 1 hour. The following antibodies were used **in Table 12.,**

Table 12: Antibodies employed for IHC

Antibodies	Company	Cat No.	Host	Dilution
SP-A	Abcam	ab87674	Rabbit	1:500
SP-B	Novus	NBP2-77431	Rabbit	1:500
SP-C	Thermo	PA5-76631	Rabbit	1:200
SP-D	Biocompare	bs-1583R	Rabbit	1:250
p21	Thermo	AHZ0422	Mouse	1:500
p16	LS Bio	LS-B1347-0.05	Rabbit	1:500
PCNA	Thermo	PA5-27214	Rabbit	1:500
Caspase 3	Cell Signaling	9662	Rabbit	1:1000

3.22 Bulk ATAC Sequencing (Assay for Transposase-Accessible Chromatin using sequencing)

For ATAC-Seq, AT2 cell isolation from 60-week-old HDAC9 KO and their matching age-littermate WT controls was performed as described above. Washed cells were counted with MOXI Z Mini Automated Cell Counter Kit (Orflo) and 50.000 cells were used for ATAC Library preparation using Tn5 Transposase from Nextera DNA Sample Preparation Kit (Illumina). Cells were pelleted and resuspended in 50µl Lysis/Transposition reaction (12.5µl THS-TD-Buffer, 2.5µl Tn5, 5µl 0.1% Digitonin and 30µl water) and was incubated at 37°C for 30min with occasional snap mixing. Following purification of the DNA fragments was done by MinElute PCR Purification Kit (Qiagen). Amplification of Library together with Indexing was performed as described elsewhere (Buenrostro et al., 2013). Libraries were mixed in equimolar ratios and sequenced on NextSeq2000 platform with 2x36bp paired-end setup. Trimmomatic version 0.39 was employed to trim reads after a quality drop below a mean of Q20 in a window of 5 nt (Bolger et al.,2014). Only reads above 15 nt were cleared for further analyses. These were mapped versus the mm10 version of the mouse genome (ensemble release 101) with STAR 2.7.10a using only unique alignments to exclude reads with uncertain arrangement. Reads were further deduplicated using Picard 2.25.5 (Picard: A set of tools (in Java) for working with next generation sequencing data in the BAM format) to avoid PCR artefacts leading to multiple copies of the same original fragment. The Macs2 peakcaller (version 2.1.1.20160309) (Zhang et al.,2008) was employed to accommodate for the range of peak widths typically expected for ATAC-seq. Minimum qvalue was set to -4 and FDR (false discovery rate) was changed to 0.0001. In order to determine thresholds for significant peaks, the data was manually inspected in IGV 2.3.52 (Robinson et al.,2011). Peaks overlapping ENCODE blacklisted regions (known misassemblies, satellite repeats) were excluded. Peaks were annotated with the promoter (TSS +- 5000 nt) of the gene most closely located to the centre of the peak based on

reference data from GENCODE v15. In order to be able to compare peaks in different samples, the resulting lists of significant peaks were overlapped and unified to represent identical regions. The counts per unified peak per sample were computed with BigWigAverageOverBed (UCSC Genome Browser Utilities, http://hgdownload.cse.ucsc.edu/downloads.html). Raw counts for unified peaks were submitted to DESeq2 (version 1.30.0) for normalization. Spearman correlations were produced to identify the degree of reproducibility between samples using R. To permit a normalized display of samples in IGV, the raw BAM files were normalized for sequencing depth (number of mapped deduplicated reads per sample) and noise level (number of reads inside peaks versus number of reads not inside peaks). Two factors were computed and applied to the original BAM files using bedtools genomecov resulting in normalized BigWig files for IGV. The footprinting analysis for transcription factors was performed according to the previous study (Bentsen et al. 2020).

3.23 RNA Sequencing

For RNA Sequencing, AT2 cell isolation from 60 week-old and 70 week-old HDAC9 KO and their matching age-littermate WT controls was performed as described above. RNA from AT2 cells was isolated using miRNeasy Micro Kit (Qiagen). To avoid contamination by genomic DNA samples were treated by on-column DNase digestion (DNase-Free DNase Set, Qiagen). Total RNA and library integrity were verified on LabChip Gx Touch 24 (Perkin Elmer). 600 ng of total RNA was used as input for SMARTer Stranded Total RNA Sample Prep Kit - HI Mammalian (Takara Bio). Sequencing was performed on the NextSeq2000 instrument (Illumina) using with 1x72bp single end setup. The resulting raw reads were assessed for quality, adapter content, and duplication rates with FastQC (Andrews S. 2010, FastQC: a quality control tool for high throughput sequence data. Available online at: http://www.bioinformatics.babraham.ac.uk/projects/fastqc.Trimmomatic version 0.39 was employed to trim reads after a quality drop below a mean of Q20 in a window of 10 nucleotides (Bolger et al., 2014). Only reads of at least 15 nucleotides were cleared for subsequent analyses. Trimmed and filtered reads were aligned versus the Ensembl mouse genome version mm10 (ensemble release 101) using STAR 2.7.10a with the parameters "--outFilterMismatchNoverLmax 0.1 --alignIntronMax 200000" (Dobin et al., 2013). The number of reads aligning to genes was counted with featureCounts 2.0.2 from the Subread package (Liao et al.,2014). Only reads mapping at least partially inside exons were admitted and aggregated per gene. Reads overlapping multiple genes or aligning to multiple regions were excluded. Differentially expressed genes were identified using DESeq2 version 1.30.0 (Love et

al., 2014). The heatmap was represented with all identified transcripts from RNA-Seq for isolated AEII cells of aged WT and HDAC9 KO animals. For each transcript, the FDR and the mean Log_2fold change were calculated, and the genes were classified as differentially expressed if the average count is >5 and p value is < 0.05. The Ensemble annotation was enriched with UniProt data (release 24.03.2017) based on Ensembl gene identifiers (Activities at the Universal Protein Resource (UniProt)).

3.24 Lipidomics

AT2 cells and BM-derived monocytes/macrophages were seeded as 10^6 cells for each condition. The cells were cultured for 48 hours. After 48 hours, the supernatant samples were collected, followed by the cell lysate samples collected in cold PBS. Free fatty acid (oxylipins) metabolites and choline phospholipid metabolites were extracted from the collected samples by adding the ethyl acetate (3x) and methanol (4x), respectively. After the centrifugation, oxylipins in upper layer and choline metabolites in supernatant were dried down. Following the resuspension in the solvent, the samples were analyzed by Agiklent 1290 Infinity Lc system coupled to a QTrap 5500 mass spectrometer (Kuhnert et al., 2022).

3.25 PLA2 and cPLA2 enzymatic activity assay

Mouse AT2 cells were seeded in 6-well plates (Density: $1x10^6$ cells/well). After 24 hours, the manufacturer's instructions were followed (Cytosolic Phospholipase A2 Assay Kit, abcam, ab133090). The read at 414 nm with reference measurement was performed using Tecan Infinite M200 PRO reader.

3.26 Statistical analysis

Statistical tests were performed using GraphPad Prism 9.1 (GraphPad Software, USA). All values were presented as Mean ± Standard Error of Mean (SEM). Statistical comparison between 2 sample groups was evaluated by Student's t-test. For 3 sample groups, one way ANOVA test was used with Tukey's post-test for the multiple comparisons. *$p<0.05$, **$p< 0.01$, and ***$p < 0.001$ values were considered significant.

4. RESULTS

4.1 Genetic ablation of HDAC9 promotes emphysema-like phenotype in the lungs of young mice

Zhang et al. reported that *Hdac9* knockout mice (HDAC9 KO mice) developed spontaneous cardiac hypertrophy only upon aging i.e. around 8-month-old (~ 34 weeks old). Thus, based on this study, we studied HDAC9 KO mice as well as WT littermates at two different age groups: young group (8-12 weeks old) and aged group (60-70 weeks old) to assess the influence of HDAC9 on lung architecture and cellular alterations.

Firstly, to investigate how HDAC9 deficiency affects the lungs of young mice, surfactant profiling, the apoptotic and proliferative status of the lungs, and stereological assessment of alveolarization were performed **(Figure 4.1 A)**. Immunostainings from serial sections of paraffin-embedded lung tissue against surfactant proteins revealed that the number of SP-A, SP-B, and SP-C positive cells tended to decrease in HDAC9 KO lungs compared to age-matched WT controls. Specifically, the number of SP-D positive cells, known to be involved in innate immune response, was significantly reduced in HDAC9 total lung **(Figure 4.1 B, C)**. Subsequently, the immunoreactivity of a proliferation marker (PCNA) decreased while apoptotic marker (caspase 3) was significantly increased in HDAC9 KO lungs **(Figure 4.1 D, E)**. Further, to investigate if HDAC9 deficiency dysregulates the lung structure and function, radial alveolar count and mean linear intercept were tested as parameters of pathological criteria in the lungs. Quantification of radial alveolar count showed a significant decrease, whereas the parameter of mean linear intercept showed a tendency to increase (**Figure 4.1 F, G**). Collectively, these results suggest that the genetic ablation of HDAC9 triggers emphysema-liked phenotype in the lung.

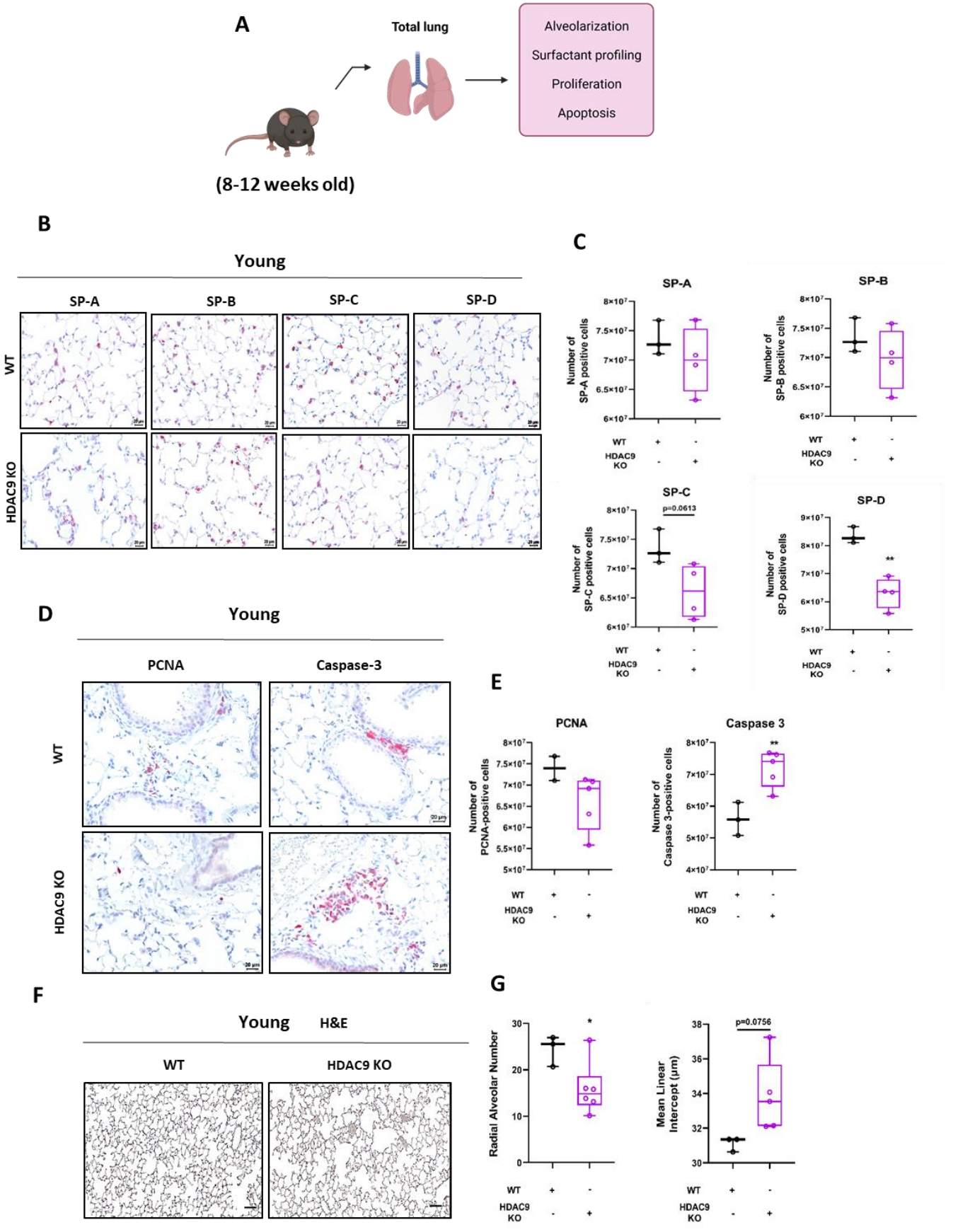

Figure 4.1: Genetic ablation of HDAC9 results in emphysema-like phenotype in the lungs of young mice. (A) Schematic experimental approach showing the investigation of surfactant protein profiling,

proliferation, apoptosis, and alveolarization in the lungs of young WT and HDAC9 KO mice. **(B)** Representative images of immunostained surfactant proteins SP-A, SP-B, SP-C, and SP-D in the lung sections from WT and HDAC9 KO mice, Scale bar=20 µm. **(C)** Quantification of SP-A, SP-B, SP-C, and SP-D positive cells in the lung sections from WT (n=3) and HDAC9 KO (n=4) mice. **(D)** Representative images for immunohistochemical detection of PCNA and caspase 3 in the lung sections from WT and HDAC9 KO mice, Scale bar=20 µm. **(E)** Quantification of PCNA and caspase 3 positive cells in the lung sections from WT (n=3) and HDAC9 KO (n=5) mice. **(F)** Representative images of hematoxylin and eosin (H&E) stained lung sections from WT and HDAC9 KO mice, Scale bar=20 µm. (G) Quantification of radial alveolar number and mean linear intercept assessment of WT (n=3) and HDAC9 KO (n=5) mice. *P < 0.05, **P < 0.01 compared with WT.

4.2 In young mice genetic ablation of HDAC9 reprograms alveolar type II cells to mesenchymal-like phenotype

AT2 cells were isolated from WT and HDAC9 KO animals based on negative bead selection and cultured for 48 hours to precisely delineate phenotypic alterations mediated by HDAC9 **(Figure 4.2 A)**. Immunostaining of SP-C and DAPI revealed HDAC9 KO-AT2 cells lost SP-C expression compared to age-matched WT controls **(Figure 4.2 B)**. Following, co-immunostaining of E-cadherin and Vimentin indicated that HDAC9 KO-AT2 cells undergo the epithelial-mesenchymal transition (EMT) **(Figure 4.2 C)**. Altogether, these results indicate that genetic ablation of HDAC9 leads to loss of epithelial cell signature including cell polarity and cell-cell adhesion by directing into EMT process.

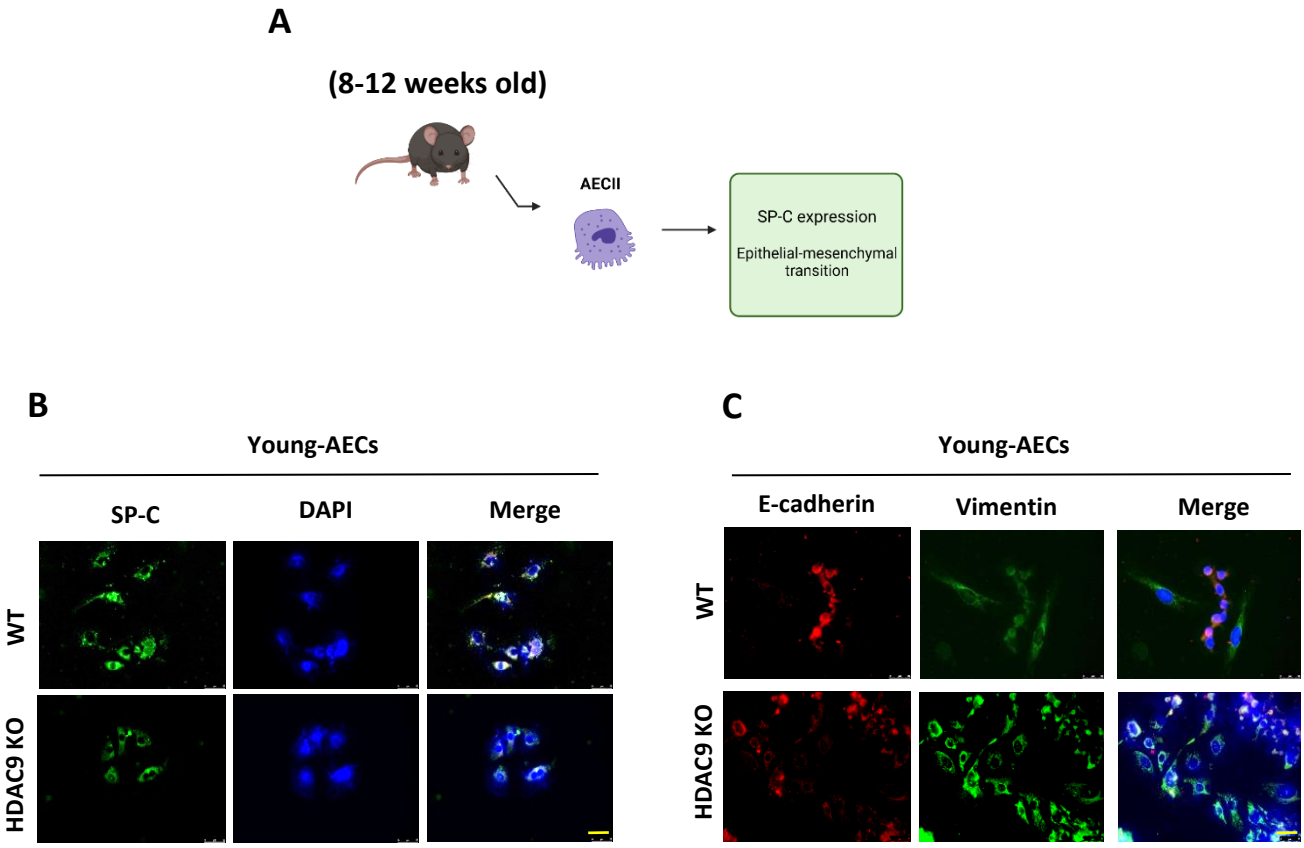

Figure 4.2: Genetic ablation of HDAC9 reprograms alveolar type II cells to mesenchymal-like phenotype. (A) Schematic experimental approach showing the assessment of SP-C expression and epithelial-mesenchymal transition in isolated alveolar type II (AT2) cells. **(B)** Representative immunofluorescence images of AT2 cells isolated from WT and HDAC9 KO mice. AT2 cells stained with SP-C (green) and nuclei counterstained with DAPI (blue). Scale bar=25 µm. The images are representative of n=3 WT and n=3 HDAC9 KO mice-AT2 cells. **(C)** Representative immunofluorescence images of AT2 cells isolated from WT and HDAC9 KO mice. AT2 cells stained with E-cadherin (red), Vimentin (green), and nuclei counterstained with DAPI (blue). Scale bar=25 µm. The images are representative of n=3 WT and n=3 HDAC9 KO mice-AT2 cells.

4.3 Genetic ablation of HDAC9 in the lungs of young mice contributes to the development of premature aging signature via upregulation of p21 and p16

To investigate the senescence-like changes in genetically HDAC9-ablated young mice, immunostainings against senescence markers, p21 and p16, were performed from serial sections of paraffin-embedded lung tissues. HDAC9 KO young mice showed an increasing

trend of both senescence markers compared to WT control mice **(Figure 4.3 A-C)**. These results suggest that HDAC9 deficiency is linked to initiation of premature senescence.

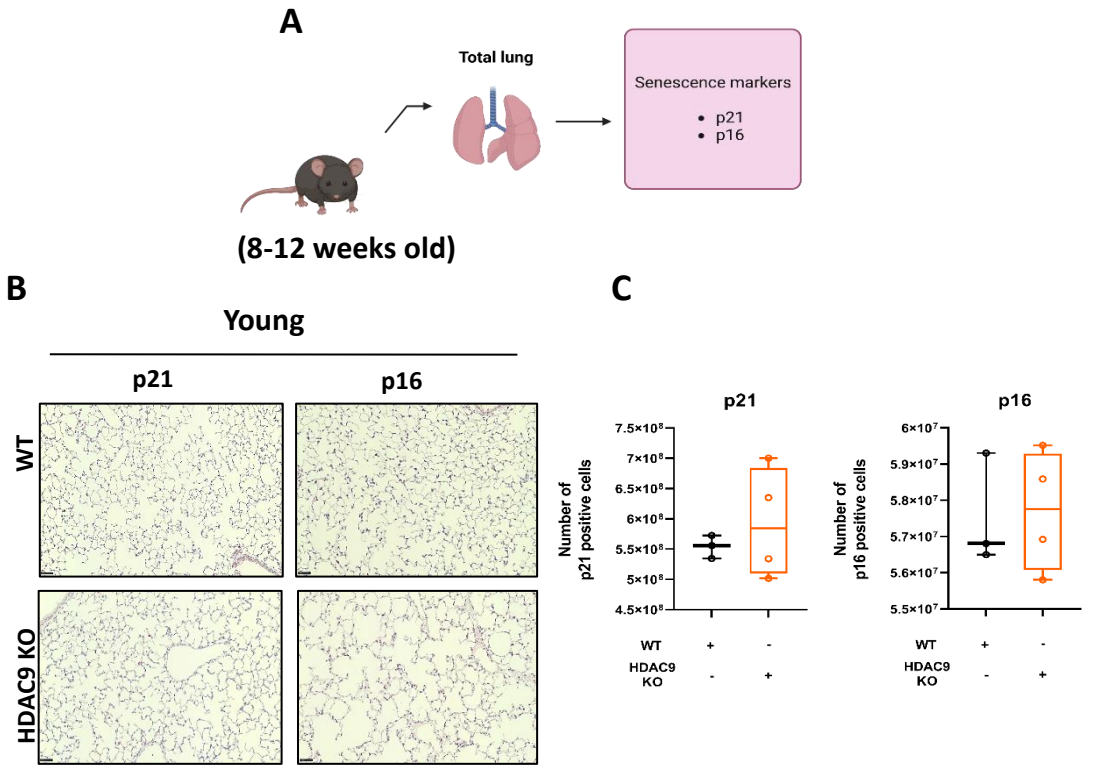

Figure 4.3: Genetic ablation of HDAC9 results in upregulation of senescence markers in the lungs of young mice. (A) Schematic experimental approach showing the investigation of the senescence markers in the total lungs. **(B)** Representative images of immunostained p21 and p16 proteins in the lung sections from WT and HDAC9 KO mice, Scale bar=50 µm. **(C)** Quantification of p21 and p16 positive cells in the lung sections from WT (n=3) and HDAC9 KO (n=4) mice. No significance, compared with WT.

4.4 Genetic ablation of HDAC9 promotes the development of cellular senescence and senescence-associated secretory phenotype (SASP)

To understand how Hdac9 is altered upon aging and how the HDAC9 deficiency alters the SAS-phenotype in AT2 cells. AT2 cells were isolated from 3 different age groups of WT mice: (i) young mice: 8-12 weeks old, (ii) aged mice group I: 34 weeks old, and (iii) aged mice group: 60 weeks old) **(Figure 4.4 A)**. Here, HDAC9 protein expression was confirmed to be reduced drastically during aging **(Figure 4.4 B)**. Further, to investigate the sign of replicative senescence, telomere length was measured in AT2 cells isolated from young age group WT and HDAC9 KO mice and this confirmed that HDAC9 deficiency points out potential DNA damage

response **(Figure 4.4 C)**. Following, co-immunostaining of p21 and HDAC9 was performed in isolated AT2 cells obtained from WT and HDAC9 KO mice. p21 expression was significantly higher when HDAC9 was deficient **(Figure 4.4 D)**. Furthermore, we assessed another common method of cellular senescence by staining isolated AT2 cells with β-galactosidase (β-GAL) activity at pH 6.0, a histochemical assay that is called "senescence-associated β-GAL" (SA-β-GAL). In accordance with p21, this marker was also highly expressed in HDAC9 KO-AT2 cells compared to WT-AT2 cells **(Figure 4.4 E)**. Lastly, mRNA expression profiling of SASP factors revealed the significant upregulation of *Mmp3* and *Cdkn1a* along with the increased trend of pro-inflammatory cytokines (*Il6* and *Il1a*) in HDAC9 KO-AT2 cells **(Figure 4.4 F)**. Collectively, these results suggest that genetic ablation of HDAC9 in AT2 cells leads to senescence-associated secretory phenotype.

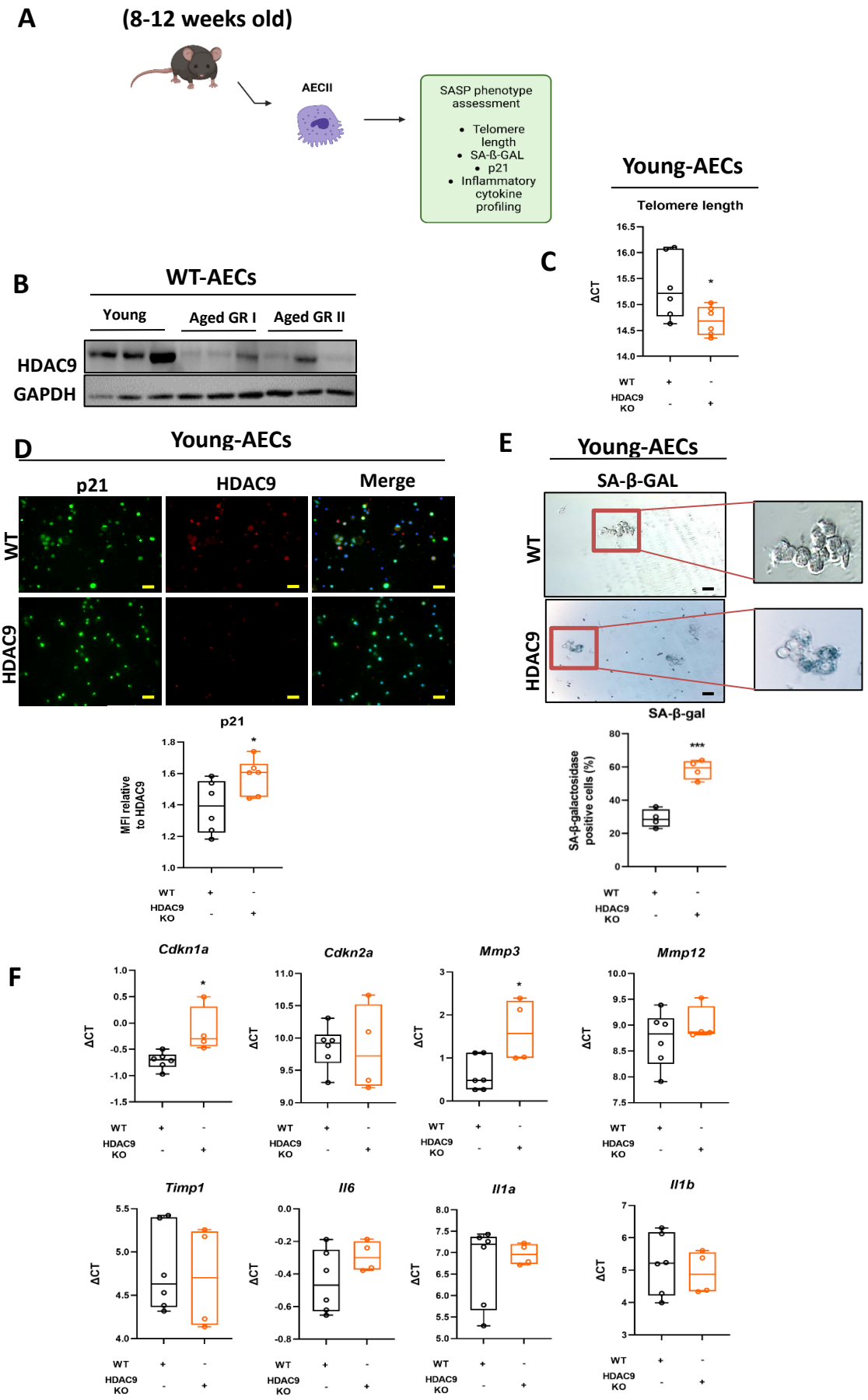

Figure 4.4: In young mice, genetic ablation of HDAC9 in AT2 cells leads to senescence-associated secretory phenotype. (A) Schematic experimental approach evaluating SASP factors in the isolated

AT2 cells. **(B)** Western blotting analysis of HDAC9 and GAPDH (loading control) in isolated AT2 cells from WT mice for 3 different age groups; n= 3 biological replicates per group. **(C)** Relative mRNA expression of telomere length in AT2 cells isolated from WT and HDAC9 KO mice; n=3 biological replicates, 2 technical replicates. **(D)** Representative immunofluorescence images of AT2 cells isolated from WT and HDAC9 KO mice. AT2 cells stained with p21 (green), HDAC9 (red), and nuclei counterstained with DAPI (blue). Scale bar=25 µm. Quantification of the mean fluorescence intensity (MFI) of p21 in AT2 cells isolated from WT and HDAC9 KO mice; n=6 biological replicates. **(E)** Representative images of senescence-associated beta-galactosidase (SA-β-gal) stainings in the isolated AT2 cells from WT and HDAC9 KO mice. Scale bar=25 µm. Quantification of SA-β-gal positive cells in AT2 cells; n=4 biological replicates per group. **(F)** Relative mRNA expression of SASP factors (*Cdkn1a*, *Cdkn2a*, *Mmp3*, *Mmp12*, *Timp1*, *Il6*, *Il1a*, *Il1b*) in AT2 cells isolated from WT and HDAC9 KO mice; n=2-3 biological replicates, 2 technical replicates. *P < 0.05, *** P < 0.001 compared with WT.

4.5 Genetic ablation of HDAC9 with aging drives emphysema-like phenotype in the lung

To determine the functional role of HDAC9 deficiency on chronological aging, 60-70 weeks old WT and HDAC9 KO mouse lungs were evaluated for surfactant profiling, apoptotic and proliferative status, as well as stereological assessment of alveolarization **(Figure 4.5 A)**. Immunostainings from serial paraffin lung sections against surfactant proteins revealed that the number of SP-C positive cells was significantly reduced in HDAC9 KO lungs. Even though SP-A and SP-D-positive cells had the tendency to be decreased, they did not show statistical differences between the compared groups. Interestingly, SP-B-positive cells were detected to be elevated in HDAC9 KO lungs versus WT controls **(Figure 4.5 B, C)**. Further, HDAC9 KO lungs showed decreased proliferation and increased apoptosis compared to age-matched controls **(Figure 4.5 D, E)**. In addition, radial alveolar count and mean linear intercept were tested. Quantification of radial alveolar count showed a significant decrease, whereas the parameter of mean linear intercept was significantly increased (**Figure 4.5 F, G**). Collectively, these results suggest that genetic ablation of HDAC9 upon aging worsens the lung structure and shows emphysema-liked phenotype in the lung.

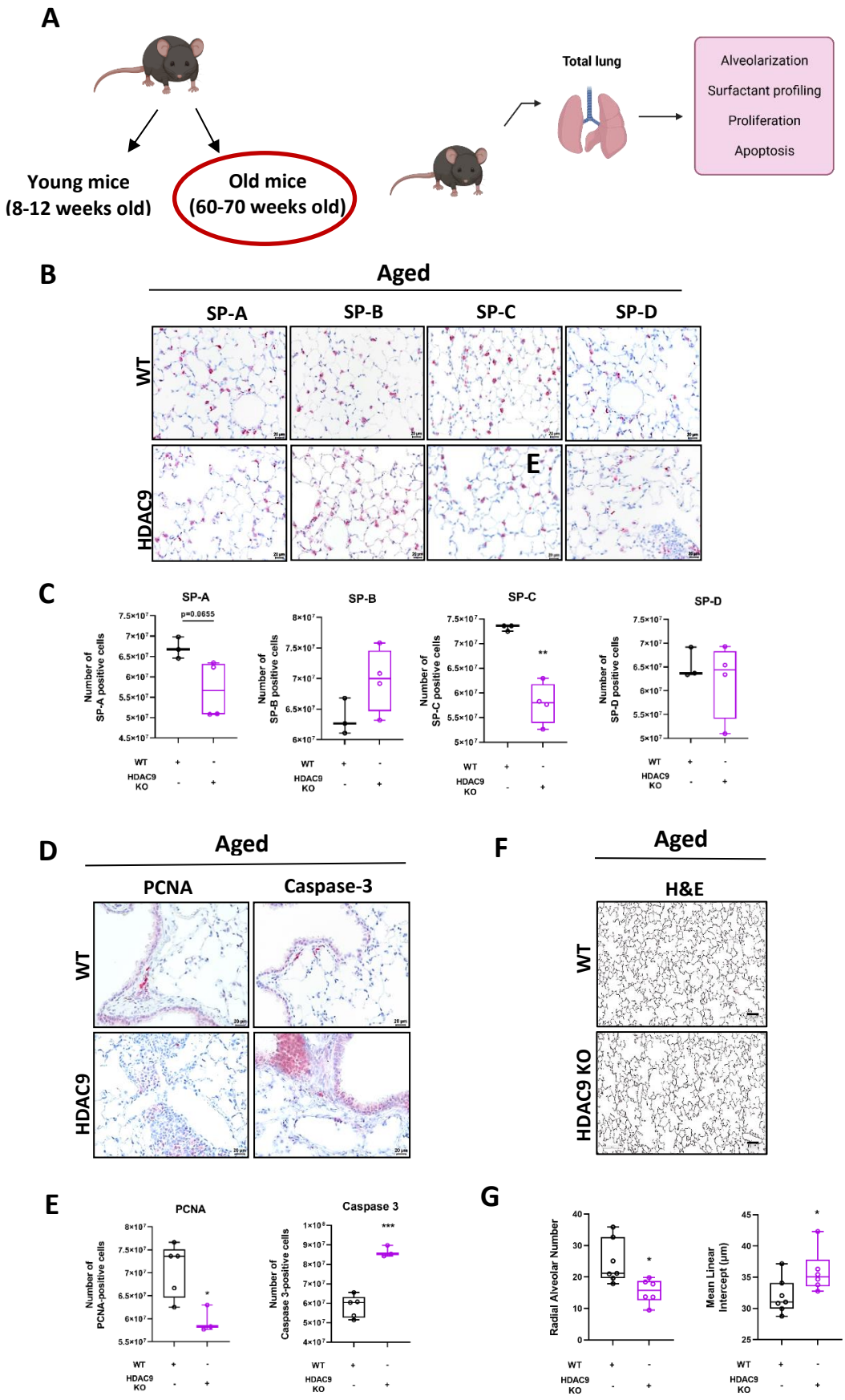

Figure 4.5: Aged HDAC9 KO mouse lungs display deteriorated lung structure along with emphysema-like phenotype. (A) Schematic experimental approach showing the investigation of

surfactant profiling, proliferation, apoptosis, and alveolarization in the aging total lungs. **(B)** Representative images of immunostained surfactant proteins A, B, C, and D in the lung sections from aged WT and HDAC9 KO mice, Scale bar=20 µm. **(C)** Quantification of SP-A, B, C, and D positive cells in the lung sections from aged WT (n=3) and HDAC9 KO (n=4) mice. **(D)** Representative images for immunohistochemical detection of PCNA and caspase 3 in the lung sections from aged WT and HDAC9 KO mice, Scale bar=20 µm. **(E)** Quantification of PCNA and caspase 3 positive cells in the lung sections from aged WT (n=5) and HDAC9 KO (n=3) mice. **(F)** Representative images of hematoxylin and eosin (H&E) stained lung sections from aged WT and HDAC9 KO mice, Scale bar=20 µm. (G) Quantification of radial alveolar number and mean linear intercept assessment of aged WT (n=7) and HDAC9 KO (n=6) mice. *P < 0.05, **P < 0.01, ***P < 0.001 compared with WT.

4.6 Genetic ablation of HDAC9 with aging promotes the expression of senescence markers

To study the senescence response in HDAC9-ablated aged lungs, immunostainings for p21 and p16 were performed from paraffin lung sections. The number of p21-positive cells did not show any significant change but the number of p16-positive cells displayed a higher count in aged HDAC9 KO mice vs WT control mice **(Figure 4.6 A-C)**. These results suggest that HDAC9 deficiency upon old age enhances senescence response in the lung compared to their WT old age mice.

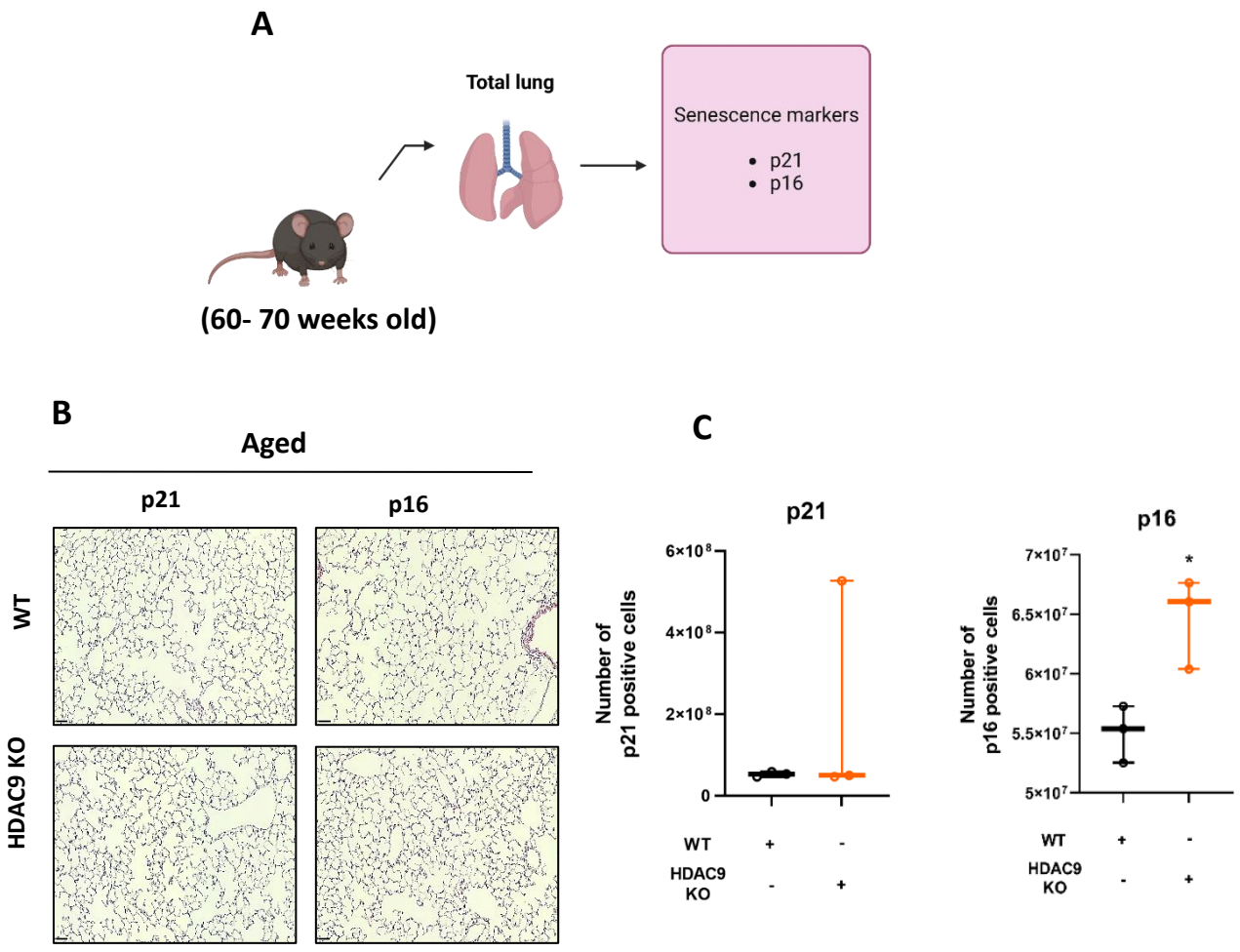

Figure 4.6: Aged HDAC9 KO mice exhibit an increased expression of senescence marker, p16. (A) Schematic experimental plan showing the evaluation of the senescence markers in the aged total lungs. **(B)** Representative images of immunostained p21 and p16 proteins in the lung sections from aged WT and HDAC9 KO mice, Scale bar=50 µm. **(C)** Quantification of p21 and p16 positive cells in the lung sections from aged WT (n=3) and HDAC9 KO (n=3) mice. *P < 0.05 compared with WT.

4.7 AT2 cells isolated from aged HDAC9 KO mice demonstrates aggravated SASP

To study the effect of chronological aging upon HDAC9 deficiency on the cellular level, SASP-related factors were planned to check in isolated AT2 cells **(Figure 4.7 A)**. The number of SA-β-GAL-positive cells was higher in aged HDAC9 KO-AT2 cells compared to age-matched controls **(Figure 4.7 B)**. In addition, mRNA expression profiling of SASP-associated genes revealed the significant upregulation of *Cdkn1a*, *Il6*, *Il1b*, and *iNOS* in HDAC9 KO-AT2 cells **(Figure 4.7 C)**. Similar to the results from young mice, aged HDAC9 KO-AT2 cells displayed higher apoptotic response and reduced proliferation capacity compared to their WT age group AT2 cells **(Figure 4.7 D)**. Collectively, these results in concordance with young mice confirm that HDAC9 deficiency in aged AT2 cells worsens SASP, which is already initiated at young age.

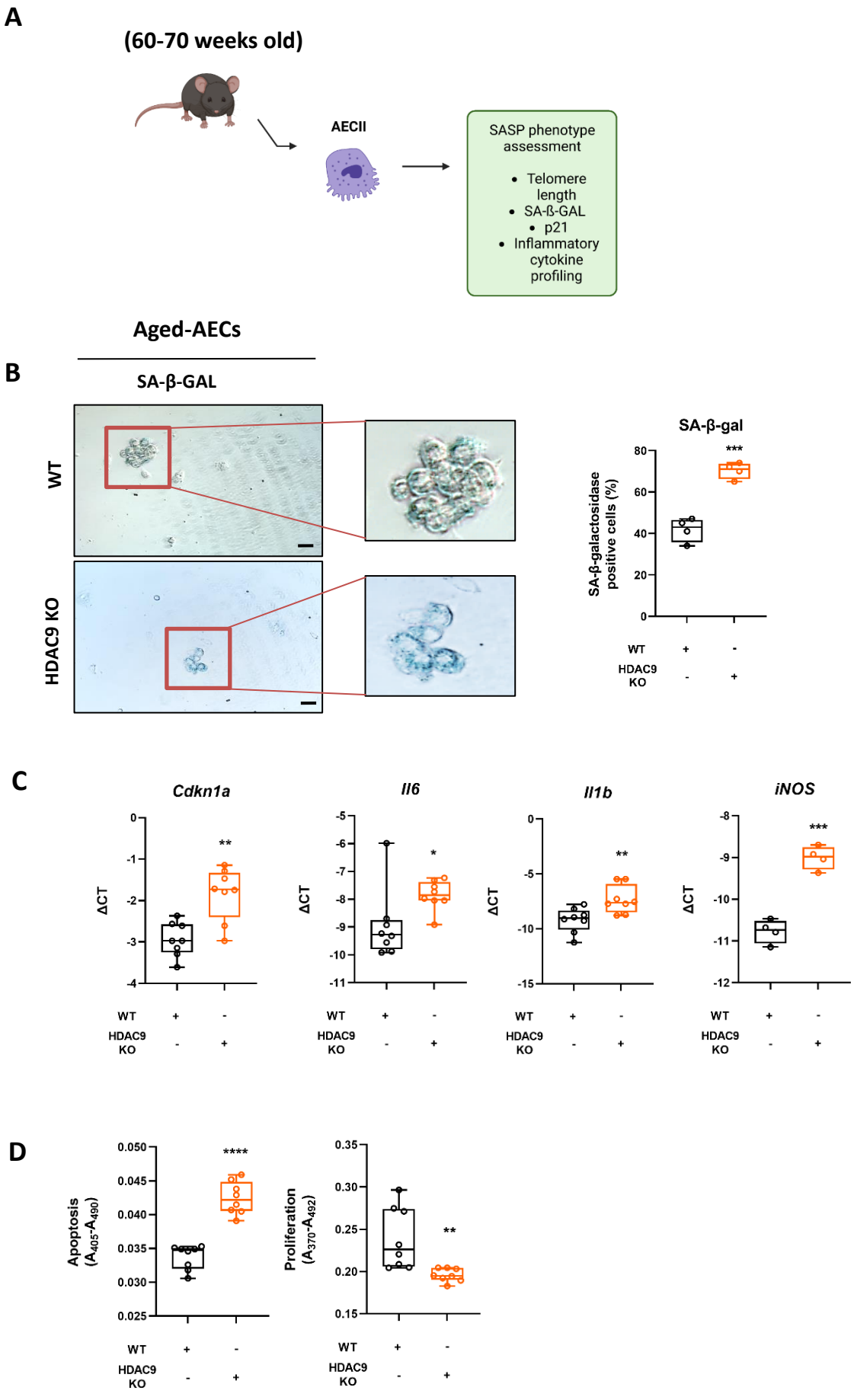
A
(60-70 weeks old)
AECII
SASP phenotype assessment
Telomere length
SA-ß-GAL
p21
Inflammatory cytokine profiling
B
Aged-AECs
SA-β-GAL
WT
HDAC9 KO
SA-β-gal
SA-β-galactosidase positive cells (%)
***
WT
HDAC9 KO
C
Cdkn1a
Il6
Il1b
iNOS
ΔCT
**
*
**
***
D
Apoptosis (A405-A490)
Proliferation (A370-A492)
****
**

Figure 4.7: AT2 cells isolated from aged HDAC9 KO mouse lungs display aggravated senescence-associated secretory phenotype. (A) Schematic experimental approach evaluating SASP factors in the isolated AT2 cells from aged mice. **(B)** Representative images of senescence-associated beta-galactosidase (SA-β-gal) stainings in the isolated AT2 cells from aged WT and HDAC9 KO mice. Scale bar=25 µm. Quantification of SA-β-gal positive cells in aged AT2 cells; n=4 biological replicates per group. **(C)** Relative mRNA expression of SASP factors (Cdkn1a, Il6, Il1b, iNOS) in AT2 cells isolated from aged WT and HDAC9 KO mice; n=2-4 biological replicates, 2 technical replicates. **(D)** Quantification of apoptosis and proliferation in AT2 cells (n=4-7 biological replicates, 2 technical replicates). *P < 0.05, **P < 0.01, ***P < 0.001 compared with WT.

4.8 HDAC9 deficient aged lungs display the altered abundance of epithelial cells of subpopulations

Flow cytometry protocol using 25 different fluorochromes, was performed to identify the cell population changes and their molecular signature in lung samples of aged WT and HDAC9 KO mice. In the analysis, $CD45^+$ and $CD44^+$ cell populations were separated based on a gating strategy along with subdivision of $CD117^+$ and $EpCam^+$ cells. While $CD117^+$ epithelial cells showed 14% of reduction, $EpCam^+$ cells showed 3% of reduction in HDAC9 KO mice **(Figure 4.8 A)**. Interestingly, the total abundance of $CD45^-$cells was significantly increased in HDAC9 KO mice versus WT controls. On the other hand, we observed that fibroblasts, vascular smooth muscle cells (VSMCs), lymphatic endothelial cells (LECs), and vascular endothelial cells (VECs) obtained from HDAC9 KO mice displayed higher abundance, whereas the only epithelial cell population seemed to be affected and reduced **(Figure 4.8 B, C)**.

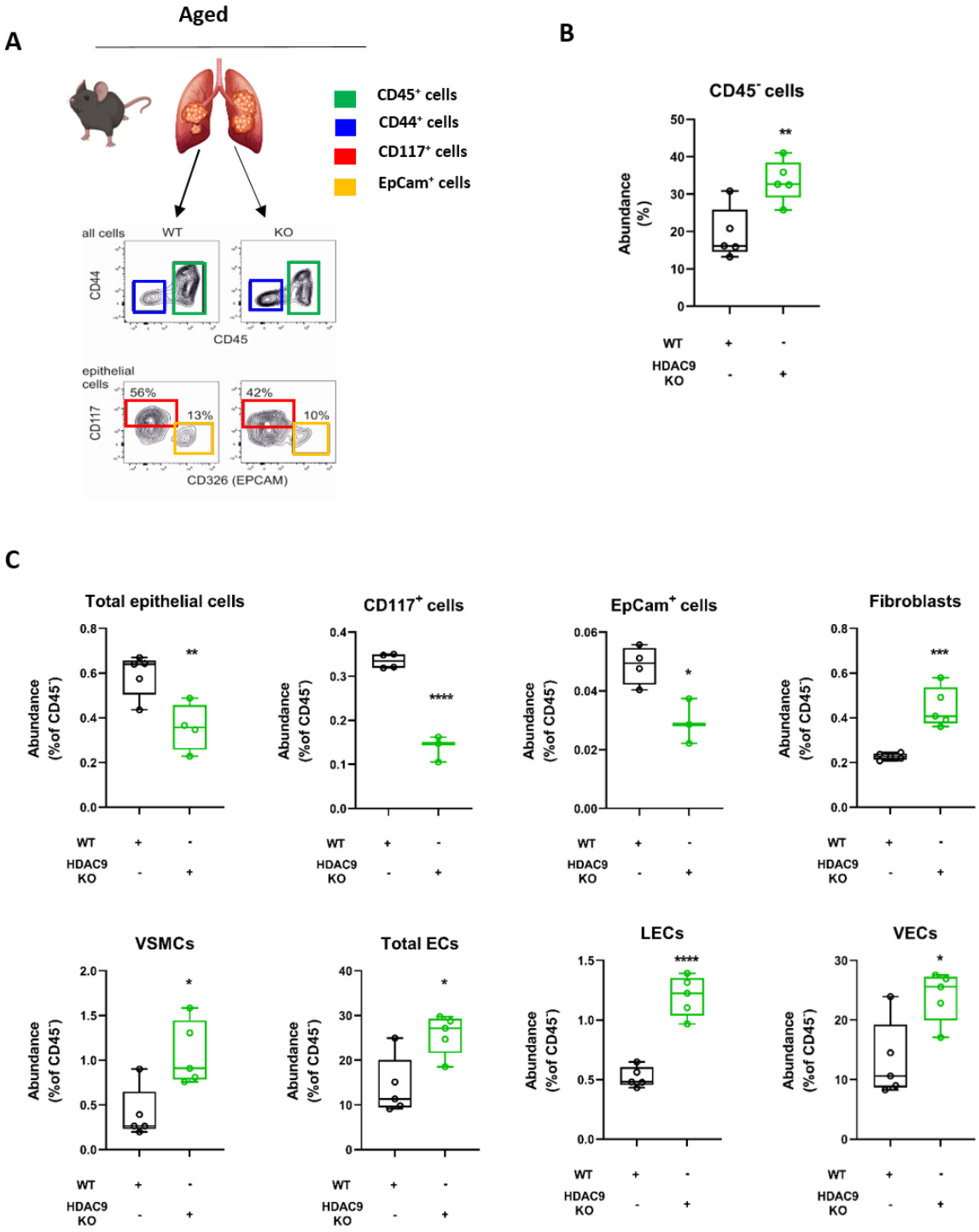

Figure 4.8: Aged HDAC9 KO mouse lungs display reduced only the abundance of the epithelial cell population. (A) Representative FACS plotting demonstrating $CD45^+$, $CD44^+$ ($CD45^-$), $CD117^+$, and $EpCam^+$ cells in freshly isolated total lungs from aged WT and HDAC9 KO mouse lungs (n=5 per group). **(B)** Percentage of $CD45^-$ cells abundance in aged WT and HDAC9 KO mouse lungs; n=5. **(C)** Percentage of total epithelial cells including $CD117^+$ and $EpCam^+$ epithelial cells, fibroblasts, vascular smooth muscle cells (VSMCs), and total endothelial cells (Ecs) including lymphatic endothelial cells

(LECs) and vascular endothelial cells (VECs) within CD45- population; n=3-5. *P < 0.05, **P < 0.01, ***P < 0.001, ****P < 0.0001 compared with WT.

4.9 HDAC9 deficient aged lungs display enhanced adaptive immune responses

As previous data sets pointed out towards heightened inflammatory response as a part of SASP, FACS analysis also confirmed that aged HDAC9 KO mice undergo dysregulated inflammatory response. Even though the total population of $CD45^+$ cells in HDAC9 KO mice significantly decreased, $CD8^+$ T (increase by %6) cells were enriched within $CD45^+$ population in HDAC9 KO mice versus WT control **(Figure 4.9 A, B)**. Importantly, we have observed an increase of total T cell and B cell abundance as well as $CD8^+$ T cells and $CD8^+/CD4^+$ T cell ratio in HDAC9 KO mice, whereas interstitial macrophages were decreased **(Figure 4.9 C)**. Altogether, these results suggest there is an imbalance of healthy inflammatory response and chronic adaptive immunity is dominantly in charge of the inflammatory response through enriched T and B cells in aged HDAC9 KO mouse lungs.

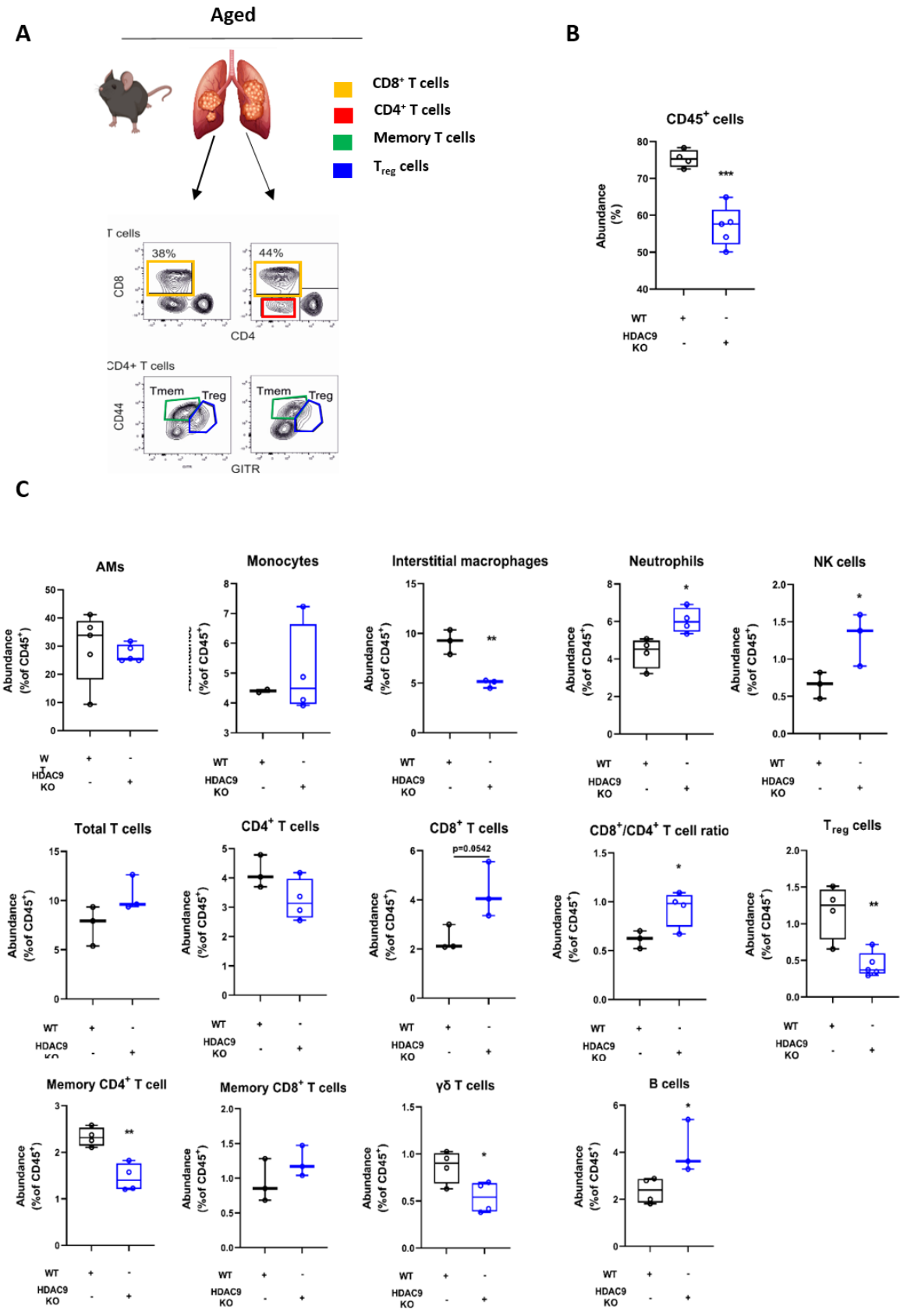

Figure 4.9: Aged HDAC9 KO mouse lungs display enhanced T and B-cell responses. (A) Representative FACS plotting demonstrating $CD8^+$, $CD4^+$, memory T cells, and regulatory T (Treg) cells in freshly isolated lungs from WT (n=4) and HDAC9 KO mice (n=5). **(B)** Percentage of $CD45^+$

cells abundance in aged WT (n=4) and HDAC9 KO mice (n=5). **(C)** Percentage of alveolar macrophages (AMs), monocytes, interstitial macrophages, neutrophils, natural killer (NK) cells, total T cells including $CD8^+$, $CD4^+$, $CD8^+/CD4^+$ ratio, Treg, memory $CD8^+$ T cells, $CD4^+$ T cells, γδT cells and B cells within $CD45^+$ population; n=3-5. *P < 0.05, **P < 0.01, ***P < 0.001, compared with WT.

4.10 Genetic ablation of HDAC9 leads to inflammatory phenotype via BALT formation during aging

To investigate the effect of aging upon HDAC9 ablation over lung characteristics, a histopathological examination was performed with hematoxylin and eosin (H&E) stainings from young and aged mice paraffin blocks. H&E-stained lung sections revealed the forming of inflamed regions in aged HDAC9 KO mice versus age-matched WT control mice as well as young mice groups (**Figure 4.10 A**). Bronchus-associated lymphoid tissue (BALT) does not form in the normal lung but is present in different diseases. To understand which cell population is located within BALT formation, immunofluorescence stainings were performed. As shown in **Figure 4.10 B**, these inflamed regions in HDAC9 KO lungs contained heavily immune cells rather than pancytokeratin-positive cells, which indicated there was no tumor formation. In fact, these regions displayed a dominant T cell recruitment with a little proportion of macrophages, and B cell population was not detected within BALT formation. Collectively, these results suggest HDAC9 ablation leads to inflammatory lung phenotype once the aging hits and inflamed regions consist of T cells and macrophages.

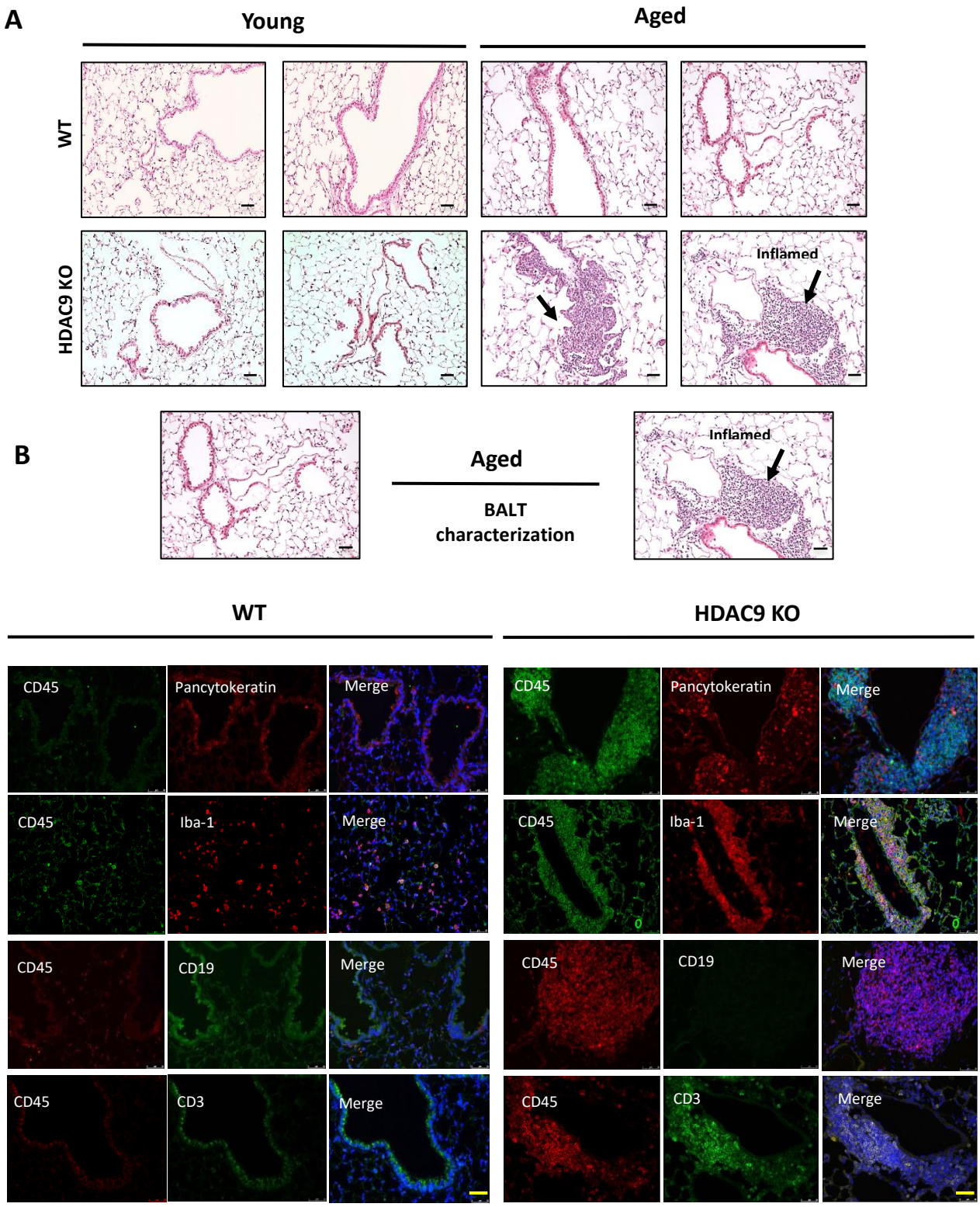

Figure 4.10: Aging upon genetic ablation of HDAC9 promotes lung inflammation via iBALT formation. (A) Representative pictures of hematoxylin and eosin (H&E) stained sections from young and aged WT and HDAC9 KO mice; n=8 per group. Scale bar= 20 µm. **(B)** Representative immunofluorescence images of tissue sections from WT and HDAC9 KO mice. The sections stained with CD45 (all hematopoietic cells marker, green), pancytokeratin (red), Iba1 (macrophage marker, red),

CD19 (B cell marker, green), CD3 (T cell marker, green), and nuclei counterstained with DAPI (blue). Scale bar=50 µm. n=6 biological replicates per group.

4.11 HDAC9-mediated transcriptional regulation of metabolic pathways upregulates with aging

To identify the molecular mechanisms underlying the phenotypic alterations in AT2 cells isolated from the aged HDAC9 deficiency mice, RNA and ATAC-sequencing were performed **(Figure 4.11 A)**. For RNA-sequencing, AT2 cells from 2 advanced age mice were used: (i) 60 weeks old, and (ii) 70 weeks old. As shown in **Figure 4.11 B** from 60-week-old mice, the genes involved in lysosomal degradation, RNA polymerase II regulation, proteosome, cysteine/glutamate transporter pathway, and inositol phosphate metabolic pathway were upregulated in HDAC9 KO-AT2 cells versus WT controls. The same analysis also revealed that the genes coding metalloproteinases, enzymes responsible for cytochrome, and receptors for ubiquitine ligase substrate were downregulated in HDAC9 KO-AT2 cells. In addition, gene set enrichment analysis identified the imbalance of catabolism and anabolism of metabolites **(Figure 4.11 B, C)**. As regards 70-week-old mice, RNA sequencing revealed upregulated gene expression linked to phospholipid enzymes, cysteine/glutamate receptors, and metalloproteinases in HDAC9 KO-AT2 cells versus WT controls. Importantly, *Pla2g12b*, phospholipase A family enzyme, was striking as one of the most upregulated targets. Moreover, the reactome analysis identified sialic acid metabolism, purine metabolism, and glycerophospholipid biosynthesis as the most enriched pathways in HDAC9 KO-AT2 cells **(Figure 4.11 D, E)**. Collectively, these data suggest that the metabolic pathways are majorly regulated in aged HDAC9 KO mouse lungs.

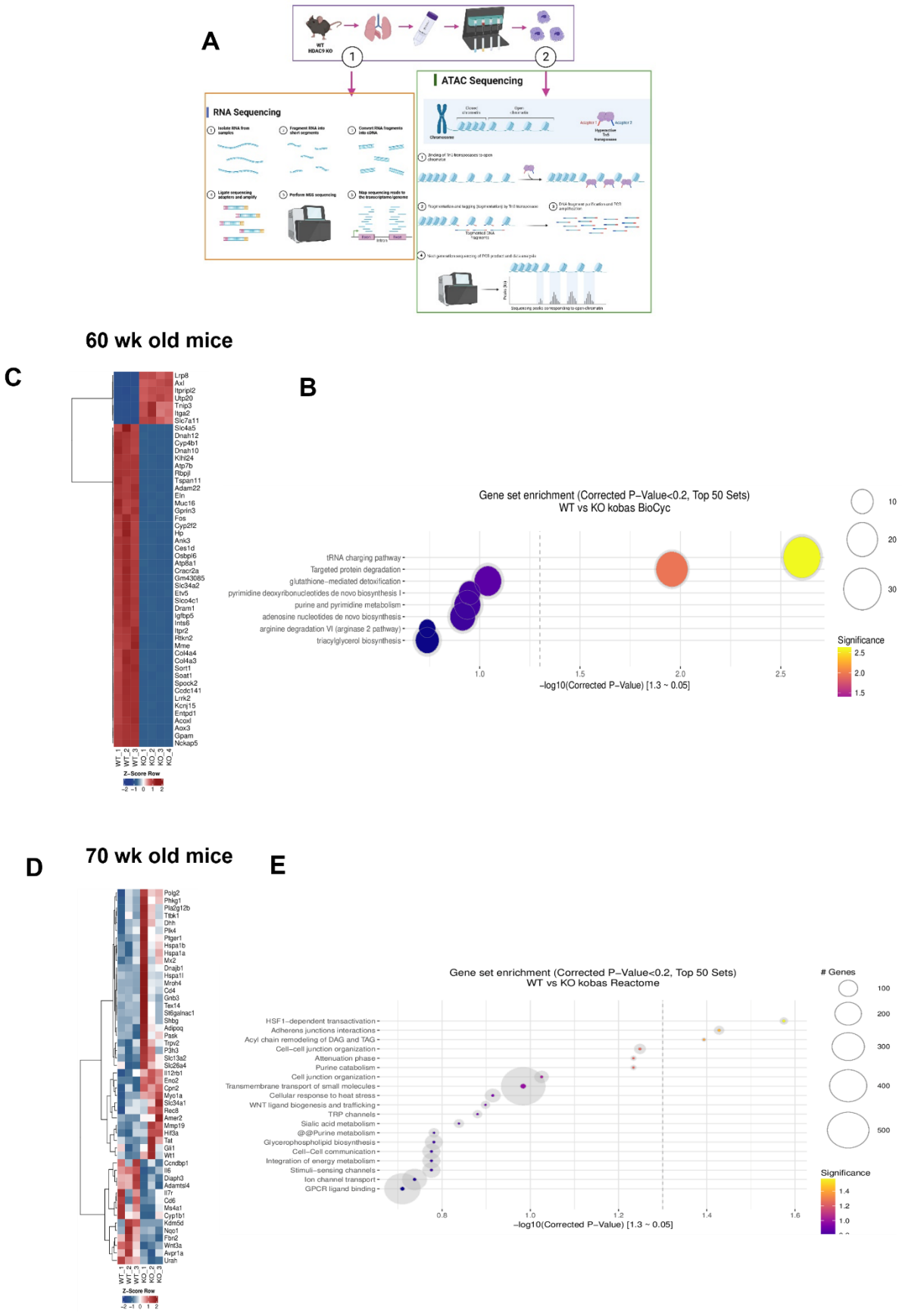

Figure 4.11: RNA Sequencing in HDAC9 KO-AT2 cells from 2 groups of advanced age identifies major regulation of metabolic pathways. (A) Schematic experimental approaches showing the

isolation of AT2 cells from WT and HDAC9 KO mice concerning RNA and ATAC-Sequencings. **(B, C)** While heatmap displays the differentially expressed genes, pathway analysis reveals mitochondrial metabolic pathways concerning biosynthesis and degradation of the metabolites are affected in 60 weeks-old WT (n=3) and HDAC9 KO (n=4) mice. **(D, E)** While heatmap displays the differentially expressed genes, pathway analysis reveals metabolic pathways including glycerophospholipid synthesis are affected in 70 weeks-old WT (n=3) and HDAC9 KO (n=3) mice.

4.12 Foot-printing of HDAC9-mediated transcriptional factors elucidates chromatin accessibility of lipid metabolism-related gene promoters in aged HDAC9 KO mice

HDAC9 is an enzyme known to induce histone deacetylation to block gene transcription by targeting the promoter regions as a scaffold factor in the transcriptional co-repressor complex. We performed ATAC-sequencing analysis to find how HDAC9 in aged AT2 cells affects the chromatin structure and interacts with which transcription factors (TFs) involved in metabolic pathway genes, which were identified to be upregulated in RNA-sequencing. Firstly, ATAC-sequencing revealed a change in *cis*-regulatory elements including promoters and enhancers in HDAC9 KO-AT2 cells. Assigned peaks to open and closed chromatin regions were represented in pie charts. As shown in **Figure 4.12 A**, around 17% of the peaks for open regions and around 38% of the peaks for closed regions are within promoters in HDAC9 KO-AT2 cells. Peak annotation analysis via KEGG aligned with phospholipase and ERK1/2 cascade as the most enriched peaks in HDAC9 KO-AT2 cells **(Figure 4.12 B)**. The foot-printing of the transcription factor binding site (TFBS) motifs was provided by TOBIAS analysis to predict TFs and their binding sites within the promoters. As shown in **Figure 4.12 C and D**, CEBPE, CEBPB, CEBPG, and NFE2 showed the highest binding score of TFBS within promoters in HDAC9 KO-AT2 cells. Interestingly, these TFs are known to bind to the promoter of gene family called PLA2 (phospholipase A2 family). This data set specifically confirmed the lack of HDAC9-mediated repressive response directly interacts with TFs involved in phospholipase family genes, also detected in RNA-sequencing obtained from 70-week-old HDAC9 KO-AT2 cells. Collectively, these results suggest there was an alteration of lipid metabolism-related chromatin accessibility with aging upon genetic ablation of HDAC9.

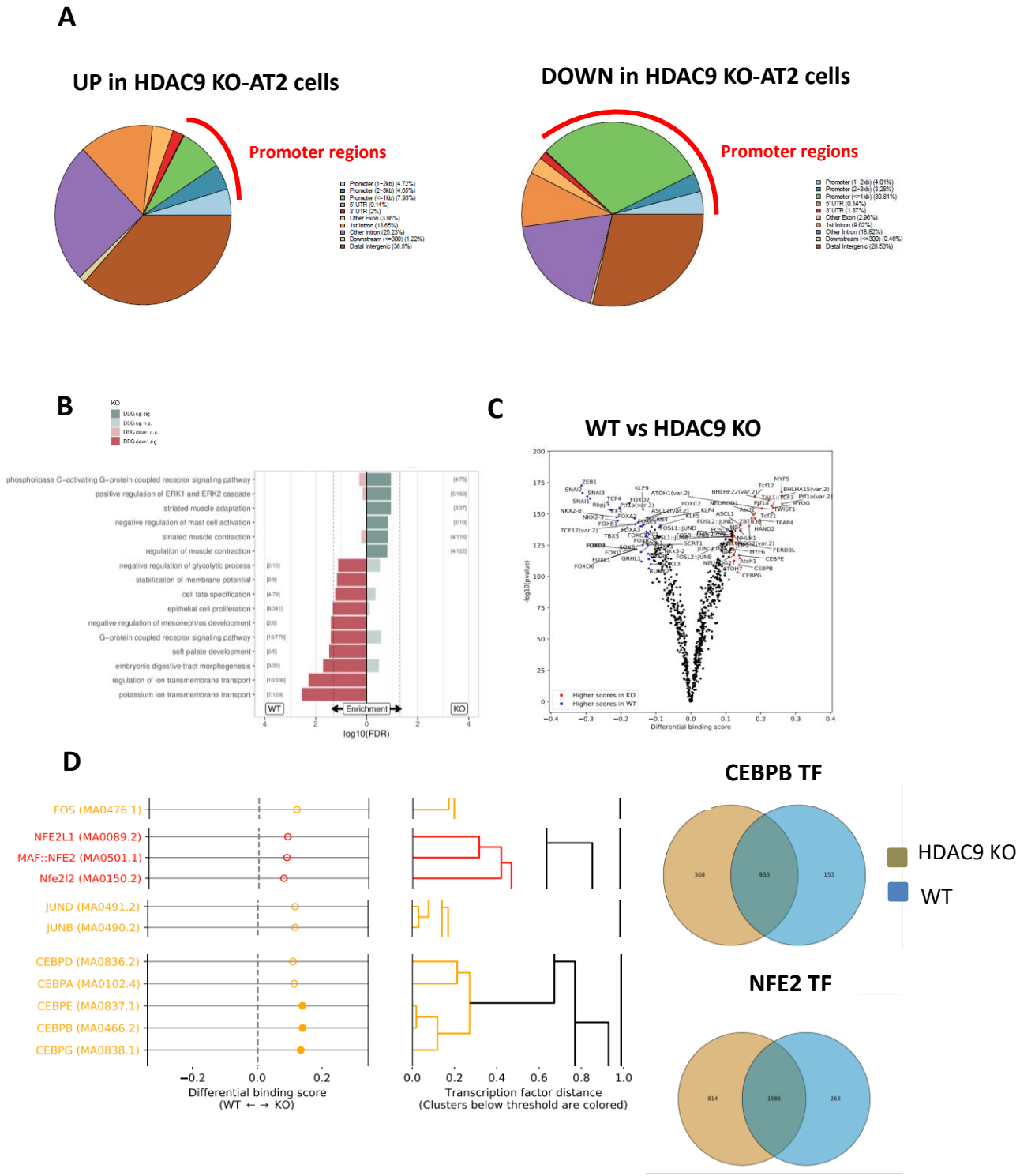

Figure 4.12: ATAC Sequencing elucidates chromatin accessibility of lipid metabolism-related gene promoters in aged HDAC9 KO mice. (A) The pie charts display all potential on and off-binding sites overlapping with promoter regions of protein- coding genes as well as intronic and exonic chromosomal regions in HDAC9 KO-AT2 cells. **(B)** Pathways analysis shows significantly enriched gene sets in WT and HDAC9 KO-AT 2 cells. **(C)** The volcano plot of pairwise comparison of transcription factors (TFs) between WT and HDAC9 KO-AT2 cells shows the differentially binding activity based on -log10 (p value) provided by TOBIAS analysis. Each dot represents one investigated TF motif; specific TFs for HDAC9 KO-AT2 are labeled in red, specific TFs for WT-AT2 are in blue. **(D)** The positions of NFE and CEBPB transcription factors are highlighted in WT-AT2 vs. HDAC9 KO-AT2 cells as tree and pie chart displays. Clusters of investigated TF motifs based on overlapping of

binding-sites are shown. Global TF clusters considering TF binding location are represented as excerpts and individual TFs are highlighted as rows. The trees of the differential binding score and TF distance display the genomic positional place of each TF binding site. 0.2 as tree depth represents 80% of the overlapping motifs. Clusters of TFs (indicated by unique IDs) overlapping more than 50% are colored in red/orange; (n=2 per group).

4.13 Aging with HDAC9 deficiency leads to metabolic modulation of choline pathway in AT2 cells

As RNA and ATAC-sequencing data sets suggest the regulation of the phospholipids upon HDAC9 deficiency in AT2 cells, we performed metabolic profilings of choline phospholipid metabolites and phospholipids resulting in free fatty acid metabolites. AT2 cells from young and aged WT and HDAC9 KO mice were isolated based on negative bead selection and cultured for 48 hours in an air-liquid interface system. After 48 hours, supernatant and cell lysates were collected. Targeted metabolic pathway analysis was performed through LC-MS/MS **(Figure 4.13 A)**. A total of 19 metabolites were detected and quantified from cell lysate samples of young mice-AT2 cells. The most abundant phospholipids including choline and glycerophosphocholine were identified within cell lysates. However, there was no significant change between WT vs HDAC9 KO-AT2 cells as well as the other detected amino acids **(Figure 4.13 B, C)**. On the other hand, from aged AT2 cells, a total of 29 metabolites were detected and quantified. Normally, choline is converted into phosphocholine (PC) and PC metabolizes CDP-Choline into phosphatidylcholine (PtdCho) and subsequently, glycerophosphocholine (GPC). As shown in **Figure 4.13 D and E**, levels of phosphorylcholine, the functional group of PC, and GPC (5x higher than young mice) were significantly reduced in HDAC9 KO-AT2 cells versus WT, whereas choline levels remain unaltered. In addition, ornithine can be metabolized into glutamate and we observed elevated levels of glutamate (10x higher than young mice) while ornithine was reduced in HDAC9 KO-AT2 cells. Folate and sarcosine, as players of folate-mediated one-carbon metabolism, were decreased in HDAC9 KO-AT2 cells compared to WT-AT2 cells. These metabolites are important to the choline oxidation pathway in mitochondria. Since choline depletion is linked to amino acid metabolism, glycine (5x higher than young mice) and leucine-isoleucine level were reduced as a consequence in HDAC9 KO-AT2 cells. Lastly, there was a decreased trend for carnitin metabolite (200x higher than in young mice), which is a cellular stress marker dependent on choline for energy metabolism. Collectively, these results suggest that PC biosynthesis (CDP-

choline branch of Kennedy pathway) was altered with aging upon genetic deletion of HDAC9 in AT2 cells.

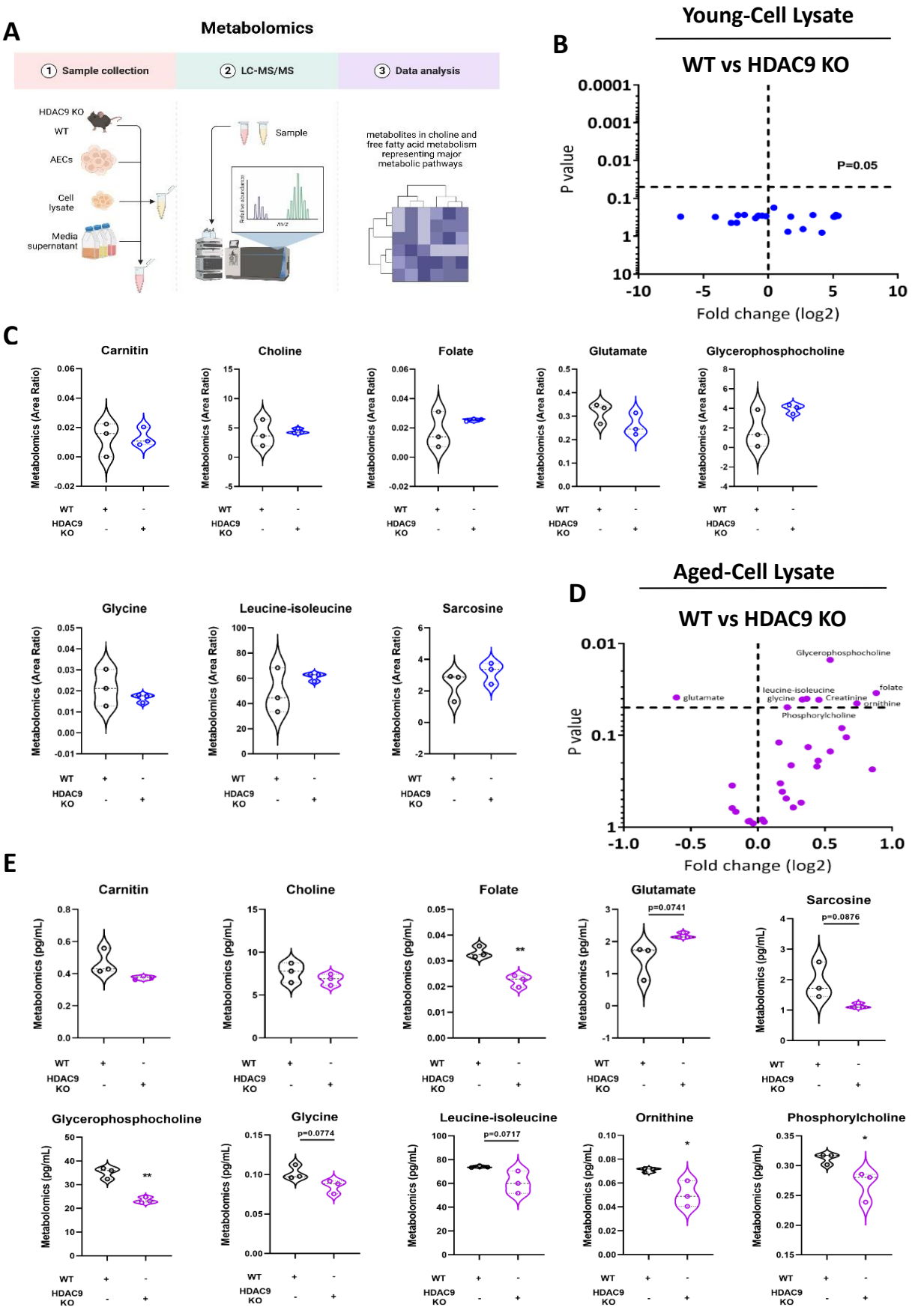

Figure 4.13: Metabolic profiling of cell lysates reveals the alteration of the choline pathway in AT2 cells with aging upon genetic deletion of HDAC9. (A) Schematic experimental approach showing metabolome analysis for choline and free fatty acid metabolites in AT2 cells from WT and HDAC9 KO mice concerning the young and aged mice. **(B, C)** Volcano plot indicates choline pathway metabolites from cell lysate samples of young WT and HDAC9 KO mice; n=3. X-axis shows fold change based on log2 and y-axis shows p-value as 0.05 of threshold. The values of the metabolites are normalized and represented as area ratio. There is no significant difference regarding highly enriched choline metabolites in WT vs. HDAC9 KO-AT2 cells as the box and violin plots indicate. **(D, E)** Volcano plot indicates choline pathway metabolites from cell lysate samples of aged WT and HDAC9 KO mice; n=3. X-axis shows fold change based on log2 and y-axis shows p-value as 0.05 of threshold. The values of the metabolites are normalized and represented as pg/mL. The significantly altered choline metabolites in WT vs. HDAC9 KO-AT2 cells were folate, ornitihine, glycerophosphocholine, and phosphorylcholine as the box and violin plots indicate. *P < 0.05, **P < 0.01 compared with WT.

4.14 Aging HDAC9 deficiency alters the releasing of choline phospholipid metabolites and uptake into AT2 cells

After investigating the production of choline phospholipid metabolites, we focused on releasing these metabolites into the extracellular environment as another crucial aspect. To study this point, supernatant samples were collected from 48-hour-cultured AT2 cells obtained from young and aged mice. Metabolic pathway analysis was performed through LC-MS/MS. As shown in **Figure 4.14A and B**, 23 metabolites in total were detected and quantified from young mice-AT2 cells. Glycerophosphocholine was found significantly higher in young HDAC9 KO-AT2 cells compared to WT controls. The higher level of this metabolite in the supernatant is best explained by choline conversion into glycerophosphocholine. In accordance, the choline levels were reduced in HDAC9 KO-AT2 cells. As a result of choline-betaine branch within Kennedy pathway, the level of carnitine and sarcosine were elevated in HDAC9 KO-AT2 cells versus control. Amino acid metabolism is known to be linked to choline/betain supplementation and choline/betain oxidative demethylation process within the mitochondria. The circulating levels of alanine, aspartate, proline, and glutamate amino acids were also higher in the supernatant, whereas leucine-isoleucine level was less in HDAC9 KO-AT2 cells. In respect of aged AT2 cells' amino acid metabolism **(Figure 4.14 C, D)**, valine, tryptophan, methionine, and phenylalanine levels were higher along with elevated levels of carnitine and sarcosine in HDAC9 KO cells. In this data, there were 3 striking metabolites: choline, glycerophosphocholine, and cystine. While choline (23x higher than young mice) was elevated, glycerophosphocholine (6,5x higher than young mice) and cystine were reduced in HDAC9

KO-AT2 cells. This suggests choline is not only converted to betaine and enters into methionine-homocystine-cystine but also not metabolized to PC-glycerophosphocholine branch. Collectively, these results indicate that there is broken cycle of CDP-choline, which affects the circulating levels of downstream metabolites with aging upon genetic deletion of HDAC9.

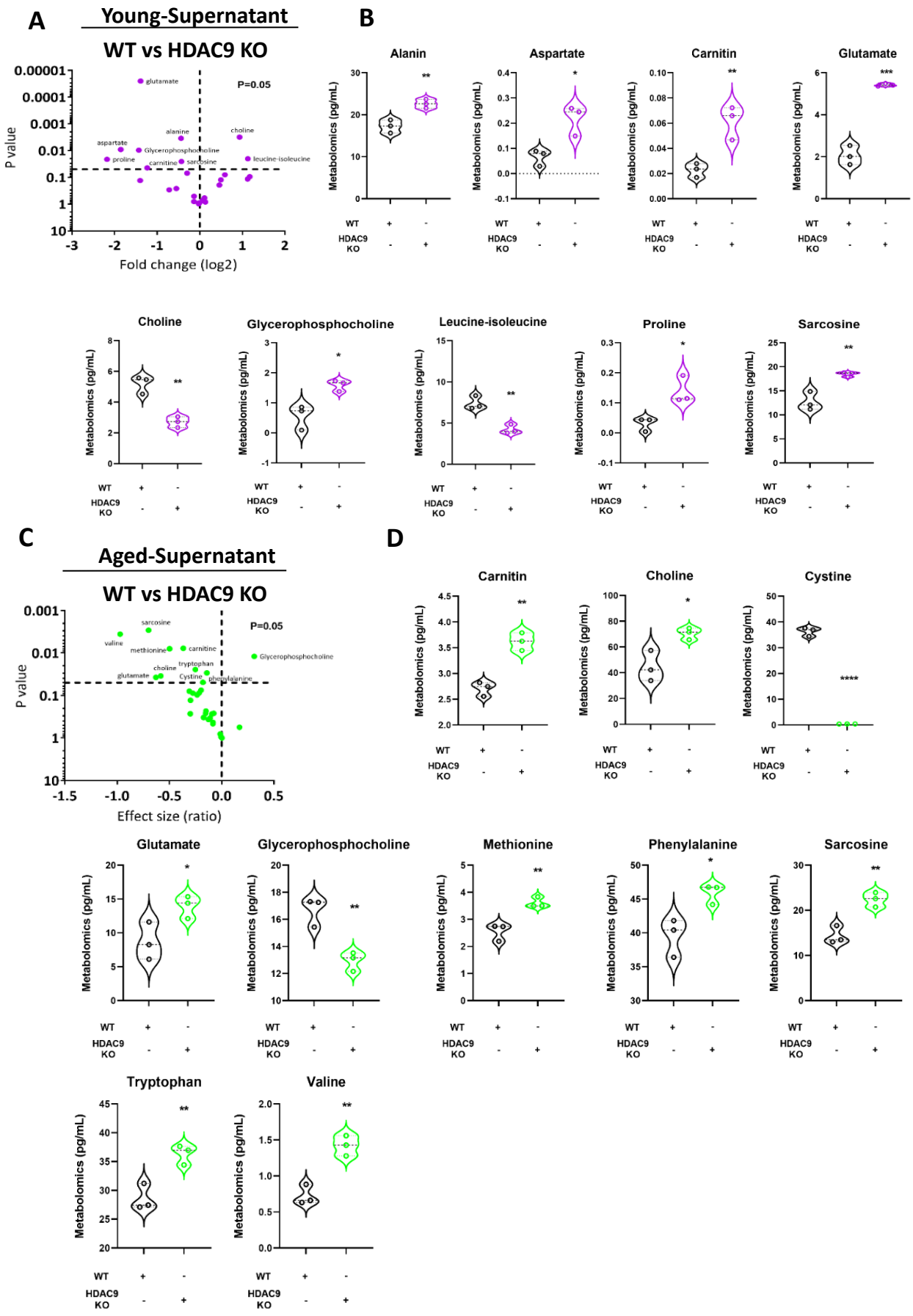

Figure 4.14: Metabolic profiling of supernatants reveals the alteration of choline pathway in aged HDAC9 deficient-AT2 cells. (A, B) Volcano plot indicates choline pathway metabolites from

supernatant samples of young WT and HDAC9 KO mice; n=3. X-axis shows fold change based on log2 and y-axis shows p-value as 0.05 of threshold. The values of the metabolites are normalized and represented as pg/mL. The altered choline metabolites in WT vs. HDAC9 KO-AT2 cells were alanine, aspartate, carnitin, glutamate, choline, glycerophosphocholine, leucine-isoleucine, proline and sarcosine as the box and violin plots indicate. **(C, D)** Volcano plot indicates choline pathway metabolites from cell lysate samples of aged WT and HDAC9 KO mice; n=3. X-axis shows fold change based on log2 and y-axis shows p-value as 0.05 of the threshold. The values of the metabolites are normalized and represented as pg/mL. The altered choline metabolites in WT vs. HDAC9 KO-AT2 cells were carnitin, choline, cystine, glutamate, glycerophosphocholine, methionine, phenylalanine, sarcosine, tryptophan, and valine as the box and violin plots indicate. *P < 0.05, **P < 0.01, ***P < 0.001, ****P < 0.0001 compared with WT.

4.15 Altered choline metabolism with aging upon genetic deletion of HDAC9 switches into free fatty acid metabolism

Phosphatidylcholine, the product of choline phospholipid metabolism, is normally metabolized via phospholipase A2 (PLA2) to direct the whole pathway into the conversion of the glycerophospcholine-choline axis. However, when there is a stress or need, PLA2 can join to arachidonic acid (AA) metabolism branch. As the previous results obtained from RNA- and ATAC-sequencing of aged mice pointed out PLA family and choline phospholipid metabolome profiling displayed aberrant regulation, we decided to study the metabolite changes from arachidonic acid via PLA2 for the next step. For that purpose, AT2 cells were isolated from aged WT and HDAC9 KO-AT2 cells. After 48 hours, the cell lysate and supernatant were collected and metabolic profiling against free fatty acids (oxylipins) was performed through LC-MS/MS. As shown in **Figure 4.15 A and B**, 10 metabolites in total were detected and quantified from cell lysates obtained from aged AT2 cells. There was no significant change between WT vs HDAC9 KO-AT2 cells. With respect to aged AT2 cells supernatant **(Figure 4.15 C, D)**, total of 19 metabolites were detected and quantified. The levels of circulating arachidonic acid and its percursor, linolenic acid were higher in supernatant of HDAC9 KO-AT2 cells versus control. PGE2 and PGG2 were also significantly elevated in HDAC9 KO-AT2. These 2 pro-inflammatory lipid metabolites are derived from AA via cyclooxygenases. Interestingly, 12_HETE levels were significantly high in supernatant of HDAC9 KO-AT2. This simply means that AA is alternatively metabolized by 12-lipoxygenases, another metabolic branch within AA pathway. Collectively, these results suggest that aberrant regulation of choline phospholipid metabolism is forced towards AA pathway response in aged HDAC9 deficient AT2 cells.

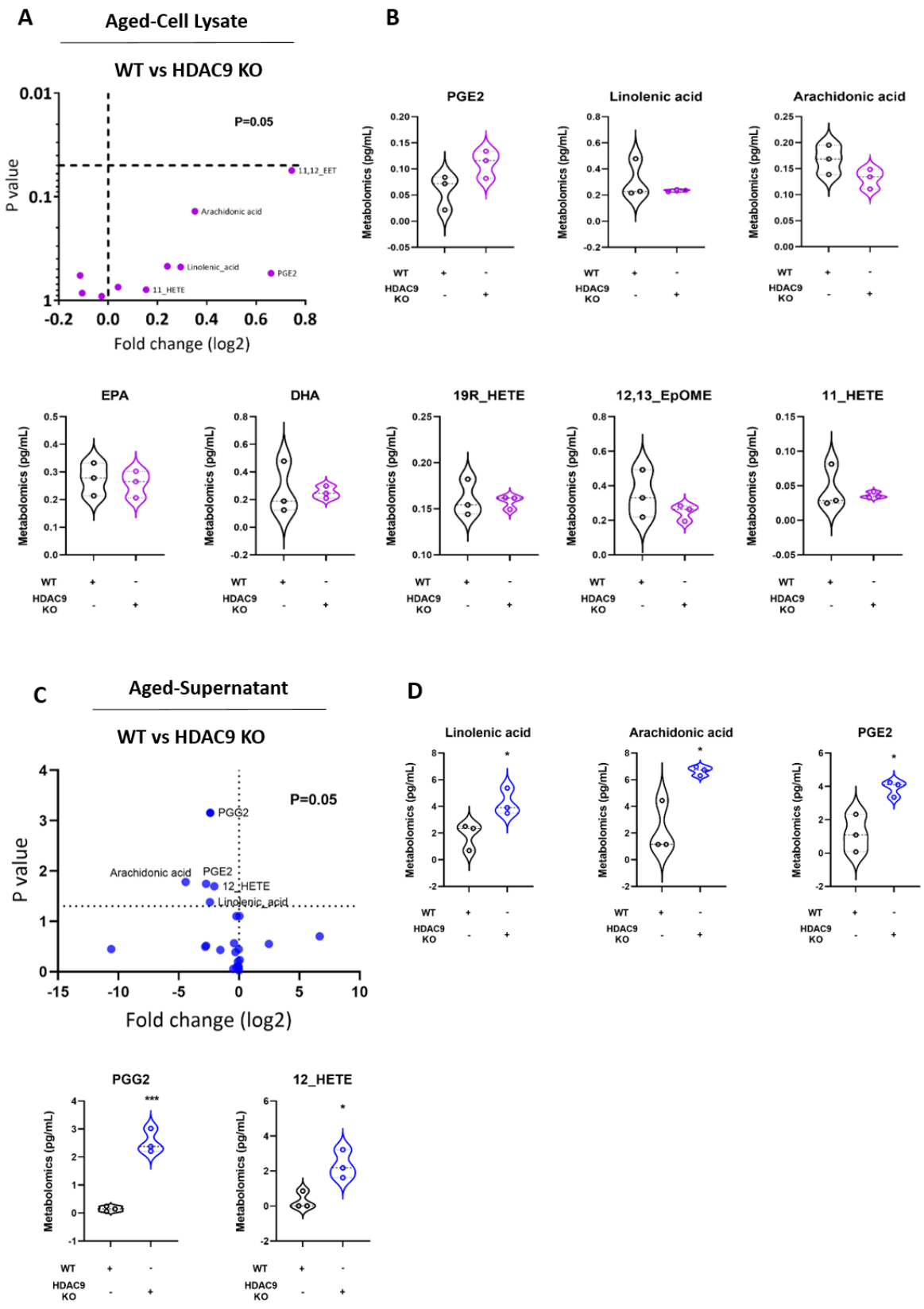

Figure 4.15: Altered choline metabolism with aging upon genetic deletion of HDAC9 switches into free fatty acid metabolism. (A, B) Volcano plot indicates free fatty acid metabolites from cell lysate samples of aged WT and HDAC9 KO mice; n=3. X-axis shows fold change based on log2 and y-axis

shows p-value as 0.05 of the threshold. The values of the metabolites are normalized and represented as pg/mL. There is no significant difference regarding highly enriched free fatty acid metabolites in WT vs. HDAC9 KO-AT2 cells as the box and violin plots indicate. **(C, D)** Volcano plot indicates free fatty acid metabolites from supernatant samples of aged WT and HDAC9 KO mice; n=3. X-axis shows fold change based on log2 and y-axis shows p-value as 0.05 of the threshold. The values of the metabolites are normalized and represented as pg/mL. The altered free fatty acid metabolites in WT vs. HDAC9 KO-AT2 cells were linolenic acid, arachidonic acid, PGE2, PGG2, and 12_HETE as the box and violin plots indicate. *P < 0.05, ***P < 0.001 compared with WT.

4.16 HDAC9 ablation boosts cPLA2 activation

As the levels of prostaglandins were elevated in the supernatant of aged HDAC9 KO-AT2 cells, we assessed the regulation of cPLA2 (cytosolic phospholipase 2), the key enzyme of the AA pathway. AT2 cells were isolated from young and aged WT and HDAC9 KO mice and seeded into an 8-well plate. Co-immunostaining of cPLA2 and HDAC9 for both aged groups revealed that the mean fluorescence intensity of cPLA2 upregulated in HDAC9 KO-AT2 cells versus WT independently of aging **(Figure 4.16 A, B)**. As shown in **Figure 4.16 C and D**, protein expression analysis of AA components (cPLA2, COX1) and its targets (Annexin A1, pERK) confirmed the upregulation of cPLA2 and its down-stream branch. In addition, the enzymatic activity of the super family of PLA2 displayed an increase as a trend in aged HDAC9 KO-AT2 cells, whereas cPLA2 had markedly higher activity. Collectively, these results indicate HDAC9 ablation in AT2 cells differentially affects the expression and enzyme activity of cPLA2.

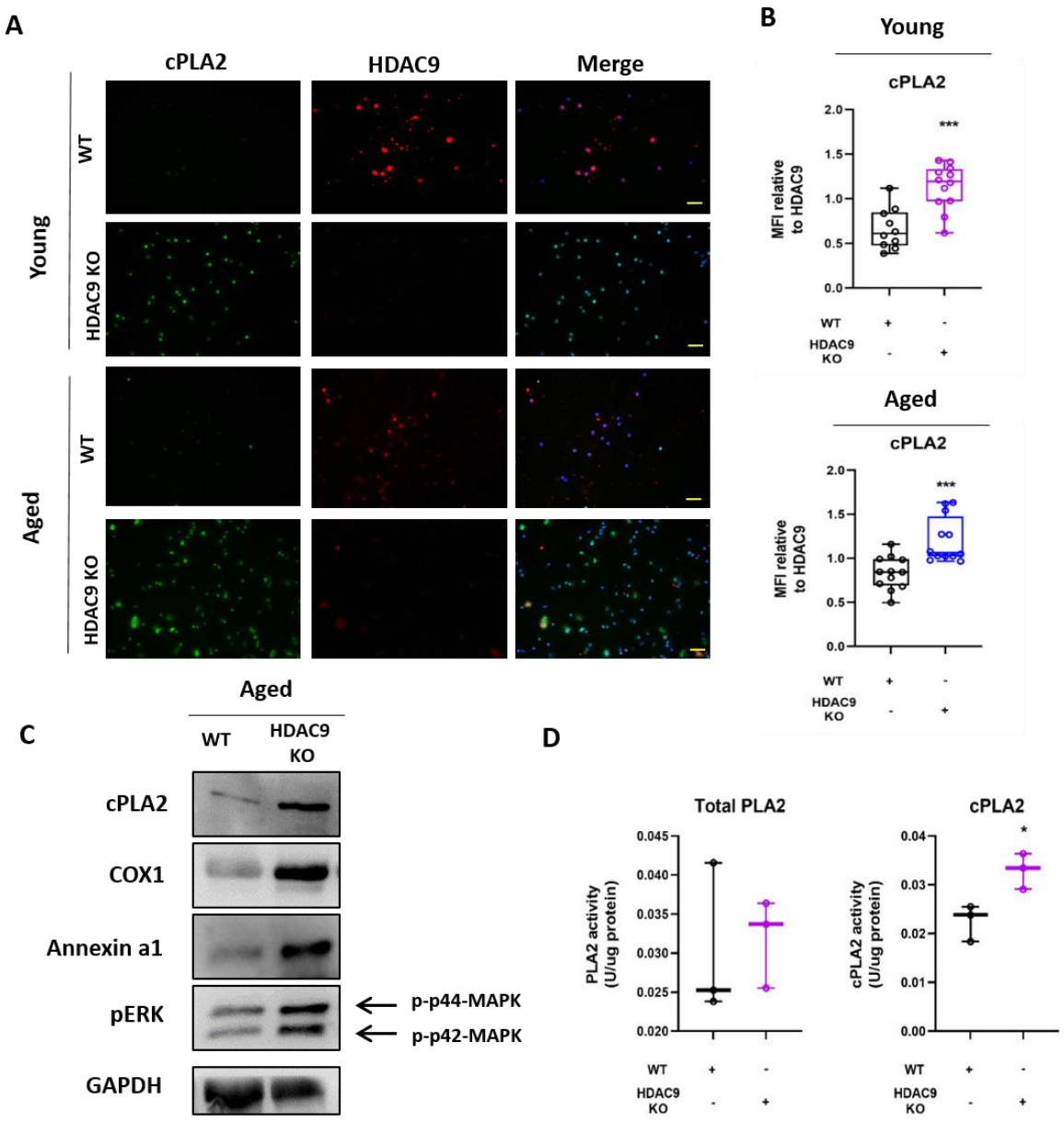

Figure 4.16: Genetic ablation of HDAC9 boosts cPLA2 activation. (A, B) Representative immunofluorescence images of AT2 cells isolated from WT and HDAC9 KO mice. AT2 cells stained with cPLA2 (green), HDAC9 (red), and nuclei counterstained with DAPI (blue). Scale bar=25 µm. The images are representative of n=3 WT and n=3 HDAC9 KO mice-AT2 cells for young and aged groups. Quantification of the mean fluorescence intensity (MFI) of cPLA2 in AT2 cells isolated from WT and HDAC9 KO mice for young and aged groups; n=6 biological replicates; n=2 technical replicates. ***P < 0.001 compared with WT-HDAC9. **(C, D)** Western blotting analysis of cPLA2, COX1, Annexin a1, pERK (p-p44-MAPK and p-p42-MAPK), and GAPDH (loading control) in isolated AT2 cells from aged WT and HDAC9 KO mice; n= 3. The enzymatic activity assays of total PLA2 and cPLA2 from isolated AT2 cells from WT and HDAC9 KO mice were normalized and represented as U/ug. n=3 biological replicates, *P < 0.05 compared with WT.

4.17 Silencing of HDAC9 gene induces imbalance of pro-inflammatory and anti-inflammatory response in alveolar macrophages

As the FACS analysis of aged HDAC9 KO mouse lungs showed alterations in the number of macrophages, we assessed whether HDAC9 deficiency alters the phenotypic switches of immune cells. As alveolar macrophages are the most abundant resident cell population in the lung, we assessed at first in alveolar macrophages whether HDAC9 deficiency alters the phenotypic switches. Alveolar macrophages (MH-S cell line) were transfected with specific siRNA against HDAC9 and inflammatory cytokine profiling was performed (**Figure 4.17 A**). Knockdown efficiency against HDAC9 was validated (**Figure 4.17 B**). As shown in **Figure 4.17 C and D**, mRNA expression of pro-inflammatory genes (*Il1β,Il6,Tnfα*) was significantly upregulated upon HDAC9 silencing along with upregulated anti-inflammatory genes (*Mmp9,Il10, Tgfβ*). Collectively, these results indicate that silencing of HDAC9 creates an imbalance between pro- and anti-inflammatory responses.

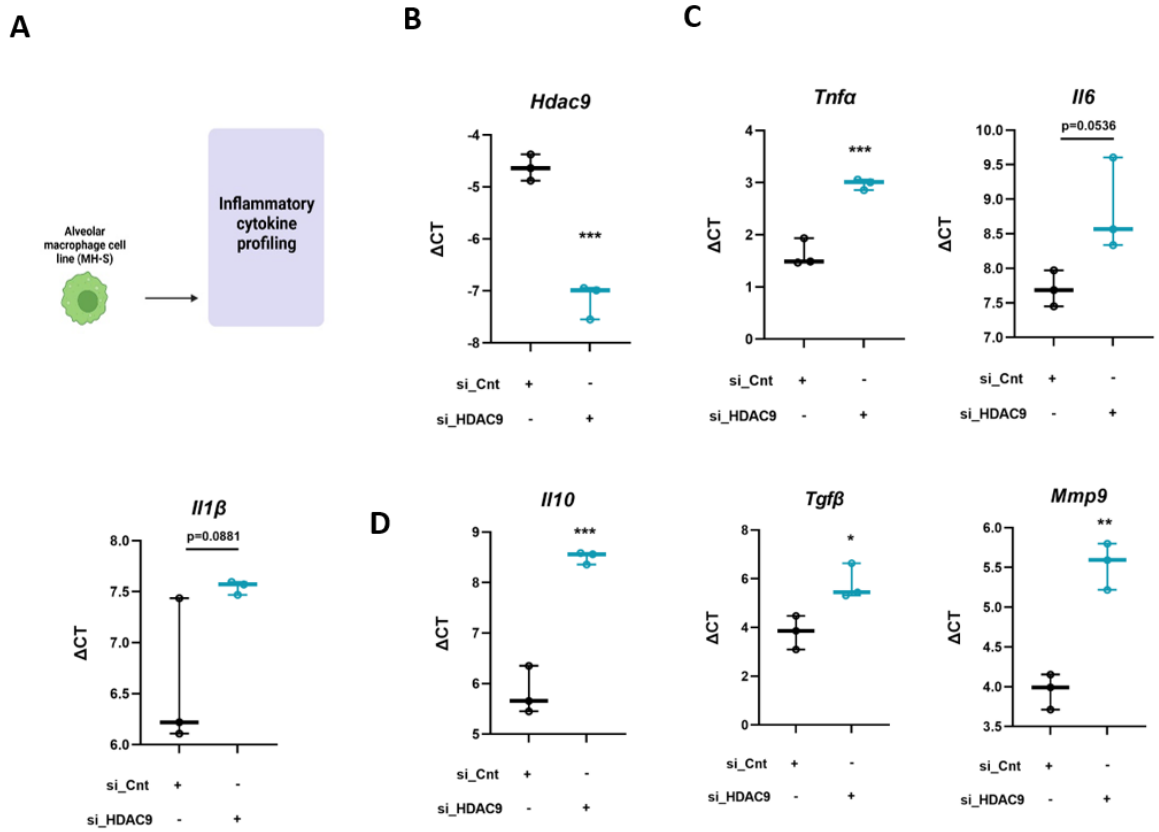

Figure 4.17: Silencing of HDAC9 gene promotes imbalance of pro-inflammatory and anti-inflammatory response in alveolar macrophages. (A) Schematic experimental plan showing performing inflammatory cytokine profiling in alveolar macrophage cell line (MH-S). **(B)** Relative mRNA expression of HDAC9 displaying the knockdown efficiency of siRNA. **(C, D)** Relative mRNA

expression of M1 macrophage markers (*Il6, Il1β, Tnfα, Il8*) and M2 macrophage markers (*Il10, Mmp9, Tgfβ*) in undifferentiated alveolar macrophages (n=3). *P < 0.05 and **P < 0.01 compared with control (si_Cnt).

4.18 Alveolar epithelial cell-alveolar macrophage crosstalk leads to proliferative response

Silencing of HDAC9 did not induce a proliferative response after 24 hours; however, significantly increased the response in alveolar macrophages after 48 hours **(Figure 4.18 A).** As shown in **Figure 4.18 B and C**, alveolar macrophages were cultured for 24 hours with the media of isolated AT2 cells from HDAC9 KO mice. The culture media from the 24 hours sharply induced proliferation in HDAC9-depleted alveolar macrophages. Altogether, these results suggest that alveolar epithelial cell-alveolar macrophage crosstalk enhances proliferative response of alveolar macrophages upon HDAC9 silencing.

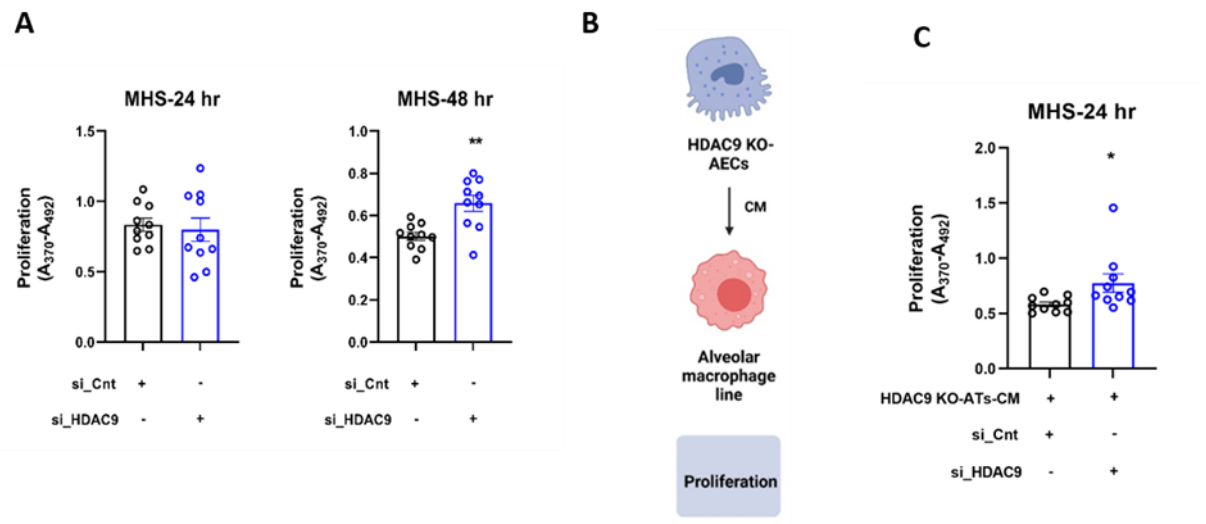

Figure 4.18: Alveolar epithelial cell-alveolar macrophage crosstalk leads to proliferative response. **(A)** Quantification of proliferation and apoptosis of alveolar macrophages (n=5 biological replicates, 2 technical replicates). **(B)** Experimental scheme showing the culturing alveolar macrophages in the presence of media of HDAC9-AT2s to perform proliferation and apoptosis assays. **(C)** Quantification of proliferation and apoptosis of alveolar macrophages (n=5 biological replicates, 2 technical replicates). *P < 0.05, **P < 0.01 compared with control (si_Cnt).

4.19 Genetic ablation of HDAC9 promotes pro-inflammatory M1-phenotype irrespectively of aging

To test whether HDAC9 deficiency alters the phenotypic switches of immune cells, undifferentiated BM-derived macrophages (M0) from young and aged WT and HDAC9 KO

mice were polarized into M1 and M2 macrophages in the presence of MCSF. After polarization, inflammatory cytokine profiling was carried out **(Figure 4.19 A)**. Firstly, HDAC9 expression was significantly higher in M1 and M2-macrophages of the young group, whereas it had an increased trend in M2-macrophages of the aged group **(Figure 4.19 B)**. As shown in **Figure 4.19 C and D,** mRNA expression profiling for the young group revealed that HDAC9 KO-M1-macrophages mainly expressed M1 markers (*Il6* and *Tnfα*), whereas HDAC9 KO-M2-macrophages expressed only one M2 marker at high level (*Tgfβ*). The high expression of pro-inflammatory genes *Il1β* and *Tnfα* was confirmed in aged HDAC9 KO-M1 macrophages similar to the young group **(Figure 4.19 E)**. Interestingly, HDAC9 KO-M2 macrophages displayed an increased expression trend of M2 (*Mmp9, Tgfβ*) markers. Altogether, these results indicate that the genetic ablation of HDAC9 enhances pro-inflammatory M1-phenotype irrespectively of aging.

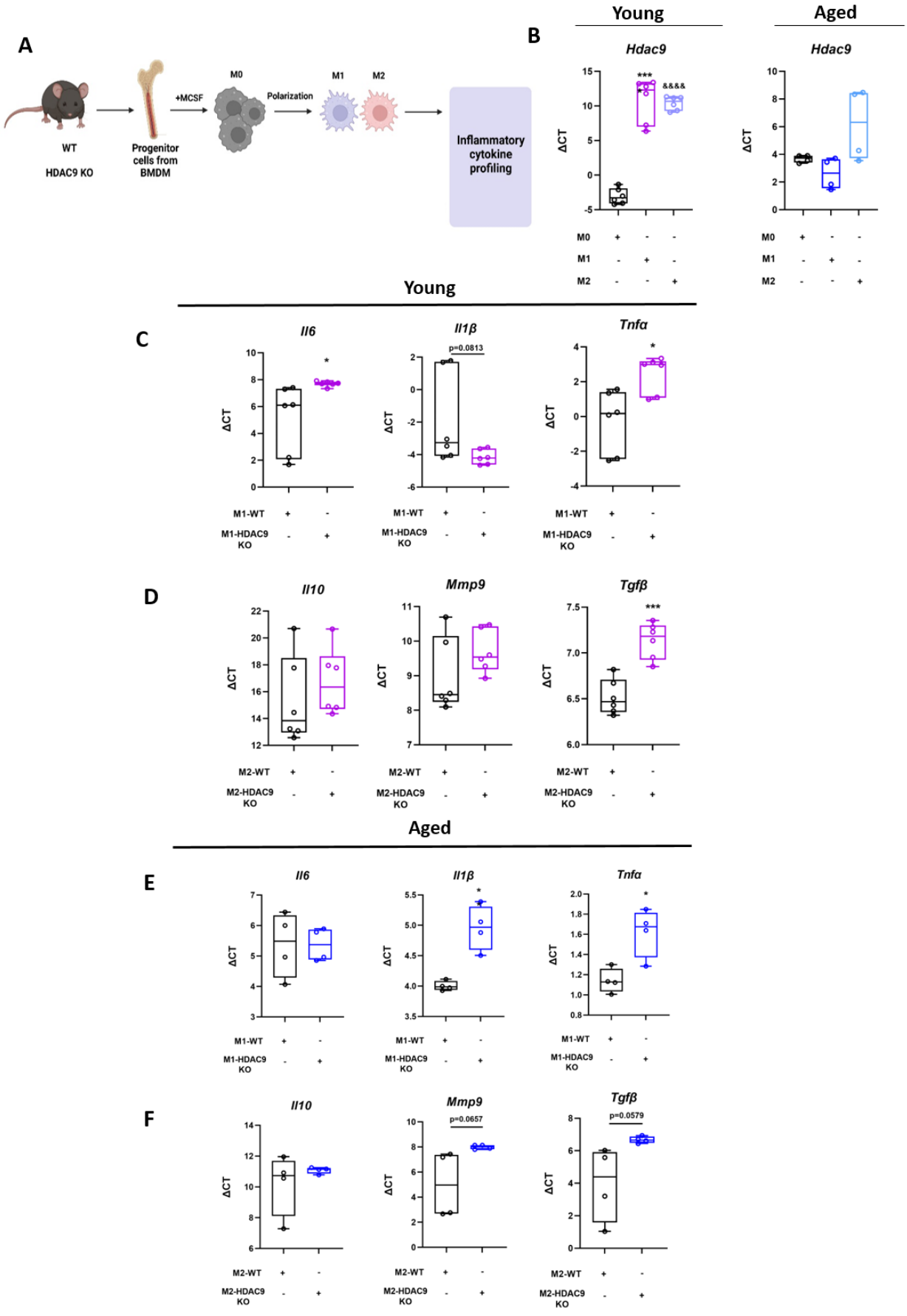
A
WT
HDAC9 KO
Progenitor cells from BMDM
+MCSF
M0
Polarization
M1
M2
Inflammatory cytokine profiling
B
Young
Aged
Hdac9
ΔCT
***
&&&&
M0
M1
M2
C
Young
Il6
Il1β
p=0.0813
Tnfα
M1-WT
M1-HDAC9 KO
D
Il10
Mmp9
Tgfβ
M2-WT
M2-HDAC9 KO
Aged
E
F
p=0.0657
p=0.0579

Figure 4.19: Genetic ablation of HDAC9 promotes pro-inflammatory M1-phenotype derived from BM irrespectively of aging. (A) Schematic experimental plan showing the generation of BMDMs (bone marrow-derived macrophages, M0) in vitro, their polarization into M1 and M2-macrophages and performing inflammatory cytokine profiling of them. M-CSF (macrophage colony-stimulating factor) was used to maintain M0 macrophages for 7 days. **(B)** Relative mRNA expression of HDAC9 in M0, M1 and M2 macrophages from young (n=6 per group) and aged (n=4 per group) of WT and HDAC9 KO mice. ****P < 0.0001 and $^{\&\&\&\&}$P < 0.0001 compared with M0. **(C, D)** Relative mRNA expression of M1 macrophage markers (*Il6, Il1β, Tnfα*) and M2 macrophage markers (*Il10, Mmp9, Tgfβ*) in polarized M1 and M2 macrophages from young WT and HDAC9 KO mice (n=6 per group). *P < 0.05 and ***P < 0.001 compared with M1-WT or M2-WT. **(E, F)** Relative mRNA expression of M1 macrophage markers (*Il6, Il1β, Tnfα*) and M2 macrophage markers (*Il10, Mmp9, Tgfβ*) in polarized M1 and M2 macrophages from aged WT and HDAC9 KO mice (n=4 per group). *P < 0.05 and **P < 0.01 compared with M1-WT or M2-WT.

4.20 Silencing of HDAC9 did not alter the releasing of choline phospholipid metabolites from BM-derived M1 and M2 macrophages

For the metabolomic analysis, supernatant samples were collected after HDAC9 silencing upon the polarization of M0 into M1 and M2-macrophages **(Figure 4.20 A)**. As shown in **Figure 4.20 B and C**, 36 metabolites in total were detected and quantified in the supernatant of M1-macrophages. The most abundant phospholipids including phosphorylcholine and glycerophosphocholine were identified within the supernatant. However, there was no significant change upon HDAC9 depletion in M1-macrophages. With respect to M2-macrophages, a total of 31 metabolites was detected. Only the circulating level of agmatine was found significantly higher **(Figure 4.20 D, E)**. Collectively, these results indicate that HDAC9 depletion did not induce the release of choline phospholipid metabolites from M1 and M2 macrophages.

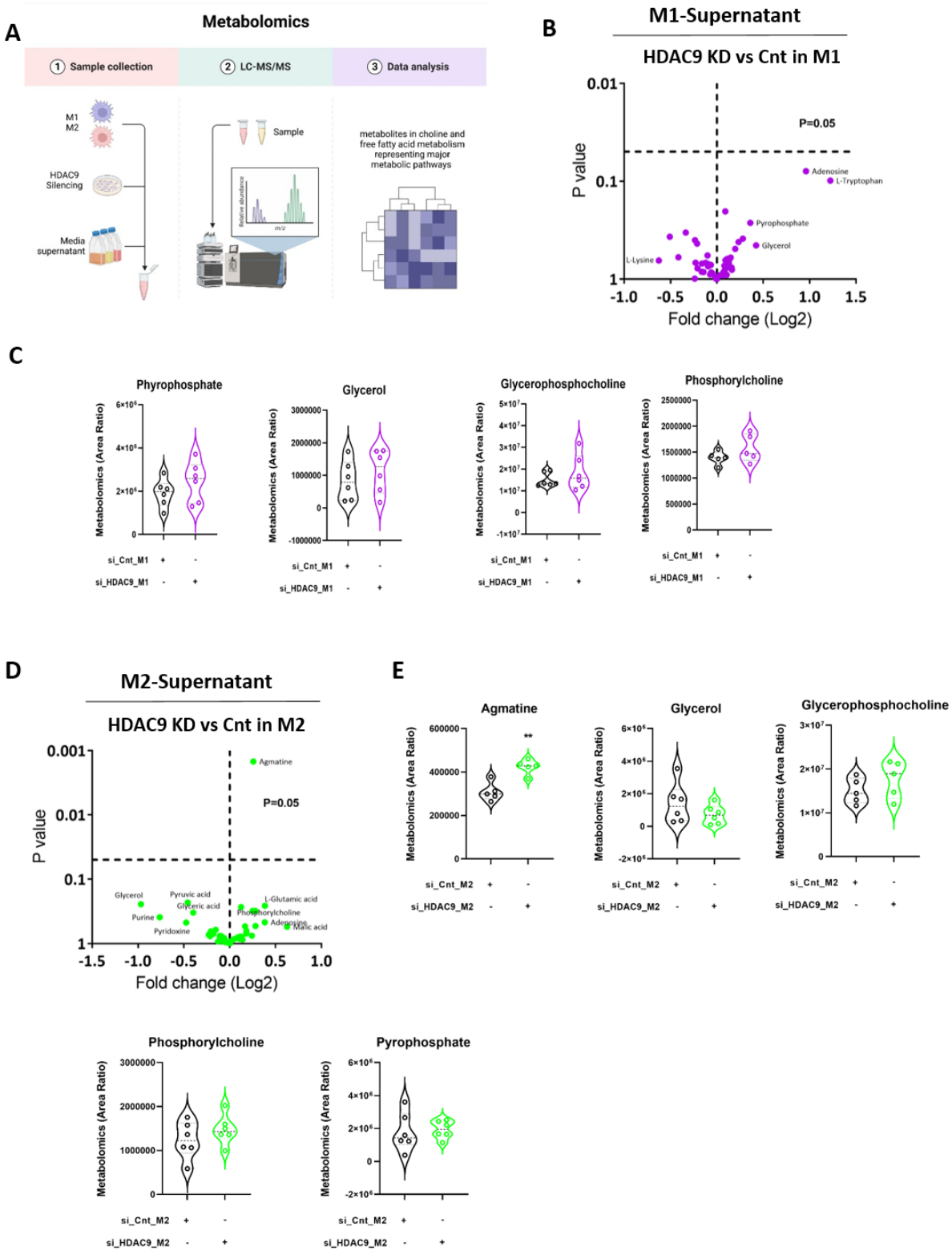

Figure 4.20: The metabolome profiling of choline pathway revealed an increased level of agmatine in M2 macrophages upon genetic depletion of HDAC9. (A) Schematic experimental approach showing metabolome analysis for choline and free fatty acid metabolites in HDAC9-depleted M1 and M2 macrophages. **(B, C)** Volcano plot indicates choline pathway metabolites from supernatant samples of M1 macrophages; n=5-6. X-axis shows fold change based on log2 and y-axis shows p-value as 0.05

of the threshold. The values of the metabolites are normalized and represented as area ratio. There is no significant difference regarding highly enriched choline metabolites in M1 macrophages as the box and violin plots indicate. **(D, E)** Volcano plot indicates choline pathway metabolites from supernatant samples of M2 macrophages; n=5-6. X-axis shows fold change based on log2 and y-axis shows p-value as 0.05 of the threshold. The values of the metabolites are normalized and represented as area ratio. The significantly altered metabolite in M2 macrophages was agmatine as the box and violin plots indicate. **P < 0.01 compared with control (Si_Cnt_M2).

4.21 Depletion of HDAC9 in M1 macrophages leads to alteration of free fatty acid metabolite amounts

Along with the same experimental approach of AT2 cells, metabolic profiling against free fatty acids (oxylipins) was performed also in M1 and M2-macrophages. As shown in **Figure 4.21 A and B**, 20 metabolites in total were detected and quantified from supernatant obtained from M1-macrophages. The levels of circulating of linolenic acid were higher in supernatant of HDAC9 depleted-M1 macrophages versus control, whereas TBX2 (Thromboxane A2) level was interestingly lower. Regarding of M2-macrophages, total of 30 metabolites were detected; however, there was no significant change between HDAC9 depleted-M2 macrophages versus control **(Figure 4.21 C and D)**.Collectively, these results suggest that aberrant regulation of AA pathway response in M1-macrophages upon HDAC9 depletion.

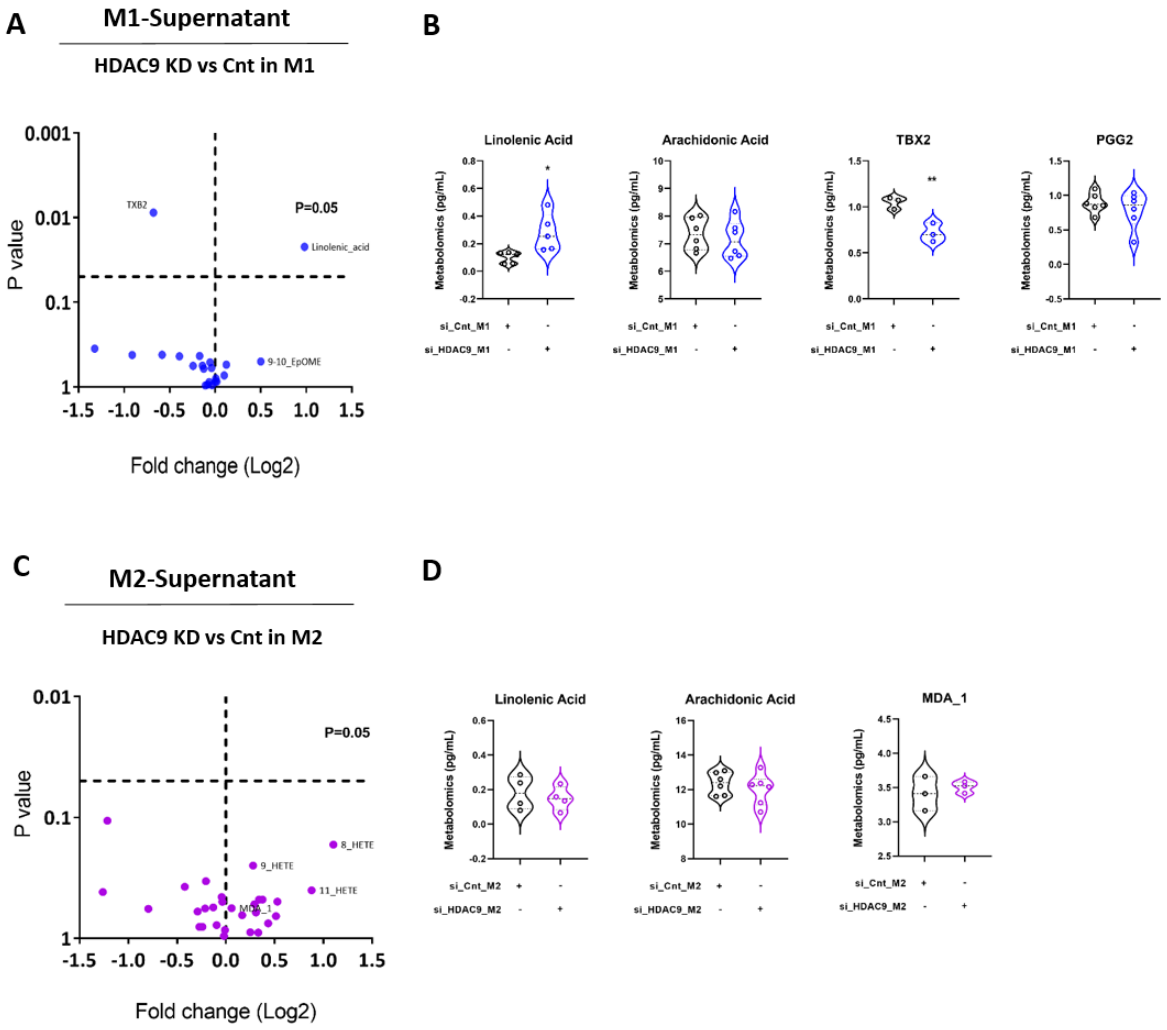

Figure 4.21: Depletion of HDAC9 in M1 macrophages leads to alteration of free fatty acid metabolite content. (A, B) Volcano plot indicates free fatty acid metabolites from supernatant samples of M1 macrophages; n=3-6. X-axis shows fold change based on log2 and y-axis shows the p-value as 0.05 of the threshold. The values of the metabolites are normalized and represented as pg/mL. The significantly altered metabolites in M1 macrophages were linolenic acid and TBX2 as the box and violin plots indicate. *P < 0.05 and **P < 0.01 compared with control (si_Cnt_M1). **(C, D)** Volcano plot indicates free fatty acid metabolites from supernatant samples of M2 macrophages; n=3-6. X-axis shows fold change based on log2 and y-axis shows p-value as 0.05 of the threshold. The values of the metabolites are normalized and represented as pg/mL. There is no significant difference regarding highly enriched free fatty metabolites as the box and violin plots indicate. *P < 0.05 compared with control (Si_Cnt_M2).

5. DISCUSSION

In healthy aging concept, organ functions decline with chronological aging and this phenomenon is associated with epigenetic changes, genomic instability, telomere attrition, dysregulated tissue regeneration, and reduced stem cell function. Accelerated aging is an unhealthy form of physiological aging occurred by accumulated senescent cells. Cellular senescence is a prominent and conserved response to many levels of cellular stress to prevent the circulation of damaged cells. Senescent cells play a vital role in aging process by senescence-associated secretory phenotype. However, elimination of these cells via pharmacological or genetic approach extends the lifespan of murine models and delay the manifestation of age-related diseases. On the other hand, prematurely aged tissues show persistent senescence response. Premature aging disorders do not manifest all features of healthy physiological aging and are linked to accelerated aging of one specific organ rather than whole organism aging. Cluster of symptoms in premature aging disorders might be occurred based on molecular signature changes such as epigenetic players, HDACs. This current study provides a strong evidence that HDAC9 deficiency initiates cellular senescence and premature lung aging response resulting in inflammatory phenotype. Accordingly, targeting HDAC9 deficient cells might offer a therapeutic approach to delay premature aging response and extend the lifespan. This mentioned notion is based on the following results: (1) Genetic ablation of HDAC9 triggers the accelerated lung aging response within AT2 cells and alters epithelial cell plasticity; (2) Aging upon genetic ablation of HDAC9 worsens lung structure along with chronic SAS-phenotype; (3) HDAC9 deficient lung with aging alters chromatin structure and impacts the related gene expression; (4) Observed inflammatory phenotype in aged HDAC9 deficient lungs is occurred by the contribution of pro-inflammatory lipid mediators by AT2 cells; (5) Altered signature of immunometabolic response within HDAC9 deficient-bone marrow-derived cells verifies the crosstalk of organs beyond lung.

5.1 Genetic ablation of HDAC9 contributes to accelerated lung aging, with disrupted epithelial cell characteristics and elevated cellular senescence signature

In the present study, we characterized HDAC9 deficient mice as a mouse model of accelerated cellular senescence, dominantly for AT2 cells aspect. Increased cellular senescence has been associated with the decline in the abundance of AT2 cells along with the loss of their stem cell function. AT2 cells are one of the major cell types in the lung responsible for producing surfactant, a complex mixture of lipids and proteins that reduce surface tension in the alveoli and prevent lung collapse. The composition and production of pulmonary surfactants are

impaired as age-related changes (Brandenberger C. and Mühlfeld C., 2017). Surfactant proteins are divided into 2 groups: (1) hydrophilic ones, SP-A and SP-D, and (2) hydrophobic ones, SP-B and SP-C. SP-A and SP-D are known to be part of the innate immune system since they have C-terminal lectin domain, responsible for binding sites found on bacteria and virus particles. SP-B and SP-C proteins are stored and secreted into the lung airways. Both are responsible for maintaining the biophysical properties by regulating surface tension of the lung. SP-B is known to exhibit anti-microbial activity, while genetic polymorphism on SP-C is linked to interstitial fibrosis, an age-related lung disease (Han S.and Mallampall R.K., 2015). To test the effect of HDAC9 deficiency over surfactant phospholipids, we performed surfactant profiling (SP-A, SP-B, SP-C, and SP-D) within the lung samples (Figure 4.1 B, C). Our investigation clearly demonstrated that HDAC9-deficient lungs have reduced levels of surfactant proteins when compared to age-matched WT controls. Decline in the number of SP-C and SP-D positive cells specifically indicates that there is a dysregulation of gas exchange function and loss of protective immune response in HDAC9 deficient lungs. Therefore, HDAC9-deficient lungs might be prone to viral and bacterial infections more frequently with age as well.

Cellular senescence is defined as a cell cycle arrest response, manifested by aberrant proliferation or deleterious stimuli to block the proliferation of dysfunctional cells (Kumari R. and Parmjit J., 2021). In this regard, we observed that HDAC9-deficient lung cells are not capable of maintaining proliferative capacity, yet prone to apoptotic faith (Figure 4.1 D, E). Loss of proliferative features of HDAC9 deficient-resident lung cells is in line with the previously observed cellular senescence characteristics.

Decades of enormous research have addressed that cellular senescence is an important driving mechanism for premature aging and age-related chronic lung diseases. At a cellular level, emphysema is defined as alveolar epithelial cell death and loss of regeneration of epithelial surface, leading to alveolar wall destruction and dysregulated gas exchange (Lin C.R. et al., 2022). In this study, genetic ablation of HDAC9 was confirmed to initiate emphysema-like phenotype, based on the radial alveolar count and mean linear intercept parameters as pathological criteria within the lungs (Figure 4.1 F, G). Collectively, these results affirm that genetic ablation of HDAC9 alters pulmonary surfactant compositions and regenerative capacity of cells with reduced proliferative feature within lung. Here, the production of pulmonary surfactants and their release process into alveolar compartments might also be affected by HDAC9 deficiency, independently from proliferative and apoptotic response of surfactant protein-positive cells. The altered surfactant composition and subsequent lung architectural

changes upon HDAC9 genetic depletion suggests lung functional impairment and breathing difficulties in these mice.

Chronic lung diseases and aging are closely associated to epithelial-mesenchymal transition (EMT), a cellular process where epithelial cells undergo mesenchymal cell phenotype. EMT and aging has been linked to specifically development of age-related fibrosis in lung as well as heart. Even though the main reason for this phenomenon is still unclear, we know that telomere length decreases with aging, while the levels of EMT-related proteins are elevated. On the other hand, aging is also connected to accumulation of senescent cells. These cells show SASP, defined by elevated levels of pro-inflammatory cytokines, reactive oxygen species, and metalloproteinases. Increase manifestation of SASP by senescent cells automatically affects surrounding cells in a harmful way, which leads to eventually age-related diseases (Imran AMS et al., 2021). Senescent fibroblast cells might influence the initiation of EMT process in the surrounding epithelial cells. In accordance, we observed that HDAC9 deficient-AT2 cells lost the epithelial cell signature when compared to age-matched WT-AT2 cells (Figure 4.2 B, C). Here, the results affirm that these new mesenchymal-like cells clearly exhibit reprogramming of AT2 cells upon HDAC9 depletion.

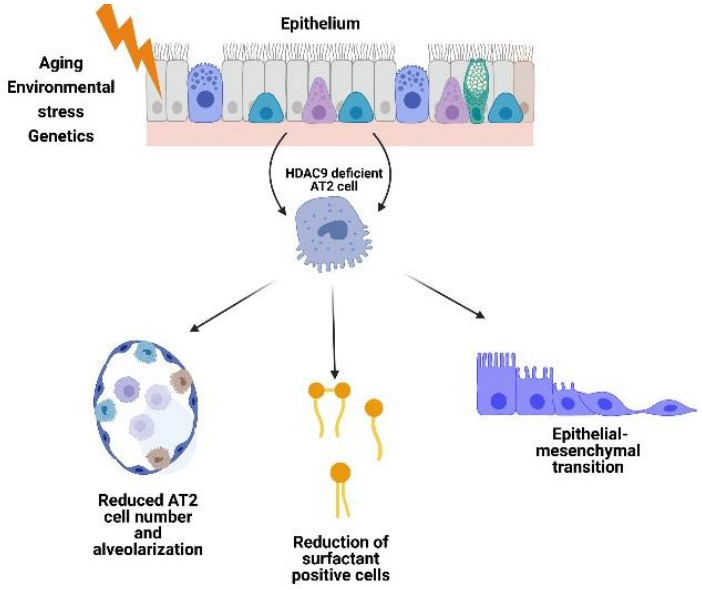

Figure 5.1: Summary of genetic ablation of HDAC9 over disrupted epithelial cell characteristics. Generated by Biorender.

The role of HDACs in cellular senescence and premature aging concepts is a wide-open and controversial topic. Several studies investigated the relation between HDAC inhibition (HDACi) and prevention of SASP in cancer field. Here, HDAC inhibitors were used as anti-cancer therapeutic approach, allowing the low toxicity for normal healthy cells and initiation of senescence response in cancer cells. This approach is named as therapy-induced senescence and used in combination with classic chemotherapy for cancer

patients (Faheem et al., 2020). However, the effect of HDACs regarding senescence within normal cells remains unclear. There is no known drug so far to slow human aging even though some such as metformin, was tested with this aim. Interestingly, HDACi was shown to extend lifespan in short-lived species through slowing down aging. For instance, inhibition of HDA complex, class II HDACs, leads to DNA damage and osmotic stress resistance by regulating aging. Silencing HDA homologs prevents aging-related deleterious process and extends the lifespan in *C. elegans* and *Drosophila*. Specifically, valproic acid and the heterocyclic anti-convulsant trimeadione were proven in *C.elegans* to delay aging (Evason et al., 2008 and McIntyre et al. 2019). In the literature, HDAC inhibition was proposed as an approach to combat aging and its manifestations. On the other hand, several studies suggest the HDAC downregulation is involved in induction of aging process. For example, HDAC1 and HDAC4 were shown to be downregulated in senescent fibroblasts (Di Giorgi et al., 2021, Place et al. 2005 and Han et al., 2016). In another recent study, downregulation of HDAC2 and HDAC7 were reported to induce senescence response in dermal fibroblast (Warnon et al., 2021). Notably, controversial results exist with regard to HDAC9. It is known that HDAC9 is a negative regulator of adipogenic differentiation and its expression was increased in adipose tissue while declined in the brain tissue with aging (Chatterjee et al.,2011 and Weintraub et al., NIH project abstract). Moreover, HDAC9 expression was shown to elevated in aging spermatogonial stem cells. When these cells were exposed to rapamycin, anti-aging drug, HDAC9 expression was recovered (Kofman et al., 2013). In our study, we claim that genetic ablation of HDAC9 provokes cellular senescence and premature aging response in AT2 cell-manner. Widely used senescence markers, p21 and p16, exhibited increased expression throughout the whole HDAC9-ablated lungs (Figure 4.3 B. C). Due to the previous data obtained from surfactant profiling and dysregulated EMT process (Figure 4.1 B, C and Figure 4.2 A-C), we decided to focus on specifically AT2 cells for the evaluation of senescence aspect. Firstly, we confirmed that HDAC9 protein expression significantly reduced with aging in isolated HDAC9 KO-AT2 cells. The opposite correlation between ETM process and telomere length led us further to investigate the telomere length of isolated AT2 cells from WT and HDAC9 KO animals. These data suggest that HDAC9 ablation initiates DNA damage response, as a sign of replicative senescence since telomere length declined. HDAC9 deficient senescent AT2 cells elicit profound SAS-phenotypic changes as a stress response, where p21 expression, SA-β-GAL, pro-inflammatory cytokines and metalloproteinases slightly increased when compared to age-matched WT-AT2 cells (Figure 4.4 A-F). These data strongly confirms that genetic ablation of HDAC9 drives the initiation of cellular senescence and premature aging

response and maintain SASP at basal level within AT2 cells. Based on these findings, following points should be highlighted: (1) HDAC9 encodes multiple protein isoforms in human and mice, where some of the isoforms show distinct patterns of cellular localization (Petrie et al., 2003). Nuclear or cytoplasmic localization of HDAC9 isoforms regulates a wide range of cellular mechanisms. Based on the above findings, we presume that lack of HDAC9 isoforms-specific to the lung initiates cellular senescence and premature aging by basal level of SASP. In this regard, our study differs from the previous studies claiming that HDACi in general improves the anti-aging response. (2) This study characterizes HDAC9 deficient mice as mouse model of accelerated cellular senescence. These mice exhibit the SAS-phenotype at basal level without any additional second hit such as external stimuli to trigger early-aging response.

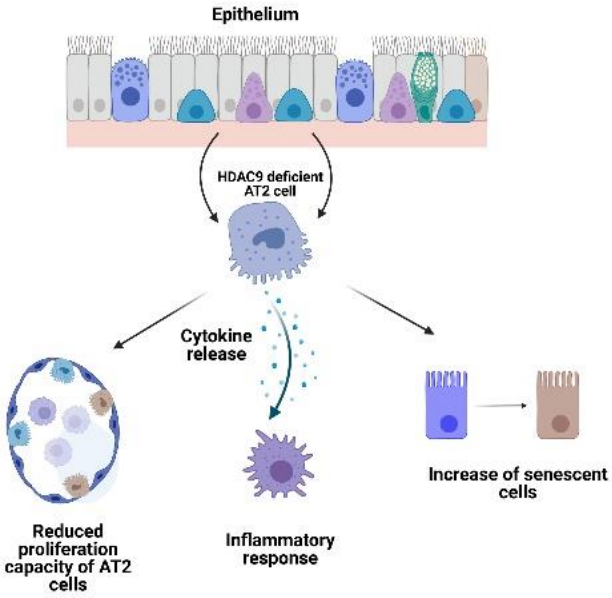

Figure 5.2: Summary of genetic ablation of HDAC9 over disrupted epithelial cell characteristics and elevated cellular senescence signature. Generated by Biorender.

5.2 Aging upon genetic ablation of HDAC9 manifests the aggravated lung structure, with the substantial premature senescence phenotype

To address specifically the effect of chronological aging upon genetic ablation of HDAC9 within lung and AT2 cells, two different age groups were selected as 60- and 70-week-old mice. The results from surfactant profiling, apoptotic and proliferative status, and stereological assessment of alveolarization indicate that aging upon HDAC9 depletion worsens lung structure along with emphysema-like phenotype. Here, the profound changes of cellular senescence started at an early age within the lung due to genetic ablation of HDAC9 become visible and prominent. In addition, the number of cells expressing Surfactant protein family members and their proliferative capacity naturally decrease at basal level in WT animals with aging (decline

range: $0.5x10^7$-$2x10^7$cells, Figure 4.1 C, E and Figure 4.5 C, E). Importantly, HDAC9 depletion aggravates age-related phenotypical alterations. Specifically, p16 expression is significantly elevated in HDAC9 ablated aged lung (Figure 4.6 C), indicating that physiological aging in addition to HDAC9 deficiency-mediated senescence enhances the senescence response. HDAC9 deficient AT2 cells elicit elevated SAS-phenotypic changes, where p21 expression, SA-β-GAL positive cell number, and pro-inflammatory cytokines (*Il6, Il1β, iNOS*) significantly increased with physiological aging (Figure 4.7 B, C). Moreover, senescent HDAC9 deficient AT2 cells with aging lost the proliferative capacity, whereas apoptotic response was significantly increased (Figure 4.7 D). Since AT2 cells are accepted as stem-like cells, this might be a hint that HDAC9 loss leads to stem cell exhaustion.

Physiological age-related changes in the respiratory system transform the cellular landscape of the lungs. To evaluate the impact of aging upon genetic ablation of HDAC9, we employed FACS approach. The two major findings from this approach strongly evidence a crucial role of HDAC9 in altering the cellular landscape of aged lungs based on the imbalanced abundance of cell populations. This includes a significant reduction of $CD117^+$ (progenitor epithelial cells, known as proto-oncogene C-kit) and $EpCAM^+$ (known as stem cell marker) epithelial cell populations, among all the $CD44^+$ cells in HDAC9 KO lungs (Figure 4.8 B, C). As epithelial cells expressing these two stem cell markers declined, this might point out towards the impact of HDAC9 on the regenerative stem cell population within the aged lung. The increased abundance of other all $CD44^+$ cells (fibroblast, endothelial cells, vascular smooth muscle cells) is an indicator of lung remodeling with age upon HDAC9 ablation. However, only 1 out of 8 aged HDAC9 KO animals showed significant fibrotic scar within the lung (data not shown), and needs further assessment of pulmonary vascular remodeling. On the other hand, an increased proportion of adaptive immune cells ($CD8^+$/$CD4^+$ T cell ratio and B cells) and a decline in innate immune cells (AMs or IMs) was observed in the lungs of HDAC9 KO mice (Figure 4.9 C). These data suggest an imbalance of healthy inflammatory response between innate and adaptive immunities. Chronic adaptive immunity response seems to be in charge through the enriched T and B cells with aging upon genetic ablation of HDAC9. This chronic inflammatory response is in concordance with the substantial SAS-phenotype in aging organism.

5.3 Chronologically aged HDAC9 deficient lung exhibits alterations of chromatin changes, activating the metabolic pathway-related genes

HDAC9 has NES (nuclear export signal) short target peptide, which enables the translocation between nucleus and cytoplasm. Considering the nuclear resident isoforms of HDAC9 and investigating the impact of their loss, RNA sequencing of isolated senescent AT2 cells from aged animals (60 and 70-week old mice) was performed. The results from RNA sequencing indicate that HDAC9-mediated transcriptional landscape is potentially responsible for drastic alterations in metabolic pathways of AT2 cells with aging. Loss of HDAC9 function leads to major regulation of the genes involved in lysosomal degradation, RNA polymerase II regulation, proteosome, cysteine/glutamate transporter pathway, inositol phosphate metabolic pathway, phospholipid enzymes, cysteine/glutamate receptors, and metalloproteinases. Interestingly, *Pla2g12b*, phospholipase A family enzyme, was one of the most upregulated targets in HDAC9 KO-AT2 cells (Figure 4.11 D). Overall, the prominent changes in metabolism indicate the influence of HDAC9 on endoplasmic reticulum (ER) stress, leading to alterations in mitochondrial calcium transfer. The prolonged ER stress might be a triggered molecular mechanism in the metabolic dysregulation with aging. This concept is in line with the HDAC inhibitors provoking ER stress and facilitating ER-mitochondria tight binding (Chen et al., 2017). Another interesting finding from the RNA-seq is the upregulation of lysosomal degradation-related genes. Recycling of complex lipids, proteins, and nucleic acids is controlled by lysosomes and abrupt event in the process leads to lysosomal stress response-related diseases. Recently, HDAC inhibitors have been reported to be used for the treatment of some of the pediatric lysosomal storage disorders (LSDs). Here, HDAC inhibition activates the transcription of lysosomal genes (Annunziata et al., 2019). Along the same lines, the absence of HDAC9 function in aging AT2 cells might mimic a similar scenario, where the transcriptional activity of lysosomal degradation gene (*Lrp8*) was enhanced (Figure 4.11 C).

Upon nuclear translocation, HDAC9 mainly acts as scaffold protein by being a negative regulator of gene transcription through co-repressor complex. In general, HDACs are considered to induce histone deacetylation in the promoter regions of corresponding genes (Petrie et al., 2003). TOBIAS analysis of aged HDAC9 KO-AT2 cells demonstrated around 17% of the peaks for open regions and around 38% of the peaks for closed regions within promoters. The following transcription factors (TFs) showed the highest binding score within corresponding promoter sequences: CEBPE, CEBPB, CEBPG, and NFE2. These TFs are known to bind to the promoter of gene family called PLA2 (phospholipase A2 family) (Figure

4.12 A-D). Here, we speculate that HDAC9-mediated repressor complex is removed from the promoter region and allows to interaction of these TFs, leading to the upregulation of the phospholipase family genes expression. This data set specifically confirmed chromatin accessibility regarding PLA family with aging upon genetic ablation of HDAC9 in AT2 cells.

5.4 Chronological aging upon genetic ablation of HDAC9 plays a vital role in chronic inflammatory lung phenotype via lipid pro-inflammatory mediators

Changes in metabolic profiling are a prominent part of SAS-phenotype in cellular senescence and premature aging. Senescence is a cellular process where the cell undergoes cell cycle arrest while maintaining its metabolism. Phospholipids play a crucial role in membrane remodeling during senescence. Integration of transcriptomics and lipidomics exhibit that lipid-related genes are expressed differentially in senescent cells. This suggests that lipid composition alters at the global level, leading to excessive morphological changes by cell membrane remodeling. After this membrane remodeling, the senescent cells adopt SAS-phenotype, releasing a wide range of regulators into the surrounding environment and eventually inducing an inflammatory response within the tissue. All these mentioned changes are lipid composition-related within the cell membrane (Millner A. and Atilla-Gokcumen E.G., 2020). In the current study, we show that glycerolipids and fatty acids are the regulators of initiation and maintenance of senescent HDAC9-deficient AT2 cells and their inflammatory components. In a cell, the levels of the metabolites are determined by the following two factors: (1) the production of a metabolite within the cell, (2) the release and uptake of the metabolites through transporters into/from the surrounding environment. The higher levels of glycerophosphocholine in the supernatant were found in the face of no significant differences regarding the production of the choline metabolites in HDAC9 KO AT2 cells when compared to WT-AT2 cells (Figure 4.13 B, C and (Figure 4.14 B, C). This can be best explained by choline conversion into glycerophosphocholine and release into supernatant. In accordance, the choline levels were reduced in HDAC9 KO-AT2 cells, suggesting that choline was consumed for the glycerophosphocholine conversion (Figure 4.14 B). Another possibility for the decline in choline levels might be choline uptake by the transporters back inside the cells. Moreover, we observed that amino acid metabolism related to choline/betaine supplementation within Kennedy pathway was highly active in HDAC9 KO-AT2 cells (elevated levels of carnitine, sarcosine, alanine, aspartate, proline, and glutamate amino acids) (Figure 4.14 B). This suggests that senescent HDAC9 KO-AT2 cells have dysregulation of metabolites regarding release and uptake rather than production at a young age.

(2) Senescent HDAC9-deficient AT2 cells during aging showed elevated levels of phosphorylcholine, the functional group of PC, and GPC, whereas choline levels were not significantly changed when compared to aged WT-AT2 cells (Figure 4.13 D, E). Here, the production of choline metabolite within cell lysate was not affected by aging upon genetic ablation of HDAC9. However, the conversion of choline into phosphorylcholine and GPC was abruptly disturbed within aged HDAC9 KO-AT2 cells. A decline in these two downstream metabolites level might be occurred by either any disturbance in choline kinase axis or CDP-choline-phosphatidylcholine-phospholipase A2 axis. On the other hand, the release of choline produced from aged HDAC9 KO-AT2 cells was significantly elevated in the supernatant, while glycerophosphocholine and cystine were reduced (Figure 4.14 C, D). Normally, choline can be preferentially converted to betaine and entered into methionine-homocystine-cystine pathway or metabolized to PC-glycerophosphocholine branch. However, here we observed that choline was accumulated in the supernatant rather than further being metabolized. This could be due to a dysfunction of the transporters such as choline transporter (SLC5A7) or choline transporter-like proteins (CTL1 and CTL2), which are responsible for choline uptake. Collectively, these results indicate that there is a broken cycle of CDP-choline, which affects the circulating levels of downstream metabolites during aging upon genetic deletion of HDAC9. Since the pathway loop cannot be completed, thus aging senescent HDAC9 deficient-AT2 cells try to compensate for the metabolic activity by redirecting into free fatty acid branch via phospholipase A2 (PLA2).

(3) Phosphotidylcholine, the product of choline phospholipid metabolism, is normally metabolized by PLA2 to direct the whole pathway into the conversion of glycerophospcholine-choline axis. However, when there is a stress stimulus, PLA2 can join to arachidonic acid (AA) metabolism branch. PLA2 was recommended to be a major target from the ATAC- and RNA-sequencing that could be modulated and plays a key role in the metabolic switch in HDAC9 KO-AT2 cells. The metabolite levels did not show any change between aged WT vs HDAC9 KO-AT2 cells, suggesting the production process was not affected by either aging or genetic ablation of HDAC9 (Figure 4.15 A, B). However, the levels of circulating arachidonic acid and its precursor, linolenic acid were higher in the supernatant of aged HDAC9 KO-AT2 cells. In addition, the release of PGE2 and PGG2, pro-inflammatory downstream lipid metabolites derived from AA via cyclooxygenases (COX1 and COX2), were significantly elevated in aged HDAC9 KO-AT2 (Figure 4.15 C, D). Here, it seems that these pro-inflammatory lipid mediators are accumulated in the extracellular environment, which eventually might create a chronic stimulating signal to the neighbor cells. Due to this accumulation, they also might act

as a chemo-attractant for inflammatory cells and facilitate their migration towards the lung. Collectively, these results suggest that abrupted choline phospholipid metabolism might be directed towards AA pathway response via PLA2 to compensate for the required metabolic activity of the cells during aging upon HDAC9 deficiency.

(4) As the levels of prostaglandins were elevated, we focus on the main key enzyme cPLA2 (cytosolic phospholipase 2) within AA pathway. Mean fluorescence intensity of cPLA2 upregulated in HDAC9 KO-AT2 cells versus WT independently from aging (Figure 4.16 A, B). This data evidenced that cPLA2 is activated upon HDAC9 deficiency within senescent AT2 cells at a young age and prominently retained during aging. Moreover, protein expression analysis of cPLA2 and COX1 within AA pathway and its targets (Annexin A1, pERK) upregulated. In addition, the enzymatic activity of cPLA2 was remarkably higher while the total super family of PLA2 enzymatic activity did not show any significant difference (Figure 4.16 C, D). Collectively, these results suggest HDAC9 ablation in AT2 cells during aging boosts the expression and enzyme activity of cPLA2.

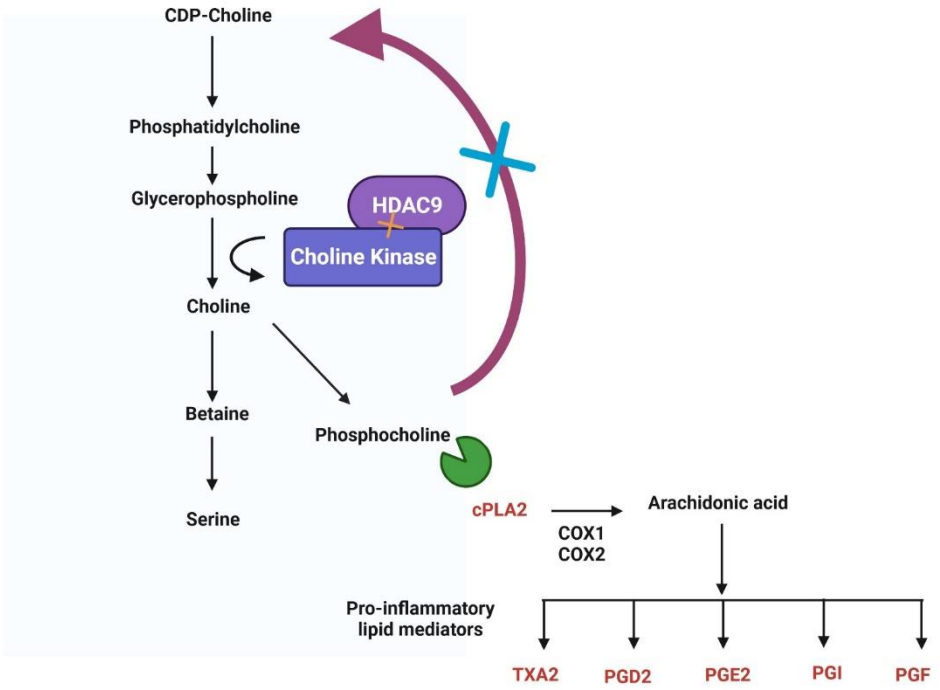

Figure 5.3: Schematic representative of broken choline phospholipid metabolism and its switch into free fatty acid metabolism via cPLA2.Generated by Biorender.

5.5 Altered immunometabolic response is present as internal organ communication beyond the lung with genetic ablation of HDAC9

Bronchus-associated lymphoid tissue (BALT) does not form in the normal lung but is present in different diseases. Leukocytes infiltrate the lung and assemble BALT structure, where T and B cells are located with stromal cells and endothelial cells. Interestingly, this structure is retained, independently from inflammation even though the inflammatory response is resolved. BALT is also reported to participate in pulmonary immune response and alters the manifestation of a disease (Hwang J.Y. et al., 2016). BALT structures are in cross-talk with innate immunity cells as well. For instance, cigarette smoke-induced BALT formation in COPD was reported to activate macrophages in B cell-dependent manner (John-Schuste G. et al., 2014). In this current study, we discovered that HDAC9-deficient lungs assemble BALT structures during aging (Figure 4.10 A). Immunofluorescence stainings clearly showed that assembled BALT areas consisted of predominantly T cells and a small portion of $Iba1^{+}$ macrophages (Figure 4.10 B). We speculate that the release of pro-inflammatory lipid mediators by senescent AT2 cells might provoke the infiltration of T cells inside the lung by acting as an attractant stimulation. Macrophage accumulation within BALT and the surrounding area might be due to organ communication between bone marrow and lung via systemic circulation.

To explore how HDAC9 deficiency affects the BM-derived macrophages and alters their phenotypic switches, inflammatory cytokine profiling was carried out. Based on the findings, we observed that: (1) HDAC9 was expressed equally higher in both M1 and M2-macrophages at a young age, whereas aged M2-macrophages expressed HDAC9 significantly higher. This data suggests that HDAC9 expression is in correlation with anti-inflammatory M2-macrophage phenotype during aging (Figure 4.19 B). Moreover, HDAC9 KO-M1-macrophages mainly expressed inflammatory genes (*Il6* and *Tnfα* for young, *Il1β* and *Tnfα* for the aged group, Figure 4.19 C-F) independently from age. It seems that HDAC depletion induces pro-inflammatory gene expression, supporting SAS-phenotype and physiological aging. On the other hand, *Tgfβ* expression from HDAC9 KO-M2-macrophages was promising even from the young age (Figure 4.19 D, F). *Tgfβ* is a gene associated with EMT. The upregulation of this gene is known to contribute the metabolic dysfunction, inflammation, and reduced generation capacity (Imran S.A.M. et al, 2021). In this regard, we speculate that HDAC9 KO-M2-macrophages fuel the retained substantial pro-inflammatory phenotype. Altogether, these results indicate that the genetic ablation of HDAC9 enhances the pro-inflammatory M1-phenotype irrespectively of aging. It seems that HDAC9 has a protective effect against inflammatory response.

(2) Alveolar macrophages (AMs) are the most abundant resident cell population in the lung. Apart from BM-derived macrophages, we also investigated the phenotypic response of AM toward HDAC9 depletion. Interestingly, both of pro-inflammatory genes (*Il1β,Il6,Tnfα*) and anti-inflammatory genes (*Mmp9,Il10, Tgfβ*) were upregulated in HDAC9 depleted M1-and M2-macrophages respectively (Figure 4.17 C, D). This contradicting data might be interpreted as the compensatory response of the immune system. In other words, the upregulation of anti-inflammatory genes might be an attempt to calm down the induced pro-inflammatory response that occurred by HDAC9 deficiency and maintain tissue homeostasis.

(3) Another aspect to investigate was the cross-talk between alveolar epithelial cells and alveolar macrophages regarding the proliferative capacity. As AT2 cells and AMs are the first cells in contact with pathogens, they must function simultaneously to eliminate pathogens by minimizing the damage within the lung. The paracrine communication between these 2 cells occurs via direct cell-cell contact or secreting molecules. AT2 cells carry ligands (CD200, CD47, and PDL-1) against extracellular membrane proteins of AMs (CD200R, SIRP1α, and PD-1), allowing the maintenance of the cross-talk. Apart from gap junctions, extracellular vesicles, and soluble regulators are used to communicate as well. Whether AT2 cells are the first to activate AM inflammatory response is still disputatious, it is known that both cells can stimulate each other to trigger a cellular response (Bissonnette E. Y et al., 2020). In the current study, alveolar macrophages exhibited higher proliferation in the presence of extended time point (Figure 4.18 A). However, the interaction of HDAC9 KO-AT2 cells in a culture system led AMs to display proliferative response in a shorter time point (Figure 4.18 C). Altogether, we concluded that alveolar epithelial cell-alveolar macrophage crosstalk enhances proliferative response upon HDAC9 silencing.

(4) The association between choline phospholipid metabolism and immune responsiveness of macrophages was reported and choline transporter-like protein 1 (CTL1) was highlighted for macrophage choline uptake (Snider S.A. et al., 2018). Towards, lipidomics was performed to evaluate how HDAC9 deficiency alters immunometabolic responses as internal organ communication beyond the lung. However, HDAC9 depletion did not induce the release of choline phospholipid metabolites from BM-derived M1 and M2 macrophages (Figure 4.20 B-E). When it comes to AA pathway, the levels of circulating linolenic acid were higher in HDAC9 depleted-M1 macrophages, whereas TBX2 level was interestingly low (Figure 4.21 B). Here, it seems that upstream metabolite, linolenic acid cannot be converted into prostaglandins properly. On the other hand, HDAC9-depleted-M2 macrophages did not show

any significant change. This data suggests that free fatty acid metabolism initially takes place in M1-macrophages upon HDAC9 depletion. However, the release of prostaglandins is not strong as observed in AT2 cells.

5.6 Conclusion

In this current study, we conclude that HDAC9 deficiency drives a cellular senescence and premature aging phenotype. Physiological aging upon genetic ablation of HDAC9 promotes SAS-phenotype with the contribution of pro-inflammatory lipid mediators released by AT2 cells. This may happen as two-tailed manner: (1) in nucleus, absence of HDAC9 scaffolded-repressive complex upon the corresponding promoter regions initiates transcriptional activity of PLA2 family genes, which encode inflammatory lipid mediators; (2) in cytoplasm, these inflammatory lipid mediators of AA pathway are produced in a higher rate to compensate the metabolic activity as HDAC9 deficient-AT2 cells cannot complete the loop of choline phospholipids metabolism during cellular senescence and aging. The broken cycle of choline metabolism is switched into AA pathway through upregulated cPLA2 activity. The released inflammatory lipid mediators (prostaglandins) may act as chemoattractant stimuli to accelerate the infiltration of immune cells, more dominantly T cell population. Based on this infiltration, BALT formation is occured as a final inflammatory manifestation within the lung.

We additionally concluded that HDAC9 deficiency alters immunometabolic response as internal organ communication beyond the lung. In the same line with the accelerated cellular senescence phenotype, the response of pro-inflammatory lipid mediators and the expression of pro-inflammatory genes in HDAC9 deficient-M1 macrophages were upregulated. Moreover, HDAC9-depleted alveolar macrophages exhibited increased proliferation when exposed to the media of HDAC9 KO-AT2 cells. This suggests that the metabolites released by HDAC9 KO-AT2 cells might affect the proliferation-related pathway of alveolar macrophage by cross-talk manner. Lastly, HDAC9 KO animal line might be considered as a mouse model of the accelerated cellular senescence without additional stimulus externally. Collectively, this study is important to understand the association of HDAC9 deficiency and the accelerated cellular senescence and aging.

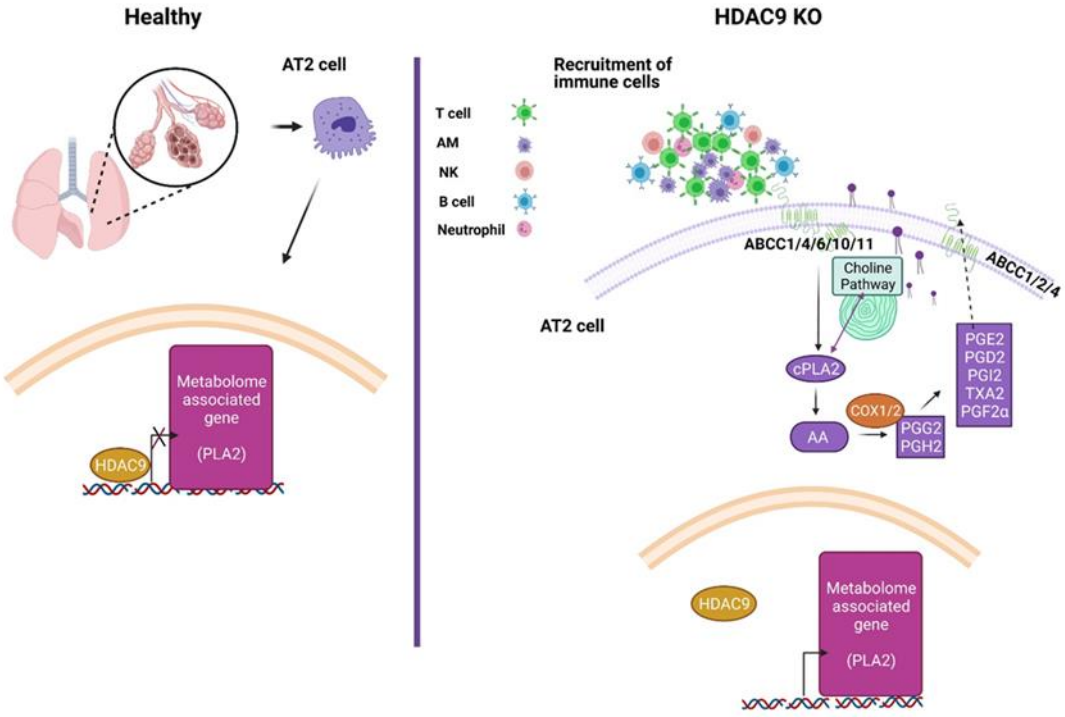

Figure 5.4: Proposed mechanism of initiated SAS-phenotype via the lack of HDAC9-mediated repressor complex. In healty AT2 cells, HDAC9-mediated repressor complex binds to the corresponding promoter regions of PLA2 family, blocking the transcriptional activity of the genes in . In the lack of HDAC9-mediated repressor complex, the related transription factors CEBPE, CEBPB, CEBPG, and NFE) bind to the promoter regions and the transcriptional activity of PLA2 is initiated. Upon this transcriptional activity, arachidonic pathway response is upregulated in the cytoplasm due to the incompleted choline pathway. cPLA2 actively metabolized the membrane phospholipids into arachidonic acid as a compensate response. AA is further metabolized to the prostaglandins via COX1/2 enzymes. The produced pro-inflammatory prostaglandins are released through the membrane transporters and act as a chemoattractant stimuli for the recruitment of various immune cells. Generated by Biorender.

5.7 Future Perspectives

Future experiments should be addressing the following points:

1. In this current study, we used global HDAC9 KO animals and investigated accelareated cellular senescence phenotype. In order to understand whether cellular senescence-associated inflammatory phenotype is specific to HDAC9 KO-AT2 cells, epithelial-specific HDAC9 *knockout* animals should be generated and SASP-related studies should be further conducted.

2. Lung compliance and hemodynamic studies should be carried out to analyze the effect of HDAC9 genetic depletion on the altered lung architectural changes and lung function.

3. In literature, HDAC9-related risk locus are known to create susceptibility for atherosclerotic stroke and coronary artery disease in humans (Prestel M. et al., 2019). In this regard, screening in HDAC9 SNPs (single nucleotide polymorphism) might be valuable to detect the tendency to the accelerated aging-related lung diseases at young age.

4. To understand how HDAC9 deficiency induce the transcriptional activity of PLA2 gene family and to determine the use of distinct TFs to bind at their respective promoters, RNA-interference tools can be employed to selectively manipulate each TF and observe the resulting effects on gene expression.

5. The binding protein partners of HDAC9, involving choline and AA pathways in the cytoplasm, should be characterized by mass spectometry. To determine if the observed phenotype is based on cPLA2-induced senescence, HDAC9-cPLA2 axis should be investigated with immunoprecipitation experiments. cPLA2 inhibitors can be used to reverse the inflammatory response through pro-inflammatory lipid mediators releasing. Additionally, cPLA2 KO animals can be cross-breeded with HDAC9 KO animals to use as a reversed phenotype-control group.

6. Choline uptake experiments should be conducted to see if there is a dysfunction of the transporters such as choline transporter (SLC5A7) or choline transporter-like proteins (CHL1 and CHL2) with HDAC9 deficiency. The rate of choline uptake can be measured

with ^{3}H choline chloride uptake. To determine the responsible transporter, RNA-interference tools against CHL1, CHL2 and SCL5A7 can be employed as well.

7. To study if the premature aging phenotype can be reversed in HDAC9 KO mice, senolytic drug experiment should be employed. Lung characteristics and inflammatory phenotype should be studied in senolytic drug-challenged in HDAC9 KO animals by lung compliance, cytokine profiling and histology.

6. SUMMARY

Age-related lung diseases are becoming an increasingly concerning public health issue worldwide.The rising prevalence of chronic lung diseases among older individuals draws attention to the need to develop preventative and curative strategies. Recent studies indicate that environmental factors such as epigenetic players are the important contributors to the development and progression of cellular senescence and aging-related diseases, but the molecular mechanisms that are at the foundation of this phenomenon are not yet well understood.

Through histological analysis, we confirmed that genetic removal of HDAC9 causes changes in the composition of pulmonary surfactants and reduces the regenerative capacity of cells in the lungs, resulting in decreased proliferation. Additionally, the depletion of HDAC9 leads to a clear reprogramming of AT2 cells, resulting in the emergence of new mesenchymal-like cells. Here, we also substantiated that genetic ablation of HDAC9 provokes cellular senescence and premature aging response in AT2 cell-manner. HDAC9-deficient AT2 cells undergoing senescence exhibit SAS phenotype as a stress response. These SASP related-changes include a slight increase in the expression of p21, SA-β-GAL, pro-inflammatory cytokines, and metalloproteinases, as compared to age-matched WT-AT2 cells. Moreover, the depletion of HDAC9 exacerbates age-related phenotypical changes, including a significant increase in p21 expression, the number of SA-β-GAL positive cells, and pro-inflammatory cytokines (*Il6, Il1β, iNOS*) in AT2 cells from HDAC9-ablated aged mice. As a final inflammatory phenotype, we also observed BALT formation in HDAC9-deficient aged lung. Immunofluorescence stainings clearly showed that assembled BALT areas consisted of predominantly T cells and a small portion of $Iba1^+$ macrophages.

A series of high-throughput studies further confirmed that HDA9 deficiency alters cellular landscape of aged lungs based on the imbalanced abundance of cell populations. This includes a significant reduction of $CD117^+$ and $EpCAM^+$ epithelial cell populations along with an increased proportion of adaptive immune cells ($CD8^+/CD4^+$ T cell ratio and B cells). Further, the results from RNA sequencing indicate that HDAC9-mediated transcriptional landscape is potentially responsible for drastic alterations in metabolic pathways of AT2 cells with aging. *Pla2g12b*, phospholipase A family enzyme, was one of the most upregulated targets in HDAC9 KO-AT2 cells. Following, ATAC-sequencing and TOBIAS analysis revealed that CEBPE, CEBPB, CEBPG, and NFE transcription factors, showed the highest binding score within corresponding promoter sequences of gene family called PLA2 (phospholipase A2 family).

Changes in metabolic profiling are a prominent part of SAS-phenotype in cellular senescence and premature aging. The levels of choline were found to be reduced in young HDAC9 KO-AT2 cells. Furthermore, we observed amino acid metabolism related to choline/betaine supplementation within the Kennedy pathway was highly active in young HDAC9 KO-AT2 cells, as evidenced by elevated levels of carnitine, sarcosine, alanine, aspartate, proline, and glutamate amino. Moreover, the physiological aging upon HDAC9 deficiency exhibits the disrupted conversion of choline into phosphorylcholine and GPC. On the other hand, the release of choline produced from aged HDAC9 KO-AT2 cells was significantly elevated in the supernatant. Further metabolic analysis of AA pathway revealed the levels of circulating arachidonic acid and linolenic acid were higher in the supernatant of aged HDAC9 KO-AT2 cells. In addition, the release of PGE2 and PGG2, pro-inflammatory downstream lipid metabolites were significantly elevated in aged HDAC9 KO-AT2. Lastly, we confirmed that key enzyme cPLA2 (cytosolic phospholipase 2) within AA pathway, showed higher enzymatic activity with upregulated protein expression in HDAC9 KO-AT2 cells.

A series of in vitro studies confirmed that HDAC9 deficiency impacts BM-derived macrophages. HDAC9 KO-M1-macrophages mainly expressed inflammatory genes (*Il6* and *Tnfα* for young, *Il1β* and *Tnfα* for the aged group). On the other hand, *Tgfβ* expression from HDAC9 KO-M2-macrophages was promising even from the young age. Apart from BM-derived macrophages, we also investigated the phenotypic response of AM toward HDAC9 depletion. Interestingly, both of pro-inflammatory genes (*Il1β,Il6,Tnfα*) and anti-inflammatory genes (*Mmp9,Il10, Tgfβ*) were upregulated in HDAC9 depleted M1-and M2- macrophages respectively. AMs also exhibited higher proliferation in the presence of the collected media from HDAC9-deficient AT2 cells. Lastly, lipidomic analysis revealed that the levels of circulating linolenic acid were higher in HDAC9 depleted-M1 macrophages, whereas TBX2 level was interestingly low.

In conclusion, this study demonstrated the absence of HDAC9 leads to premature aging and cellular senescence-associated secretory phenotype with the aid of pro-inflammatory lipid mediators that are released by AT2 cells. Prostaglandins, the released inflammatory lipid mediators, may act as chemoattractant stimuli to accelerate the infiltration of immune cells, predominantly T cells, leading to BALT formation as a final inflammatory manifestation within the lung.

7. ZUSAMMENFASSUNG

Altersbedingte Lungenerkrankungen werden weltweit zu einem zunehmend besorgniserregenden Problem der öffentlichen Gesundheit. Die steigende Prävalenz chronischer Lungenerkrankungen bei älteren Menschen lenkt zeigt die Notwendigkeit, präventive und heilende Strategien zu entwickeln. Jüngste Studien zeigen, dass Umweltfaktoren wie epigenetische Akteure eine wichtige Rolle bei der Entstehung und beim Verlauf der zellulären Seneszenz und bei altersbedingten Krankheiten spielen. Die zugrundeliegenden molekularen Mechanismen sind hingegen nur unzureichend untersucht.

Durch histologische Analysen haben wir bestätigt, dass die genetische Entfernung von HDAC9 Veränderungen in der Zusammensetzung von Lungensurfactanten verursacht und die Regenerationsfähigkeit von Zellen in der Lunge verringert, was zu einer verringerten Proliferation führt. Darüber hinaus führt die Depletion von HDAC9 zu einer deutlichen Umprogrammierung von AT2-Zellen, wodurch neue mesenchymal-ähnliche Zellen entstehen. Wir konnten auch belegen, dass die genetische Ablation von HDAC9 eine zelluläre Seneszenz und eine vorzeitige Alterungsreaktion nach Art von AT2-Zellen hervorruft. HDAC9-defiziente AT2-Zellen, welche seneszent werden, zeigen den SAS-Phänotyp als Stressreaktion. Diese SASP-bedingten Veränderungen umfassen einen im Vergleich zu altersangepassten WT-AT2-Zellen leichten Anstieg der Expression von p21, SA-β-GAL, entzündungsfördernden Zytokinen und Metalloproteinasen. Darüber hinaus verschlimmert die Depletion von HDAC9 altersbedingte phänotypische Veränderungen, einschließlich einer signifikanten Zunahme der p21-Expression, sowie der Anzahl SA-β-GAL-positiver Zellen und proinflammatorischer Zytokine (Il6, Il1β, iNOS) in AT2-Zellen gealterter Mäuse ohne HDAC9. Als letzten entzündlichen Phänotyp beobachteten wir auch die BALT-Bildung in HDAC9-defizienter gealterter Lunge. Immunfluoreszenzfärbungen zeigten deutlich, dass zusammengesetzte BALT-Bereiche überwiegend aus T-Zellen und einem kleinen Teil von Iba1+-Makrophagen bestanden.

Eine Reihe von Hochdurchsatzstudien bestätigte weiter, dass ein HDA9-Mangel die Zelllandschaft gealterter Lungen durch unausgewogene Zellpopulationsgrößen verändert. Dazu gehört eine signifikante Reduktion der CD117+- und EpCAM+-Epithelzellpopulationen zusammen mit einem erhöhten Anteil adaptiver Immunzellen (CD8+/CD4+-T-Zell-Verhältnis und B-Zellen). Darüber hinaus deuten die Ergebnisse der RNA-Sequenzierung darauf hin, dass die HDAC9-vermittelte Transkriptionslandschaft möglicherweise für drastische Veränderungen der Stoffwechselwege von AT2-Zellen mit zunehmendem Alter verantwortlich

ist. *Pla2g12b*, ein Enzym der Phospholipase-A-Familie, war eines der am stärksten hochregulierten Ziele in HDAC9-KO-AT2-Zellen. Anschließend ergaben die ATAC-Sequenzierung und die TOBIAS-Analyse, dass die Transkriptionsfaktoren CEBPE, CEBPB, CEBPG und NFE den höchsten Bindungswert innerhalb der entsprechenden Promotorsequenzen der PLA2 (Phospholipase A2-Familie) Genfamilie zeigten.

Veränderungen im Stoffwechselprofil sind ein wichtiger Bestandteil des SAS-Phänotyps bei zellulärer Seneszenz und vorzeitiger Alterung. Es wurde festgestellt, dass die Cholinspiegel in jungen HDAC9 KO-AT2-Zellen reduziert waren. Darüber hinaus beobachteten wir, dass der Aminosäurestoffwechsel im Zusammenhang mit der Cholin/Betain-Supplementierung innerhalb des Kennedy-Signalwegs in jungen HDAC9-KO-AT2-Zellen hoch aktiv war, was durch erhöhte Carnitin-, Sarcosin-, Alanin-, Aspartat-, Prolin- und Glutamat-Aminowerte belegt wurde. Darüber hinaus zeigt die physiologische Alterung bei HDAC9-Mangel die gestörte Umwandlung von Cholin in Phosphorylcholin und GPC. Andererseits war die Freisetzung von Cholin, das von gealterten HDAC9-KO-AT2-Zellen produziert wurde, im Überstand signifikant erhöht. Die weitere metabolische Analyse des AA-Signalwegs ergab, dass die Konzentrationen an zirkulierender Arachidonsäure und Linolensäure im Überstand von gealterten HDAC9-KO-AT2-Zellen höher waren. Darüber hinaus war die Freisetzung von PGE2 und PGG2, entzündungsfördernden nachgeschalteten Lipidmetaboliten, bei gealtertem HDAC9 KO-AT2 signifikant erhöht. Schließlich bestätigten wir, dass das Schlüsselenzym cPLA2 (zytosolische Phospholipase 2) des AA-Signalwegs eine höhere enzymatische Aktivität mit hochregulierter Proteinexpression in HDAC9 KO-AT2-Zellen zeigte.

Eine Reihe von In-vitro-Studien bestätigte, dass sich ein HDAC9-Mangel auf BM-Makrophagen auswirkt. HDAC9 KO-M1-Makrophagen exprimierten hauptsächlich Entzündungsgene (Il6 und Tnfα für die junge, Il1β und Tnfα für die alte Gruppe). Andererseits war die Tgfβ-Expression von HDAC9 KO-M2-Makrophagen bereits im jungen Alter vielversprechend. Abgesehen von BM-abgeleiteten Makrophagen untersuchten wir auch die phänotypische Reaktion von AM auf HDAC9-Depletion. Interessanterweise wurden sowohl entzündungsfördernde Gene (*Il1β, Il6, Tnfα*) als auch entzündungshemmende Gene (*Mmp9, Il10, Tgfβ*) in HDAC9-depletierten M1- bzw. M2-Makrophagen hochreguliert. AMs zeigten auch in Gegenwart von Medium, welches von von HDAC9-defizienten AT2-Zellen abgesammelt wurde, eine höhere Proliferation. Schließlich zeigte die lipidomische Analyse, dass die Spiegel der zirkulierenden Linolensäure in HDAC9-depletierten M1-Makrophagen höher waren, während der TBX2-Spiegel interessanterweise niedrig war.

Zusammenfassend zeigte diese Studie, dass das Fehlen von HDAC9 über entzündungsförderndee Lipidmediatoren, die von AT2-Zellen freigesetzt werden, zu vorzeitiger Alterung und zellulärem Seneszenz-assoziiertem sekretorischem Phänotyp führt. Prostaglandine, die freigesetzten entzündlichen Lipidmediatoren, können als chemoattraktive Stimuli wirken, um die Infiltration von Immunzellen, hauptsächlich T-Zellen, zu beschleunigen, was zur BALT-Bildung als letzte Manifestation der Entzündung in der Lunge führt.

8. LIST OF ABBREVIATIONS

$^{-/-}$ Homozygous Knockout of the indicated gene

7-AAD - 7-aminoactinomycin D

AA- arachidonic acid

ABTS - 2, 2'-azino-bis 3-ethylbenzothiazoline-6-sulphonic acid

AT1 - alveolar type I cells

AT2 - alveolar epithelial type II cells

BALT - Bronchus-associated lymphoid tissue

BCR - B cell receptor

BSA - Bovine serum albumin

CARE - co-chaperone adaptive response

C. elegans - *Caenorhabditis elegans*

CAR - chimeric antigen receptor

CTL1 - choline transporter-like 1 protein

CTL2 - choline transporter-like 2 protein

CHD - chromodomain helicase DNA-binding

CNVs - Copy Number Variations

COX1- cyclooxygenase 1

CpG - cytosine-phospho-guanine

cPLA2 - cytosolic phospholipase 2

COPD - chronic obstructive pulmonary disease

DDR - DNA damage response

D+Q - dasatinib and quercetin

ETC - electron transport chain

EMT - epithelial-to-mesenchymal transition

FCS - fetal bovine serum

FEV1/FVC - forced expiratory volume in 1 second/ forced vital capacity

FDR - false discovery rate

FMO - fluorescence minus one control

GPC - glycerophosphocholine

GWAS - Genome-wide association studies

LPS - Lipopolysaccharide

HAT – Histone acetyl transferase

HBSS - Hank´s Balanced Salt Solution

HDAC – Histone deacetylase

HDACi - HDAC inhibition

HDMs - histone demethylases

HGPS - Hutchinson-Gilford syndrome

HSCs - hematopoietic stem cells

HMTs - histone methyltransferases

hTERT - human telomerase reverse transcriptase

IL-8 - interleukin-8

Ifnγ - Interferon-γ

IPF - idiopathic pulmonary fibrosis

iPSCs - induced pluripotent stem cells

ISWI - imitation switch

MITR - MEF2-interacting transcriptional repressor

miRNAs – microRNAs

MH-S - mouse alveolar macrophage cells

H&E - hematoxylin and eosin

HRP - horseradish peroxidase

HPRT - hypoxanthine phosphoribosyltransferase1

MSCs - mesenchymal stromal cells

mtDNA - mitochondrial DNA

MUC5B - Mucin 5B

NES - nuclear export signal

PAGE - polyacrylamyde gel

PARP - poly ADP ribose polymerase

4-PBA - 4-phenyl butyric acid

PC - phosphocholine

PFA – paraformaldehyde

PLA2 - phospholipase A2

Ppi - protease-phosphatase inhibitor cocktail

PtdCho - phosphatidylcholine

PVDF - polyvinylidene fluoride

rmM-CSF - recombinant murine macrophage stimulating factor

RRF - ragged red fibers

ROS - reactive oxygen species

RT-qPCR - Real time Quantitative Polymerase chain reaction

SA-β-GAL - senescence-associated β-GAL

SASP - senescence-associated secretory phenotype

SDS - sodium dodecyl sulphate

SFTPA2 - surfactant-associated proteins A

SFTPC - surfactant protein C gene

SREBP - sterol-response element binding protein

S. Pneumoniae - Streptococcus Pneumoniae

TAFs- telomere-associated DDR foci

TCA - tricarboxylic acid

TCR - T cell receptor

tDDR - DDR at telomeres

TFBS - transcription factor binding site

T_{FR} - T follicular regulatory cells

TGF-b1 - transforming growth factor b1

TLRs – toll like receptors

TP53 - tumor protein 53

TRF-1 - telomere repeat binding factor-1

TBX2 - Thromboxane A2

UPR - unfolded protein response

UPS - ubiquitin-proteasome system

UTX1 - Ubiquitously Transcribed TPR on X1

9. LIST OF FIGURES

10. LIST OF TABLES

11. REFERENCES

Alder JK, Chen JJ, Lancaster L, Danoff S, Su SC, Cogan JD, Vulto I, Xie M, Qi X, Tuder RM, Phillips JA 3rd, Lansdorp PM, Loyd JE, Armanios MY. (2008). Short telomeres are a risk factor for idiopathic pulmonary fibrosis. Proc Natl Acad Sci U S A. **2**;105(35):13051-6.

Agrawal A, Agrawal S, Cao JN, Su H, Osann K, Gupta S. (2007). Altered innate immune functioning of dendritic cells in elderly humans: a role of phosphoinositide 3-kinase-signaling pathway. J Immunol. **1**;178(11):6912-22.

Anderson R, Lagnado A, Maggiorani D, Walaszczyk A, Dookun E, Chapman J, Birch J, Salmonowicz H, Ogrodnik M, Jurk D, Proctor C, Correia-Melo C, Victorelli S, Fielder E, Berlinguer-Palmini R, Owens A, Greaves LC, Kolsky KL, Parini A, Douin-Echinard V, LeBrasseur NK, Arthur HM, Tual-Chalot S, Schafer MJ, Roos CM, Miller JD, Robertson N, Mann J, Adams PD, Tchkonia T, Kirkland JL, Mialet-Perez J, Richardson GD, Passos JF. (2019). Length-independent telomere damage drives post-mitotic cardiomyocyte senescence. EMBO J. **1**;38(5):e100492.

Annunziata I, van de Vlekkert D, Wolf E, Finkelstein D, Neale G, Machado E, Mosca R, Campos Y, Tillman H, Roussel MF, Andrew Weesner J, Ellen Fremuth L, Qiu X, Han MJ, Grosveld GC, d'Azzo A. (2019). 'MYC competes with MiT/TFE in regulating lysosomal biogenesis and autophagy through an epigenetic rheostat'. Nat Commun. **9**;10(1):3623.

Ameur A, Zaghlool A, Halvardson J, Wetterbom A, Gyllensten U, Cavelier L, Feuk L. (2011). Total RNA sequencing reveals nascent transcription and widespread co-transcriptional splicing in the human brain. Nat Struct Mol Biol. **6**;18(12):1435-40.

Amor C, Feucht J, Leibold J, Ho YJ, Zhu C, Alonso-Curbelo D, Mansilla-Soto J, Boyer JA, Li X, Giavridis T, Kulick A, Houlihan S, Peerschke E, Friedman SL, Ponomarev V, Piersigilli A, Sadelain M, Lowe SW. (2020). Senolytic CAR T cells reverse senescence-associated pathologies. Nature. **583**(7814):127-132.

Araya J, Kojima J, Takasaka N, Ito S, Fujii S, Hara H, Yanagisawa H, Kobayashi K, Tsurushige C, Kawaishi M, Kamiya N, Hirano J, Odaka M, Morikawa T, Nishimura SL, Kawabata Y, Hano H, Nakayama K, Kuwano K. (2013). Insufficient autophagy in idiopathic pulmonary fibrosis. Am J Physiol Lung Cell Mol Physiol. **1**;304(1):L56-69.

Bahar R, Hartmann CH, Rodriguez KA, Denny AD, Busuttil RA, Dollé ME, Calder RB, Chisholm GB, Pollock BH, Klein CA, Vijg J. (2006). Increased cell-to-cell variation in gene expression in ageing mouse heart. Nature. **22**;441(7096):1011-4.

Balch WE, Morimoto RI, Dillin A, Kelly JW. (2008). Adapting proteostasis for disease intervention. Science. **15**;319(5865):916-9.

Balch WE, Sznajder JI, Budinger S, Finley D, Laposky AD, Cuervo AM, Benjamin IJ, Barreiro E, Morimoto RI, Postow L, Weissman AM, Gail D, Banks-Schlegel S, Croxton T, Gan W. (2014). Malfolded protein structure and proteostasis in lung diseases. Am J Respir Crit Care Med. **1**;189(1):96-103.

Baker MG, Barnard LT, Kvalsvig A, Verrall A, Zhang J, Keall M, Wilson N, Wall T, Howden-Chapman P. (2012). Increasing incidence of serious infectious diseases and inequalities in New Zealand: a national epidemiological study. Lancet**. 24**;379(9821):1112-9.

Barkauskas CE, Cronce MJ, Rackley CR, Bowie EJ, Keene DR, Stripp BR, Randell SH, Noble PW, Hogan BL. (2013). Type 2 alveolar cells are stem cells in adult lung. J Clin Invest. **123**(7):3025-36.

Basisty N, Kale A, Jeon OH, Kuehnemann C, Payne T, Rao C, Holtz A, Shah S, Sharma V, Ferrucci L, Campisi J, Schilling B. (2020). A proteomic atlas of senescence-associated secretomes for aging biomarker development. PLoS Biol. **16**;18(1):e3000599.

Behrens A, van Deursen JM, Rudolph KL, Schumacher B. (2014). Impact of genomic damage and ageing on stem cell function. Nat Cell Biol. **16**(3):201-7.

Bentsen M, Goymann P, Schultheis H, Klee K, Petrova A, Wiegandt R, Fust A, Preussner J, Kuenne C, Braun T, Kim J, Looso M. (2020). 'ATAC-seq footprinting unravels kinetics of transcription factor binding during zygotic genome activation'. Nat Commun. **26**;11(1):4267.

Bernardes de Jesus B, Vera E, Schneeberger K, Tejera AM, Ayuso E, Bosch F, Blasco MA. (2012). Telomerase gene therapy in adult and old mice delays aging and increases longevity without increasing cancer. EMBO Mol Med. **4**(8):691-704.

Birch J, Anderson RK, Correia-Melo C, Jurk D, Hewitt G, Marques FM, Green NJ, Moisey E, Birrell MA, Belvisi MG, Black F, Taylor JJ, Fisher AJ, De Soyza A, Passos JF. (2015). DNA damage response at telomeres contributes to lung aging and chronic obstructive pulmonary disease. Am J Physiol Lung Cell Mol Physiol. **15**;309(10):L1124-37.

Bissonnette EY, Lauzon-Joset JF, Debley JS, Ziegler SF. (2020). 'Cross-Talk Between Alveolar Macrophages and Lung Epithelial Cells is Essential to Maintain Lung Homeostasis'. Front Immunol. 15;11:583042.

Blackburn EH, Greider CW, Szostak JW. (2006). Telomeres and telomerase: the path from maize, Tetrahymena and yeast to human cancer and aging. Nat Med. **12**(10):1133-8.

Brandenberger C. and Mühlfeld C (2017). 'Mechanisms of lung aging'. Cell and Tissue Research **367**(3):469-480.

Brusselle GG, Joos GF, Bracke KR. (2011). New insights into the immunology of chronic obstructive pulmonary disease. Lancet. **378**: 1015–1026.

Bodas M, Patel N, Silverberg D, Walworth K, Vij N. (2017). Master Autophagy Regulator Transcription Factor EB Regulates Cigarette Smoke-Induced Autophagy Impairment and Chronic Obstructive Pulmonary Disease-Emphysema Pathogenesis. Antioxid Redox Signal. **20**;27(3):150-167.

Boe DM, Boule LA, Kovacs EJ. (2017). Innate immune responses in the ageing lung. Clin Exp Immunol. **187**(1):16-25.

Bolger AM, Lohse M, Usadel B. (2014). 'Trimmomatic: a flexible trimmer for Illumina sequence data'. Bioinformatics. **1**;30(15):2114-20.

Boehm M, Slack F. (2005). A developmental timing microRNA and its target regulate life span in C. elegans. Science. **23**;310(5756):1954-7.

Boulias K, Horvitz HR. (2012). The C. elegans microRNA mir-71 acts in neurons to promote germline-mediated longevity through regulation of DAF-16/FOXO. Cell Metab. **4**;15(4):439-50.

Bua E, Johnson J, Herbst A, Delong B, McKenzie D, Salamat S, Aiken JM. (2006). Mitochondrial DNA-deletion mutations accumulate intracellularly to detrimental levels in aged human skeletal muscle fibers. Am J Hum Genet. **79**(3):469-80.

Buenrostro JD, Giresi PG, Zaba LC, Chang HY, Greenleaf WJ.(2013). 'Transposition of native chromatin for fast and sensitive epigenomic profiling of open chromatin, DNA-binding proteins and nucleosome position'. Nat Methods. **10**(12):1213-8.

Bueno M, Lai YC, Romero Y, Brands J, St Croix CM, Kamga C, Corey C, Herazo-Maya JD, Sembrat J, Lee JS, Duncan SR, Rojas M, Shiva S, Chu CT, Mora AL. (2015). PINK1 deficiency impairs mitochondrial homeostasis and promotes lung fibrosis. J Clin Invest. **125**(2):521-38.

Burtner CR, Kennedy BK. (2010). Progeria syndromes and ageing: what is the connection? Nat Rev Mol Cell Biol. **11**(8):567-78.

Bustos ML, Huleihel L, Kapetanaki MG, Lino-Cardenas CL, Mroz L, Ellis BM, McVerry BJ, Richards TJ, Kaminski N, Cerdenes N, Mora AL, Rojas M. (2014). Aging mesenchymal stem cells fail to protect because of impaired migration and antiinflammatory response. Am J Respir Crit Care Med. **1**;189(7):787-98.

Cabrera S, Maciel M, Herrera I, Nava T, Vergara F, Gaxiola M, López-Otín C, Selman M, Pardo A. (2015). Essential role for the ATG4B protease and autophagy in bleomycin-induced pulmonary fibrosis. Autophagy. **3**;11(4):670-84

Calado RT, Young NS. (2009). Telomere diseases. N Engl J Med. **10**;361(24):2353-65.

Calderwood SK, Murshid A, Prince T. (2009). The shock of aging: molecular chaperones and the heat shock response in longevity and aging--a mini-review. Gerontology. **55**(5):550-8.

Calhoun C, Shivshankar P, Saker M, Sloane LB, Livi CB, Sharp ZD, Orihuela CJ, Adnot S, White ES, Richardson A, Le Saux CJ. (2016). Senescent Cells Contribute to the Physiological Remodeling of Aged Lungs. J Gerontol A Biol Sci Med Sci. **71**(2):153-60.

Cao K, Blair CD, Faddah DA, Kieckhaefer JE, Olive M, Erdos MR, Nabel EG, Collins FS. (2011). Progerin and telomere dysfunction collaborate to trigger cellular senescence in normal human fibroblasts. J Clin Invest. **121**(7):2833-44

Chatterjee TK, Idelman G, Blanco V, Blomkalns AL, Piegore MG Jr, Weintraub DS, Kumar S, Rajsheker S, Manka D, Rudich SM, Tang Y, Hui DY, Bassel-Duby R, Olson EN, Lingrel JB, Ho SM, Weintraub NL. (2011). 'Histone deacetylase 9 is a negative regulator of adipogenic differentiation'. J Biol Chem. 5;286(31):27836-47.

Chawla G, Deosthale P, Childress S, Wu YC, Sokol NS. (2016). A let-7-to-miR-125 MicroRNA Switch Regulates Neuronal Integrity and Lifespan in Drosophila. PLoS Genet. **10**;12(8):e1006247.

Chelvarajan L, Popa D, Liu Y, Getchell TV, Stromberg AJ, Bondada S. (2007). Molecular mechanisms underlying anti-inflammatory phenotype of neonatal splenic macrophages. J Leukoc Biol. **82**(2):403-16.

Chen Y, Tsai YH, Tseng SH.(2017). 'HDAC Inhibitors and RECK Modulate Endoplasmic Reticulum Stress in Tumor Cells'. Int J Mol Sci. **26**;18(2):258.

Chen J, Xie JJ, Jin MY, Gu YT, Wu CC, Guo WJ, Yan YZ, Zhang ZJ, Wang JL, Zhang XL, Lin Y, Sun JL, Zhu GH, Wang XY, Wu YS. (2018). Sirt6 overexpression suppresses senescence and apoptosis of nucleus pulposus cells by inducing autophagy in a model of intervertebral disc degeneration. Cell Death Dis. **19**;9(2):56.

Chen G, Kroemer G, Kepp O. (2020). Mitophagy: An Emerging Role in Aging and Age-Associated Diseases. Front Cell Dev Biol. **26**;8:200.

Chen J, Liu Z, Wang H, Qian L, Li Z, Song Q, Zhong G. (2021). SIRT6 enhances telomerase activity to protect against DNA damage and senescence in hypertrophic ligamentum flavum cells from lumbar spinal stenosis patients. Aging (Albany NY). **10**;13(4):6025-6040.

Childs BG, Durik M, Baker DJ, van Deursen JM. (2015). Cellular senescence in aging and age-related disease: from mechanisms to therapy. Nat Med. **21**(12):1424-35.

Cho SJ, Plataki M, Mitzel D, Lowry G, Rooney K, Stout-Delgado H. (2018). Decreased NLRP3 inflammasome expression in aged lung may contribute to increased susceptibility to secondary Streptococcus pneumoniae infection. Exp Gerontol. **105**:40-46.

Chocron ES, Munkácsy E, Pickering AM. (2019). Cause or casualty: The role of mitochondrial DNA in aging and age-associated disease. Biochim Biophys Acta Mol Basis Dis. **1**;1865(2):285-297.

Clapier CR, Cairns BR. (2009). The biology of chromatin remodeling complexes. Annu Rev Biochem. **78**:273-304.

Cloonan SM, Choi AM. (2016). Mitochondria in lung disease. J Clin Invest. **1**;126(3):809-20.

Cortopassi GA, Arnheim N. (1990). Detection of a specific mitochondrial DNA deletion in tissues of older humans. Nucleic Acids Res. **11**;18(23):6927-33.

Córdoba-Lanús E, Cazorla-Rivero S, Espinoza-Jiménez A, de-Torres JP, Pajares MJ, Aguirre-Jaime A, Celli B, Casanova C. (2017). Telomere shortening and accelerated aging in COPD: findings from the BODE cohort. Respir Res. **13;**18(1):59.

Cruz C, Della Rosa M, Krueger C, Gao Q, Horkai D, King M, Field L, Houseley J. (2018). Tri-methylation of histone H3 lysine 4 facilitates gene expression in ageing cells. Elife. **2**;7:e34081.

Davoli T, de Lange T. (2011). The causes and consequences of polyploidy in normal development and cancer. Annu Rev Cell Dev Biol. **27**:585-610.

de Cabo R, Mattson MP. (2019). Effects of Intermittent Fasting on Health, Aging, and Disease. N Engl J Med. **26**;381(26):2541-2551.

de Magalhães JP, Curado J, Church GM. (2009). Meta-analysis of age-related gene expression profiles identifies common signatures of aging. Bioinformatics. **1**;25(7):875-81.
Dechat T, Pfleghaar K, Sengupta K, Shimi T, Shumaker DK, Solimando L, Goldman RD. (2008). Nuclear lamins: major factors in the structural organization and function of the nucleus and chromatin. Genes Dev. **1**;22(7):832-53.

Deeks SG. (2011). HIV infection, inflammation, immunosenescence, and aging. Annu Rev Med. **62**:141-55.

Demanelis K, Jasmine F, Chen LS, Chernoff M, Tong L, Delgado D, Zhang C, Shinkle J, Sabarinathan M, Lin H, Ramirez E, Oliva M, Kim-Hellmuth S, Stranger BE, Lai TP, Aviv A, Ardlie KG, Aguet F, Ahsan H; GTEx Consortium; Doherty JA, Kibriya MG, Pierce BL. (2020). Determinants of telomere length across human tissues. Science. **11**;369(6509):eaaz6876.

Di Micco R, Krizhanovsky V, Baker D, d'Adda di Fagagna F. (2021). Cellular senescence in ageing: from mechanisms to therapeutic opportunities. Nat Rev Mol Cell Biol. **22**(2):75-95.

Di Giorgio E, Paluvai H, Dalla E, Ranzino L, Renzini A, Moresi V, Minisini M, Picco R and Brancolini C. (2021). 'HDAC4 degradation during senescence unleashes an epigenetic program driven by AP-1/p300 at selected enhancers and super-enhancers'. Genome Biol. **22**, 129.

Djeghloul D, Kuranda K, Kuzniak I, Barbieri D, Naguibneva I, Choisy C, Bories JC, Dosquet C, Pla M, Vanneaux V, Socié G, Porteu F, Garrick D, Goodhardt M. (2016). Age-Associated Decrease of the Histone Methyltransferase SUV39H1 in HSC Perturbs Heterochromatin and B Lymphoid Differentiation. Stem Cell Reports. **14**;6(6):970-984.

Dobin A, Davis CA, Schlesinger F, Drenkow J, Zaleski C, Jha S, Batut P, Chaisson M, Gingeras TR. (2013). 'STAR: ultrafast universal RNA-seq aligner'. Bioinformatics. **1**;29(1):15-21.

Dzau VJ, Inouye SK, Rowe JW, Finkelman E, Yamada T.(2019). Enabling Healthful Aging for All - The National Academy of Medicine Grand Challenge in Healthy Longevity. N Engl J Med. 31;381(18):1699-1701.

Espada J, Varela I, Flores I, Ugalde AP, Cadiñanos J, Pendás AM, Stewart CL, Tryggvason K, Blasco MA, Freije JM, López-Otín C. (2008). Nuclear envelope defects cause stem cell dysfunction in premature-aging mice. J Cell Biol. **7**;181(1):27-35.

Evason K, Collins JJ, Huang C, Hughes S, Kornfeld K. 2008). 'Valproic acid extends Caenorhabditis elegans lifespan'. Aging Cell. **7**(3):305-17.

Faggioli F, Wang T, Vijg J, Montagna C. (2012). Chromosome-specific accumulation of aneuploidy in the aging mouse brain. Hum Mol Genet. **15**;21(24):5246-53.

Faheem MM, Seligson ND, Ahmad SM, Rasool RU, Gandhi SG, Bhagat M. and Goswami A. (2020). 'Convergence of therapy-induced senescence (TIS) and EMT in multistep carcinogenesis: current opinions and emerging perspectives'. Cell Death Discovery. 6:51.

Fain SB, Altes TA, Panth SR, Evans MD, Waters B, Mugler JP 3rd, Korosec FR, Grist TM, Silverman M, Salerno M, Owers-Bradley J. (2005). Detection of age-dependent changes in healthy adult lungs with diffusion-weighted 3He MRI. Acad Radiol. **12**(11):1385-93.

Fakouri NB, Hou Y, Demarest TG, Christiansen LS, Okur MN, Mohanty JG, Croteau DL, Bohr VA. (2019). Toward understanding genomic instability, mitochondrial dysfunction and aging. FEBS J. **286**(6):1058-1073.

Fang F, Yu M, Cavanagh MM, Hutter Saunders J, Qi Q, Ye Z, Le Saux S, Sultan W, Turgano E, Dekker CL, Tian L, Weyand CM, Goronzy JJ. (2016). Expression of CD39 on Activated T Cells Impairs their Survival in Older Individuals. Cell Rep. **9**;14(5):1218-1231.

Farr JN, Fraser DG, Wang H, Jaehn K, Ogrodnik MB, Weivoda MM, Drake MT, Tchkonia T, LeBrasseur NK, Kirkland JL, Bonewald LF, Pignolo RJ, Monroe DG, Khosla S. (2016). Identification of Senescent Cells in the Bone Microenvironment. J Bone Miner Res. **31**(11):1920-1929.

Fayet G, Jansson M, Sternberg D, Moslemi AR, Blondy P, Lombès A, Fardeau M, Oldfors A. (2002). Ageing muscle: clonal expansions of mitochondrial DNA point mutations and deletions cause focal impairment of mitochondrial function. Neuromuscul Disord. **12**(5):484-93.

Feser J, Tyler J. (2011). Chromatin structure as a mediator of aging. FEBS Lett. **7**;585(13):2041-8.

Franceschi C, Bonafè M, Valensin S, Olivieri F, De Luca M, Ottaviani E, De Benedictis G. (2000). Inflamm-aging. An evolutionary perspective on immunosenescence. Ann N Y Acad Sci. **908**:244-54.

Frasca D, Diaz A, Romero M, Blomberg BB. (2017). Human peripheral late/exhausted memory B cells express a senescent-associated secretory phenotype and preferentially utilize metabolic signaling pathways. Exp Gerontol. **87**(Pt A):113-120.

Freund A, Laberge RM, Demaria M, Campisi J. (2012). Lamin B1 loss is a senescence-associated biomarker. Mol Biol Cell. **23**(11):2066-75.

Forsberg KJ, Reyes A, Wang B, Selleck EM, Sommer MO, Dantas G. (2012). The shared antibiotic resistome of soil bacteria and human pathogens. Science. **31;**337(6098):1107-11.

Fumagalli M, Rossiello F, Clerici M, Barozzi S, Cittaro D, Kaplunov JM, Bucci G, Dobreva M, Matti V, Beausejour CM, Herbig U, Longhese MP, d'Adda di Fagagna F. (2012). Telomeric DNA damage is irreparable and causes persistent DNA-damage-response activation. Nat Cell Biol. **18**;14(4):355-65.

Ganesan S, Unger BL, Comstock AT, Angel KA, Mancuso P, Martinez FJ, Sajjan US. (2013). Aberrantly activated EGFR contributes to enhanced IL-8 expression in COPD airways epithelial cells via regulation of nuclear FoxO3A. Thorax. **68**(2):131-41.

Ganuza M, Sáiz-Ladera C, Cañamero M, Gómez G, Schneider R, Blasco MA, Pisano D, Paramio JM, Santamaría D, Barbacid M.(2012). Genetic inactivation of Cdk7 leads to cell cycle arrest and induces premature aging due to adult stem cell exhaustion. EMBO J. **30**;31(11):2498-510.

Gao Z, Xu MS, Barnett TL, Xu CW. (2011). Resveratrol induces cellular senescence with attenuated mono-ubiquitination of histone H2B in glioma cells. Biochem Biophys Res Commun. **8**;407(2):271-6.

García-Río F, Pino JM, Dorgham A, Alonso A, Villamor J. (2004). Spirometric reference equations for European females and males aged 65-85 yrs. Eur Respir J. **24**(3):397-405.

Godin LM, Sandri BJ, Wagner DE, Meyer CM, Price AP, Akinnola I, Weiss DJ, Panoskaltsis-Mortari A. (2016). Decreased Laminin Expression by Human Lung Epithelial Cells and Fibroblasts Cultured in Acellular Lung Scaffolds from Aged Mice. PLoS One. **8**;11(3):e0150966.

Gorgoulis V, Adams PD, Alimonti A, Bennett DC, Bischof O, Bishop C, Campisi J, Collado M, Evangelou K, Ferbeyre G, Gil J, Hara E, Krizhanovsky V, Jurk D, Maier AB, Narita M, Niedernhofer L, Passos JF, Robbins PD, Schmitt CA, Sedivy J, Vougas K, von Zglinicki T, Zhou D, Serrano M, Demaria M. (2019). Cellular Senescence: Defining a Path Forward. Cell. **31**;179(4):813-827.

Gonzalez-Suarez I, Redwood AB, Perkins SM, Vermolen B, Lichtensztejin D, Grotsky DA, Morgado-Palacin L, Gapud EJ, Sleckman BP, Sullivan T, Sage J, Stewart CL, Mai S, Gonzalo S. (2009). Novel roles for A-type lamins in telomere biology and the DNA damage response pathway. EMBO J. **19**;28(16):2414-27.

Greer EL, Maures TJ, Hauswirth AG, Green EM, Leeman DS, Maro GS, Han S, Banko MR, Gozani O, Brunet A. (2010). Members of the H3K4 trimethylation complex regulate lifespan in a germline-dependent manner in C. elegans. Nature. **15**;466(7304):383-7.

Greer EL, Shi Y. (2012). Histone methylation: a dynamic mark in health, disease and inheritance. Nat Rev Genet. **3**;13(5):343-57.

Gregg EW, Chen H, Wagenknecht LE, Clark JM, Delahanty LM, Bantle J, Pownall HJ, Johnson KC, Safford MM, Kitabchi AE, Pi-Sunyer FX, Wing RR, Bertoni AG; Look AHEAD Research Group. (2012). Association of an intensive lifestyle intervention with remission of type 2 diabetes. JAMA. **19**;308(23):2489-96.

Griffith AV, Fallahi M, Venables T, Petrie HT. (2012). Persistent degenerative changes in thymic organ function revealed by an inducible model of organ regrowth. Aging Cell. **11**(1):169-77.

Grube K, Bürkle A. (1992). Poly(ADP-ribose) polymerase activity in mononuclear leukocytes of 13 mammalian species correlates with species-specific life span. Proc Natl Acad Sci U S A. **15;**89(24):11759-63.

Gulati S, Thannickal VJ. (2019). The Aging Lung and Idiopathic Pulmonary Fibrosis. Am J Med Sci. **357**(5):384-389.
Haas RH. (2019). Mitochondrial Dysfunction in Aging and Diseases of Aging. Biology (Basel). **17**;8(2):48.

Haberland M, Montgomery RL, Olson EN. (2009). The many roles of histone deacetylases in development and physiology: implications for disease and therapy. Nat Rev Genet. **10**(1):32-42.

Haigis MC, Sinclair DA. (2010). Mammalian sirtuins: biological insights and disease relevance. Annu Rev Pathol. **5**:253-95.

Hartl FU, Bracher A, Hayer-Hartl M. (2011). Molecular chaperones in protein folding and proteostasis. Nature. **20**;475(7356):324-32.

Harries LW, Hernandez D, Henley W, Wood AR, Holly AC, Bradley-Smith RM, Yaghootkar H, Dutta A, Murray A, Frayling TM, Guralnik JM, Bandinelli S, Singleton A, Ferrucci L, Melzer D. (2011). Human aging is characterized by focused changes in gene expression and deregulation of alternative splicing. Aging Cell. **10**(5):868-78.

Han S. and Mallampall R. K (2015). 'The Role of Surfactant in Lung Disease and Host Defense against Pulmonary Infections'. Ann Am Thorac Soc. **12**(5): 765–774.

Han X, Niu J, Zhao Y, Kong Q, Tong T, Han L. (2016). 'HDAC4 stabilizes SIRT1 via sumoylation SIRT1 to delay cellular senescence'. Clin Exp Pharmacol Physiol. **43**:41–46.

HAYFLICK L, MOORHEAD PS. (1961). The serial cultivation of human diploid cell strains. Exp Cell Res. **25**:585-621.

Hecker T, Hermenau K, Isele D, Elbert T. (2014). Corporal punishment and children's externalizing problems: a cross-sectional study of Tanzanian primary school aged children. Child Abuse Negl. **38**(5):884-92

Hemann MT, Strong MA, Hao LY, Greider CW. (2001). The shortest telomere, not average telomere length, is critical for cell viability and chromosome stability. Cell. **5**;107(1):67-77.

Herranz D, Muñoz-Martin M, Cañamero M, Mulero F, Martinez-Pastor B, Fernandez-Capetillo O, Serrano M. (2010). Sirt1 improves healthy ageing and protects from metabolic syndrome-associated cancer. Nat Commun. **12**;1:3.

Hewitt G, Jurk D, Marques FD, Correia-Melo C, Hardy T, Gackowska A, Anderson R, Taschuk M, Mann J, Passos JF. (2012). Telomeres are favoured targets of a persistent DNA damage response in ageing and stress-induced senescence. Nat Commun. **28**;3:708.

Henikoff S, Smith MM. (2015). Histone variants and epigenetics. Cold Spring Harb Perspect Biol. **5**;7(1):a019364.

Hill C, Li J, Liu D, Conforti F, Brereton CJ, Yao L, Zhou Y, Alzetani A, Chee SJ, Marshall BG, Fletcher SV, Hancock D, Ottensmeier CH, Steele AJ, Downward J, Richeldi L, Lu X, Davies DE, Jones MG, Wang Y. (2019). Autophagy inhibition-mediated epithelial-mesenchymal transition augments local myofibroblast differentiation in pulmonary fibrosis. Cell Death Dis. 7;10(8):591.

Hirani D, Alvira CM, Danopoulos S, Milla C, Donato M, Tian L, Mohr J, Dinger K, Vohlen C, Selle J, V Koningsbruggen-Rietschel S, Barbarino V, Pallasch C, Rose-John S, Odenthal M, Pryhuber GS, Mansouri S, Savai R, Seeger W, Khatri P, Al Alam D, Dötsch J, Alejandre

Alcazar MA. (2022). 'Macrophage-derived IL-6 trans-signalling as a novel target in the pathogenesis of bronchopulmonary dysplasia'. Eur Respir J. **17**;59(2):2002248.

Hoeijmakers JH. (2009). DNA damage, aging, and cancer. N Engl J Med. **8**;361(15):1475-85

Horvath S. (2013). DNA methylation age of human tissues and cell types. Genome Biol. **14**(10):R115.

Horvath S, Pirazzini C, Bacalini MG, Gentilini D, Di Blasio AM, Delledonne M, Mari D, Arosio B, Monti D, Passarino G, De Rango F, D'Aquila P, Giuliani C, Marasco E, Collino S, Descombes P, Garagnani P, Franceschi C. (2015). Decreased epigenetic age of PBMCs from Italian semi-supercentenarians and their offspring. Aging (Albany NY). **7**(12):1159-70.

Hogan BL, Barkauskas CE, Chapman HA, Epstein JA, Jain R, Hsia CC, Niklason L, Calle E, Le A, Randell SH, Rock J, Snitow M, Krummel M, Stripp BR, Vu T, White ES, Whitsett JA, Morrisey EE. (2014). Repair and regeneration of the respiratory system: complexity, plasticity, and mechanisms of lung stem cell function. Cell Stem Cell. **7;**15(2):123-38.

Houtkooper RH, Pirinen E, Auwerx J. (2012). Sirtuins as regulators of metabolism and healthspan. Nat Rev Mol Cell Biol. **7**;13(4):225-238.

Huan T, Chen G, Liu C, Bhattacharya A, Rong J, Chen BH, Seshadri S, Tanriverdi K, Freedman JE, Larson MG, Murabito JM, Levy D. (2018). Age-associated microRNA expression in human peripheral blood is associated with all-cause mortality and age-related traits. Aging Cell. 17(1):e12687.

Huang T. (2011). Next generation sequencing to characterize mitochondrial genomic DNA heteroplasmy. Curr Protoc Hum Genet. Chapter **19**:19.8.1-19.8.12.

Huna A, Salmina K, Jascenko E, Duburs G, Inashkina I, Erenpreisa J. (2011). Self-Renewal Signalling in Presenescent Tetraploid IMR90 Cells. J Aging Res. **2011**:103253.

Hwang JY, Randall TD, Silva-Sanchez A. (2016). 'Inducible Bronchus-Associated Lymphoid Tissue: Taming Inflammation in the Lung'. Front Immunol. 30;7:258.

Imran SAM, Yazid MD, Idrus RBH, Maarof M, Nordin A, Razali RA, and Lokanathan Y. (2021). 'Is There an Interconnection between Epithelial–Mesenchymal Transition (EMT) and Telomere Shortening in Aging?'. Int J Mol Sci. **22**(8): 3888.

Issa JP. (2014). Aging and epigenetic drift: a vicious cycle. J Clin Invest. **124**(1):24-9.

Ishii KJ, Koyama S, Nakagawa A, Coban C, Akira S. (2008). Host innate immune receptors and beyond: making sense of microbial infections. Cell Host Microbe. **12**;3(6):352-63.

Ito K, Barnes PJ.(2009). COPD as a disease of accelerated lung aging. Chest. **135**(1):173-180.

Jacobs KB, Yeager M, Zhou W, Wacholder S, Wang Z, Rodriguez-Santiago B, Hutchinson A, Deng X, Liu C, Horner MJ, Cullen M, Epstein CG, Burdett L, Dean MC, Chatterjee N, Sampson J, Chung CC, Kovaks J, Gapstur SM, Stevens VL, Teras LT, Gaudet MM, Albanes D, Weinstein SJ, Virtamo J, Taylor PR, Freedman ND, Abnet CC, Goldstein AM, Hu N, Yu K, Yuan JM, Liao L, Ding T, Qiao YL, Gao YT, Koh WP, Xiang YB, Tang ZZ, Fan JH, Aldrich

MC, Amos C, Blot WJ, Bock CH, Gillanders EM, Harris CC, Haiman CA, Henderson BE, Kolonel LN, Le Marchand L, McNeill LH, Rybicki BA, Schwartz AG, Signorello LB, Spitz MR, Wiencke JK, Wrensch M, Wu X, Zanetti KA, Ziegler RG, Figueroa JD, Garcia-Closas M, Malats N, Marenne G, Prokunina-Olsson L, Baris D, Schwenn M, Johnson A, Landi MT, Goldin L, Consonni D, Bertazzi PA, Rotunno M, Rajaraman P, Andersson U, Beane Freeman LE, Berg CD, Buring JE, Butler MA, Carreon T, Feychting M, Ahlbom A, Gaziano JM, Giles GG, Hallmans G, Hankinson SE, Hartge P, Henriksson R, Inskip PD, Johansen C, Landgren A, McKean-Cowdin R, Michaud DS, Melin BS, Peters U, Ruder AM, Sesso HD, Severi G, Shu XO, Visvanathan K, White E, Wolk A, Zeleniuch-Jacquotte A, Zheng W, Silverman DT, Kogevinas M, Gonzalez JR, Villa O, Li D, Duell EJ, Risch HA, Olson SH, Kooperberg C, Wolpin BM, Jiao L, Hassan M, Wheeler W, Arslan AA, Bueno-de-Mesquita HB, Fuchs CS, Gallinger S, Gross MD, Holly EA, Klein AP, LaCroix A, Mandelson MT, Petersen G, Boutron-Ruault MC, Bracci PM, Canzian F, Chang K, Cotterchio M, Giovannucci EL, Goggins M, Hoffman Bolton JA, Jenab M, Khaw KT, Krogh V, Kurtz RC, McWilliams RR, Mendelsohn JB, Rabe KG, Riboli E, Tjønneland A, Tobias GS, Trichopoulos D, Elena JW, Yu H, Amundadottir L, Stolzenberg-Solomon RZ, Kraft P, Schumacher F, Stram D, Savage SA, Mirabello L, Andrulis IL, Wunder JS, Patiño García A, Sierrasesúmaga L, Barkauskas DA, Gorlick RG, Purdue M, Chow WH, Moore LE, Schwartz KL, Davis FG, Hsing AW, Berndt SI, Black A, Wentzensen N, Brinton LA, Lissowska J, Peplonska B, McGlynn KA, Cook MB, Graubard BI, Kratz CP, Greene MH, Erickson RL, Hunter DJ, Thomas G, Hoover RN, Real FX, Fraumeni JF Jr, Caporaso NE, Tucker M, Rothman N, Pérez-Jurado LA, Chanock SJ. (2012). Detectable clonal mosaicism and its relationship to aging and cancer. Nat Genet. **6;**44(6):651-8.

Jang YY, Sharkis SJ. (2007). A low level of reactive oxygen species selects for primitive hematopoietic stem cells that may reside in the low-oxygenic niche. Blood. **15;**110(8):3056-63.

Jazin EE, Cavelier L, Eriksson I, Oreland L, Gyllensten U. (1996). Human brain contains high levels of heteroplasmy in the noncoding regions of mitochondrial DNA. Proc Natl Acad Sci U S A. **29**;93(22):12382-7.

Jin C, Li J, Green CD, Yu X, Tang X, Han D, Xian B, Wang D, Huang X, Cao X, Yan Z, Hou L, Liu J, Shukeir N, Khaitovich P, Chen CD, Zhang H, Jenuwein T, Han JD. (2011). Histone demethylase UTX-1 regulates C. elegans life span by targeting the insulin/IGF-1 signaling pathway. Cell Metab. **3**;14(2):161-72.

John-Schuster G, Hager K, Conlon TM, Irmler M, Beckers J, Eickelberg O, Yildirim AÖ. (2014). 'Cigarette smoke-induced iBALT mediates macrophage activation in a B cell-dependent manner in COPD'. Am J Physiol Lung Cell Mol Physiol. **1**;307(9):L692-706.

John-Schuster G, Günter S, Hager K, Conlon TM, Eickelberg O, Yildirim AÖ. (2016). Inflammaging increases susceptibility to cigarette smoke-induced COPD. Oncotarget. **24**;7(21):30068-83.

Just RS, Irwin JA, Parson W. (2015). Mitochondrial DNA heteroplasmy in the emerging field of massively parallel sequencing. Forensic Sci Int Genet. **18**:131-9.

Jylhävä J, Pedersen NL, Hägg S. (2017). Biological Age Predictors. EBioMedicine. **21**:29-36.

Kanfi Y, Peshti V, Gil R, Naiman S, Nahum L, Levin E, Kronfeld-Schor N, Cohen HY. (2010). SIRT6 protects against pathological damage caused by diet-induced obesity. Aging Cell. **9**(2):162-73.

Kanfi Y, Naiman S, Amir G, Peshti V, Zinman G, Nahum L, Bar-Joseph Z, Cohen HY. (2012). The sirtuin SIRT6 regulates lifespan in male mice. Nature. **22**;483(7388):218-21.

Kang Y, Zhang H, Zhao Y, Wang Y, Wang W, He Y, Zhang W, Zhang W, Zhu X, Zhou Y, Zhang L, Ju Z, Shi L. (2018). Telomere Dysfunction Disturbs Macrophage Mitochondrial Metabolism and the NLRP3 Inflammasome through the PGC-1α/TNFAIP3 Axis. Cell Rep. **27**;22(13):3493-3506.

Kawahara A, Nishi T, Hisano Y, Fukui H, Yamaguchi A, Mochizuki N. (2009). The sphingolipid transporter spns2 functions in migration of zebrafish myocardial precursors. Science. **23**;323(5913):524-7.

Kazak L, Reyes A, Holt IJ. (2012). Minimizing the damage: repair pathways keep mitochondrial DNA intact. Nat Rev Mol Cell Biol. **13**(10):659-71.

Kim E, Bisson WH, Löhr CV, Williams DE, Ho E, Dashwood RH, Rajendran P. (2016). Histone and Non-Histone Targets of Dietary Deacetylase Inhibitors. Curr Top Med Chem. **16**(7):714-31.

Kofman AE, Huszar JM, Payne CJ. (2013). 'Transcriptional analysis of histone deacetylase family members reveal similarities between differentiating and aging spermatogonial stem cells'. Stem Cell Rev**. 9**:59–64.

Koga H, Kaushik S, Cuervo AM. (2011). Protein homeostasis and aging: The importance of exquisite quality control. Ageing Res Rev. **10**(2):205-15.

Korfei M, Ruppert C, Mahavadi P, Henneke I, Markart P, Koch M, Lang G, Fink L, Bohle RM, Seeger W, Weaver TE, Guenther A. (2008). Epithelial endoplasmic reticulum stress and apoptosis in sporadic idiopathic pulmonary fibrosis. Am J Respir Crit Care Med. **15**;178(8):838-46.

Kotton DN, Morrisey EE. (2014). Lung regeneration: mechanisms, applications and emerging stem cell populations. Nat Med**. 20**(8):822-32.

Krishnan V, Chow MZ, Wang Z, Zhang L, Liu B, Liu X, Zhou Z. (2011). Histone H4 lysine 16 hypoacetylation is associated with defective DNA repair and premature senescence in Zmpste24-deficient mice. Proc Natl Acad Sci U S A. **26**;108(30):12325-30.

Krishnan V, Liu B, Zhou Z. (2011). 'Relax and Repair' to restrain aging. Aging (Albany NY). **3**(10):943-54.

Kuhnert S, Mansouri S, Rieger MA, Savai R, Avci E, Díaz-Piña G, Padmasekar M, Looso M, Hadzic S, Acker T, Klatt S, Wilhelm J, Fleming I, Sommer N, Weissmann N, Vogelmeier C, Bals R, Zeiher A, Dimmeler S, Seeger W, Pullamsetti SS. (2022). 'Association of Clonal Hematopoiesis of Indeterminate Potential with Inflammatory Gene Expression in Patients with COPD'. Cells. **5**;11(13):2121.

Kulkarni A, Anderson AG, Merullo DP, Konopka G. (2019). Beyond bulk: a review of single cell transcriptomics methodologies and applications. Curr Opin Biotechnol. **58**:129-136.

Kumari R. and Parmjit J (2021). 'Mechanisms of Cellular Senescence: Cell Cycle Arrest and Senescence Associated Secretory Phenotype'. Front Cell Dev Biol. **9**:645593.

Kurozumi M, Matsushita T, Hosokawa M, Takeda T. (1994). Age-related changes in lung structure and function in the senescence-accelerated mouse (SAM): SAM-P/1 as a new murine model of senile hyperinflation of lung. Am J Respir Crit Care Med. **149**(3 Pt 1):776-82.

Labrie JE 3rd, Sah AP, Allman DM, Cancro MP, Gerstein RM. (2004). Bone marrow microenvironmental changes underlie reduced RAG-mediated recombination and B cell generation in aged mice. J Exp Med. **16**;200(4):411-23.

Laurie CC, Laurie CA, Rice K, Doheny KF, Zelnick LR, McHugh CP, Ling H, Hetrick KN, Pugh EW, Amos C, Wei Q, Wang LE, Lee JE, Barnes KC, Hansel NN, Mathias R, Daley D, Beaty TH, Scott AF, Ruczinski I, Scharpf RB, Bierut LJ, Hartz SM, Landi MT, Freedman ND, Goldin LR, Ginsburg D, Li J, Desch KC, Strom SS, Blot WJ, Signorello LB, Ingles SA, Chanock SJ, Berndt SI, Le Marchand L, Henderson BE, Monroe KR, Heit JA, de Andrade M, Armasu SM, Regnier C, Lowe WL, Hayes MG, Marazita ML, Feingold E, Murray JC, Melbye M, Feenstra B, Kang JH, Wiggs JL, Jarvik GP, McDavid AN, Seshan VE, Mirel DB, Crenshaw A, Sharopova N, Wise A, Shen J, Crosslin DR, Levine DM, Zheng X, Udren JI, Bennett S, Nelson SC, Gogarten SM, Conomos MP, Heagerty P, Manolio T, Pasquale LR, Haiman CA, Caporaso N, Weir BS. (2012). Detectable clonal mosaicism from birth to old age and its relationship to cancer. Nat Genet. **6;**44(6):642-50.

Lamming DW, Ye L, Sabatini DM, Baur JA. (2013). Rapalogs and mTOR inhibitors as anti-aging therapeutics. J Clin Invest. **123**(3):980-9.

Lange P, Celli B, Agustí A, Boje Jensen G, Divo M, Faner R, Guerra S, Marott JL, Martinez FD, Martinez-Camblor P, Meek P, Owen CA, Petersen H, Pinto-Plata V, Schnohr P, Sood A, Soriano JB, Tesfaigzi Y, Vestbo J. (2015). Lung-Function Trajectories Leading to Chronic Obstructive Pulmonary Disease. N Engl J Med. **9**;373(2):111-22.

Lawson WE, Grant SW, Ambrosini V, Womble KE, Dawson EP, Lane KB, Markin C, Renzoni E, Lympany P, Thomas AQ, Roldan J, Scott TA, Blackwell TS, Phillips JA 3rd, Loyd JE, du Bois RM. (2004). Genetic mutations in surfactant protein C are a rare cause of sporadic cases of IPF. Thorax. **59**(11):977-80.

Lawson WE, Crossno PF, Polosukhin VV, Roldan J, Cheng DS, Lane KB, Blackwell TR, Xu C, Markin C, Ware LB, Miller GG, Loyd JE, Blackwell TS. (2008). Endoplasmic reticulum stress in alveolar epithelial cells is prominent in IPF: association with altered surfactant protein processing and herpesvirus infection. Am J Physiol Lung Cell Mol Physiol. **294**(6):L1119-26.

Lee JW, Park KD, Im JA, Kim MY, Lee DC. (2010). Mitochondrial DNA copy number in peripheral blood is associated with cognitive function in apparently healthy elderly women. Clin Chim Acta. **2;**411(7-8):592-6.

Lederer DJ, Martinez FJ. (2018). Idiopathic Pulmonary Fibrosis. N Engl J Med. **10**;378(19):1811-1823.

Ley B, Ryerson CJ, Vittinghoff E, Ryu JH, Tomassetti S, Lee JS, Poletti V, Buccioli M, Elicker BM, Jones KD, King TE Jr, Collard HR. (2012). A multidimensional index and staging system for idiopathic pulmonary fibrosis. Ann Intern Med. **15**;156(10):684-91.

Li L, Greer C, Eisenman RN, Secombe J. (2010). Essential functions of the histone demethylase lid. PLoS Genet. **24**;6(11):e1001221.

Liao Y, Smyth GK, Shi W.(2014). 'featureCounts: an efficient general purpose program for assigning sequence reads to genomic features'. Bioinformatics. **1**;30(7):923-30.

Lin CR, Bahmed K. and Kosmider B (2022). 'Impaired Alveolar Re-Epithelialization in Pulmonary Emphysema'. Cells. 11, 2055.

Linnane AW, Marzuki S, Ozawa T, Tanaka M. (1989). Mitochondrial DNA mutations as an important contributor to ageing and degenerative diseases. Lancet. **25**;1(8639):642-5.

Liu GH, Barkho BZ, Ruiz S, Diep D, Qu J, Yang SL, Panopoulos AD, Suzuki K, Kurian L, Walsh C, Thompson J, Boue S, Fung HL, Sancho-Martinez I, Zhang K, Yates J 3rd, Izpisua Belmonte JC. (2011). Recapitulation of premature ageing with iPSCs from Hutchinson-Gilford progeria syndrome. Nature. **14**;472(7342):221-5.

Liu B, Wang J, Chan KM, Tjia WM, Deng W, Guan X, Huang JD, Li KM, Chau PY, Chen DJ, Pei D, Pendas AM, Cadiñanos J, López-Otín C, Tse HF, Hutchison C, Chen J, Cao Y, Cheah KS, Tryggvason K, Zhou Z. (2005). Genomic instability in laminopathy-based premature aging. Nat Med. **11**(7):780-5.

Liu B, Yip RKh, Zhou Z. (2012). Chromatin remodeling, DNA damage repair and aging. Curr Genomics. **13**(7):533-47.

Liu W, Acín-Peréz R, Geghman KD, Manfredi G, Lu B, Li C. (2011). Pink1 regulates the oxidative phosphorylation machinery via mitochondrial fission. Proc Natl Acad Sci U S A. **2**;108(31):12920-4.

Liu X, Li C, Li Q, Chang HC, Tang YC. (2020). SIRT7 Facilitates CENP-A Nucleosome Assembly and Suppresses Intestinal Tumorigenesis. iScience. **15**;23(9):101461.
Liu L, Cheung TH, Charville GW, Hurgo BM, Leavitt T, Shih J, Brunet A, Rando TA. (2013). Chromatin modifications as determinants of muscle stem cell quiescence and chronological aging. Cell Rep. **11**;4(1):189-204

Loguercio, S., Hutt, D.M., Campos, A.R., Stoeger, T., Grant, R.A., McQuattiePimentel, A.C., Abdala-Valencia, H., Lu, Z., Joshi, N., Ridge, K., et al. (2019). Proteostasis and Energetics as Proteome Hallmarks of Aging and Influenza Challenge in Pulmonary Disease. bioRxiv. https://doi.org/10.1101/769737.

Lomas DA. (2018). New Therapeutic Targets for Alpha-1 Antitrypsin Deficiency. Chronic Obstr Pulm Dis. **6**;5(4):233-243.

López-Otín C, Blasco MA, Partridge L, Serrano M, Kroemer G. (2013). The hallmarks of aging. Cell. **6**;153(6):1194-217.

Loth KA, MacLehose R, Bucchianeri M, Crow S, Neumark-Sztainer D. (2014). Predictors of dieting and disordered eating behaviors from adolescence to young adulthood. J Adolesc Health. 55(5):705-12.

Love MI, Huber W, Anders S. (2014). 'Moderated estimation of fold change and dispersion for RNA-seq data with DESeq2'. Genome Biol. **15**(12):550.

Lord CJ, Ashworth A. (2012). The DNA damage response and cancer therapy. Nature. **18**;481(7381):287-94.

Lottes RG, Newton DA, Spyropoulos DD, Baatz JE. (2014). Alveolar type II cells maintain bioenergetic homeostasis in hypoxia through metabolic and molecular adaptation. Am J Physiol Lung Cell Mol Physiol. **15**;306(10):L947-55.

Luger K, Mäder AW, Richmond RK, Sargent DF, Richmond TJ. (1997). Crystal structure of the nucleosome core particle at 2.8 A resolution. Nature. **18**;389(6648):251-60.

Lukey PT, Harrison SA, Yang S, Man Y, Holman BF, Rashidnasab A, Azzopardi G, Grayer M, Simpson JK, Bareille P, Paul L, Woodcock HV, Toshner R, Saunders P, Molyneaux PL, Thielemans K, Wilson FJ, Mercer PF, Chambers RC, Groves AM, Fahy WA, Marshall RP, Maher TM. (2019). A randomised, placebo-controlled study of omipalisib (PI3K/mTOR) in idiopathic pulmonary fibrosis. Eur Respir J. **18**;53(3):1801992.

Maleszewska, M., Mawer, J.S.P. & Tessarz, P. (2016). Histone Modifications in Ageing and Lifespan Regulation. Curr Mol Bio Rep **2**, 26–35.

Maegawa S, Hinkal G, Kim HS, Shen L, Zhang L, Zhang J, Zhang N, Liang S, Donehower LA, Issa JP. (2010). Widespread and tissue specific age-related DNA methylation changes in mice. Genome Res. **20**(3):332-40

Massaro GD, Gail DB, Massaro D. (1975). Lung oxygen consumption and mitochondria of alveolar epithelial and endothelial cells. J Appl Physiol. **38**(4):588-92.

McIntyre LR, Daniels EG, Molenaars M, Houtkooper RH and Janssens GE. (2019).' From molecular promise to preclinical results:HDAC inhibitors in the race for healthy aging drugs'. EMBO Mol Med.**11**:e9854.

Mengel-From J, Thinggaard M, Dalgård C, Kyvik KO, Christensen K, Christiansen L. (2014). Mitochondrial DNA copy number in peripheral blood cells declines with age and is associated with general health among elderly. Hum Genet. **133**(9):1149-59.

Mercado N, Ito K, Barnes PJ. (2015). Accelerated ageing of the lung in COPD: new concepts. Thorax. **70**(5):482-9.

Meyer KC. (2010). The role of immunity and inflammation in lung senescence and susceptibility to infection in the elderly. Semin Respir Crit Care Med . **31**: 561–574.

Michikawa Y, Mazzucchelli F, Bresolin N, Scarlato G, Attardi G. (1999). Aging-dependent large accumulation of point mutations in the human mtDNA control region for replication. Science. **22**;286(5440):774-9.

Michishita E, McCord RA, Berber E, Kioi M, Padilla-Nash H, Damian M, Cheung P, Kusumoto R, Kawahara TL, Barrett JC, Chang HY, Bohr VA, Ried T, Gozani O, Chua KF. (2008). SIRT6 is a histone H3 lysine 9 deacetylase that modulates telomeric chromatin. Nature. **27**;452(7186):492-6.

Milazzo G, Mercatelli D, Di Muzio G, Triboli L, De Rosa P, Perini G, Giorgi FM. (2020). Histone Deacetylases (HDACs): Evolution, Specificity, Role in Transcriptional Complexes, and Pharmacological Actionability. Genes (Basel). **15**;11(5):556.

Millner A, Atilla-Gokcumen GE. (2020). 'Lipid Players of Cellular Senescence'. Metabolites. **21**;10(9):339.

Min JN, Tian Y, Xiao Y, Wu L, Li L, Chang S. (2013). The mINO80 chromatin remodeling complex is required for efficient telomere replication and maintenance of genome stability. Cell Res. **23**(12):1396-413.

Minucci S, Pelicci PG. (2006). Histone deacetylase inhibitors and the promise of epigenetic (and more) treatments for cancer. Nat Rev Cancer. **6**(1):38-51.

Mizushima N, Levine B, Cuervo AM, Klionsky DJ. (2008). Autophagy fights disease through cellular self-digestion. Nature. **28**;451(7182):1069-75.

Mizumura K, Cloonan SM, Nakahira K, Bhashyam AR, Cervo M, Kitada T, Glass K, Owen CA, Mahmood A, Washko GR, Hashimoto S, Ryter SW, Choi AM. (2014). Mitophagy-dependent necroptosis contributes to the pathogenesis of COPD. J Clin Invest. **124**(9):3987-4003.

Moskalev AA, Shaposhnikov MV, Plyusnina EN, Zhavoronkov A, Budovsky A, Yanai H, Fraifeld VE. (2013). The role of DNA damage and repair in aging through the prism of Koch-like criteria. Ageing Res Rev. **12**(2):661-84.

Mostoslavsky R, Chua KF, Lombard DB, Pang WW, Fischer MR, Gellon L, Liu P, Mostoslavsky G, Franco S, Murphy MM, Mills KD, Patel P, Hsu JT, Hong AL, Ford E, Cheng HL, Kennedy C, Nunez N, Bronson R, Frendewey D, Auerbach W, Valenzuela D, Karow M, Hottiger MO, Hursting S, Barrett JC, Guarente L, Mulligan R, Demple B, Yancopoulos GD, Alt FW. (2006). Genomic instability and aging-like phenotype in the absence of mammalian SIRT6. Cell. **27**;124(2):315-29.

Muiras ML, Müller M, Schächter F, Bürkle A. (1998). Increased poly(ADP-ribose) polymerase activity in lymphoblastoid cell lines from centenarians. J Mol Med (Berl). **76**(5):346-54.

Murga M, Bunting S, Montaña MF, Soria R, Mulero F, Cañamero M, Lee Y, McKinnon PJ, Nussenzweig A, Fernandez-Capetillo O. (2009). A mouse model of ATR-Seckel shows embryonic replicative stress and accelerated aging. Nat Genet. **41**(8):891-8.

Naikawadi RP, Disayabutr S, Mallavia B, Donne ML, Green G, La JL, Rock JR, Looney MR, Wolters PJ. (2016). Telomere dysfunction in alveolar epithelial cells causes lung remodeling and fibrosis. JCI Insight. **8**;1(14):e86704.

Nelson DM, Jaber-Hijazi F, Cole JJ, Robertson NA, Pawlikowski JS, Norris KT, Criscione SW, Pchelintsev NA, Piscitello D, Stong N, Rai TS, McBryan T, Otte GL, Nixon C, Clark W,

Riethman H, Wu H, Schotta G, Garcia BA, Neretti N, Baird DM, Berger SL, Adams PD. (2016). Mapping H4K20me3 onto the chromatin landscape of senescent cells indicates a function in control of cell senescence and tumor suppression through preservation of genetic and epigenetic stability. Genome Biol. **25**;17(1):158.

Nekhaeva E, Bodyak ND, Kraytsberg Y, McGrath SB, Van Orsouw NJ, Pluzhnikov A, Wei JY, Vijg J, Khrapko K. (2002). Clonally expanded mtDNA point mutations are abundant in individual cells of human tissues. Proc Natl Acad Sci U S A. **16;**99(8):5521-6.

Nicolas FE, Moxon S, de Haro JP, Calo S, Grigoriev IV, Torres-Martínez S, Moulton V, Ruiz-Vázquez RM, Dalmay T. (2010). Endogenous short RNAs generated by Dicer 2 and RNA-dependent RNA polymerase 1 regulate mRNAs in the basal fungus Mucor circinelloides. Nucleic Acids Res. **38**(16):5535-41.

Nikolich-Žugich J. (2018). The twilight of immunity: emerging concepts in aging of the immune system. Nat Immunol. **19**(1):10-19.

Nooteboom M, Johnson R, Taylor RW, Wright NA, Lightowlers RN, Kirkwood TB, Mathers JC, Turnbull DM, Greaves LC. (2010). Age-associated mitochondrial DNA mutations lead to small but significant changes in cell proliferation and apoptosis in human colonic crypts. Aging Cell. **9**(1):96-9.

Ogrodnik M, Zhu Y, Langhi LGP, Tchkonia T, Krüger P, Fielder E, Victorelli S, Ruswhandi RA, Giorgadze N, Pirtskhalava T, Podgorni O, Enikolopov G, Johnson KO, Xu M, Inman C, Palmer AK, Schafer M, Weigl M, Ikeno Y, Burns TC, Passos JF, von Zglinicki T, Kirkland JL, Jurk D. (2019). Obesity-Induced Cellular Senescence Drives Anxiety and Impairs Neurogenesis. Cell Metab. **7;**29(5):1061-1077.e8.

Oh J, Lee YD, Wagers AJ. (2014). Stem cell aging: mechanisms, regulators and therapeutic opportunities. Nat Med. **20**(8):870-80.

Olovnikov AM. (1996). Telomeres, telomerase, and aging: origin of the theory. Exp Gerontol. **31**(4):443-8.

Osoegawa A, Hiraishi H, Hashimoto T, Takumi Y, Abe M, Takeuchi H, Miyawaki M, Okamoto T, Sugio K. (2018). The Positive Relationship Between γH2AX and PD-L1 Expression in Lung Squamous Cell Carcinoma. In Vivo. **32**(1):171-177.

Osorio FG, Varela I, Lara E, Puente XS, Espada J, Santoro R, Freije JM, Fraga MF, López-Otín C. (2010). Nuclear envelope alterations generate an aging-like epigenetic pattern in mice deficient in Zmpste24 metalloprotease. Aging Cell. **9**(6):947-57.

Osorio FG, Navarro CL, Cadiñanos J, López-Mejía IC, Quirós PM, Bartoli C, Rivera J, Tazi J, Guzmán G, Varela I, Depetris D, de Carlos F, Cobo J, Andrés V, De Sandre-Giovannoli A, Freije JM, Lévy N, López-Otín C.(2011). Splicing-directed therapy in a new mouse model of human accelerated aging. Sci Transl Med. **26**;3(106):106ra107.

Palm W, de Lange T. (2008). How shelterin protects mammalian telomeres. Annu Rev Genet. **42**:301-34.

Panda A, Qian F, Mohanty S, van Duin D, Newman FK, Zhang L, Chen S, Towle V, Belshe RB, Fikrig E, Allore HG, Montgomery RR, Shaw AC. (20109. Age-associated decrease in TLR function in primary human dendritic cells predicts influenza vaccine response. J Immunol. **1**;184(5):2518-27.

Park SY, Kim JS. (2020). A short guide to histone deacetylases including recent progress on class II enzymes. Exp Mol Med. **52**(2):204-212.

Paschalaki KE, Starke RD, Hu Y, Mercado N, Margariti A, Gorgoulis VG, Randi AM, Barnes PJ. (2013). Dysfunction of endothelial progenitor cells from smokers and chronic obstructive pulmonary disease patients due to increased DNA damage and senescence. Stem Cells. **31**(12):2813-26.

Paxson JA, Gruntman AM, Davis AM, Parkin CM, Ingenito EP, Hoffman AM. (2013). Age dependence of lung mesenchymal stromal cell dynamics following pneumonectomy. Stem Cells Dev. **15**;22(24):3214-25.

Petrie K, Guidez F, Howell L, Healy L, Waxman S, Greaves M, Zelent A. (2003). 'The Histone Deacetylase 9 Gene Encodes Multiple Protein Isoforms'. JBC. **278**,18;16059 –16072.

Place RF, Noonan EJ, Giardina C. (2005). 'HDACs and the senescent phenotype of WI-38 cells'. BMC Cell Biol. **6**:37.

Plantier L, Besnard V, Xu Y, Ikegami M, Wert SE, Hunt AN, Postle AD, Whitsett JA. (2012). Activation of sterol-response element-binding proteins (SREBP) in alveolar type II cells enhances lipogenesis causing pulmonary lipotoxicity. J Biol Chem. **23**;287(13):10099-10114.

Plate L, Cooley CB, Chen JJ, Paxman RJ, Gallagher CM, Madoux F, Genereux JC, Dobbs W, Garza D, Spicer TP, Scampavia L, Brown SJ, Rosen H, Powers ET, Walter P, Hodder P, Wiseman RL, Kelly JW. (2016). Small molecule proteostasis regulators that reprogram the ER to reduce extracellular protein aggregation. Elife. **20**;5:e15550.

Prestel M, Prell-Schicker C, Webb T, Malik R, Lindner B, Ziesch N, Rex-Haffner M, Röh S, Viturawong T, Lehm M, Mokry M, den Ruijter H, Haitjema S, Asare Y, Söllner F, Najafabadi MG, Aherrahrou R, Civelek M, Samani NJ, Mann M, Haffner C, Dichgans M. (2019). 'The Atherosclerosis Risk Variant rs2107595 Mediates Allele-Specific Transcriptional Regulation of HDAC9 via E2F3 and Rb1'. Stroke. **50**(10):2651-2660.

Powers ET, Morimoto RI, Dillin A, Kelly JW, Balch WE. (2009). Biological and chemical approaches to diseases of proteostasis deficiency. Annu Rev Biochem. **78**:959-91.

Ragnauth CD, Warren DT, Liu Y, McNair R, Tajsic T, Figg N, Shroff R, Skepper J, Shanahan CM. (2010). Prelamin A acts to accelerate smooth muscle cell senescence and is a novel biomarker of human vascular aging. Circulation. **25**;121(20):2200-10.

Rashid K, Sundar IK, Gerloff J, Li D, Rahman I. (2018). Lung cellular senescence is independent of aging in a mouse model of COPD/emphysema. Sci Rep. **13**;8(1):9023.

Rawlins EL, Giangreco A. (2014). The best laid schemes of airway repair. Eur Respir J. **44**(2):299-301.
Reddy S, Comai L. (2012). Lamin A, farnesylation and aging. Exp Cell Res. **1**;318(1):1-7.

Renshaw M, Rockwell J, Engleman C, Gewirtz A, Katz J, Sambhara S. (2002). Cutting edge: impaired Toll-like receptor expression and function in aging. J Immunol. **1**;169(9):4697-701.

Richardson RB. (2014). Age-specific bone tumour incidence rates are governed by stem cell exhaustion influencing the supply and demand of progenitor cells. Mech Ageing Dev. **139**:31-40.

Richmond TJ, Davey CA. (2003). The structure of DNA in the nucleosome core. Nature. **8**;423(6936):145-50.

Robinson JT, Thorvaldsdóttir H, Winckler W, Guttman M, Lander ES, Getz G, Mesirov JP. (2011). 'Integrative genomics viewer'. Nat Biotechnol. **29**(1):24-6.

Rock J, Königshoff M. (2012). Endogenous lung regeneration: potential and limitations. Am J Respir Crit Care Med. **15**;186(12):1213-9.

Roman J, Zhu J, Ritzenthaler JD, Zelko IN. (2017). Epigenetic regulation of EC-SOD expression in aging lung fibroblasts: Role of histone acetylation. Free Radic Biol Med. **112**:212-223.

Romero F, Summer R. (2017). Protein Folding and the Challenges of Maintaining Endoplasmic Reticulum Proteostasis in Idiopathic Pulmonary Fibrosis. Ann Am Thorac Soc. **14**(Supplement_5):S410-S413.

Ron-Harel N, Santos D, Ghergurovich JM, Sage PT, Reddy A, Lovitch SB, Dephoure N, Satterstrom FK, Sheffer M, Spinelli JB, Gygi S, Rabinowitz JD, Sharpe AH, Haigis MC. (2016). Mitochondrial Biogenesis and Proteome Remodeling Promote One-Carbon Metabolism for T Cell Activation. Cell Metab. **12**;24(1):104-17.

Ropero S, Esteller M. (2007). The role of histone deacetylases (HDACs) in human cancer. Mol Oncol. **1**(1):19-25.

Rothfuss O, Gasser T, Patenge N. (2010). Analysis of differential DNA damage in the mitochondrial genome employing a semi-long run real-time PCR approach. Nucleic Acids Res. **38**(4):e24

Rossi DJ, Bryder D, Seita J, Nussenzweig A, Hoeijmakers J, Weissman IL. (2007). Deficiencies in DNA damage repair limit the function of haematopoietic stem cells with age. Nature. **7**;447(7145):725-9

Rossiello, F., Jurk, D., Passos, J.F. (2022). Telomere dysfunction in ageing and age-related diseases. Nat Cell Biol **24,** 135–147.

Rossignol R, Faustin B, Rocher C, Malgat M, Mazat JP, Letellier T. (2003). Mitochondrial threshold effects. Biochem J. **15**;370(Pt 3):751-62.

Rubinsztein DC, Mariño G, Kroemer G. (2011). Autophagy and aging. Cell. **2**;146(5):682-95.

Sage PT, Tan CL, Freeman GJ, Haigis M, Sharpe AH. (2015). Defective TFH Cell Function and Increased TFR Cells Contribute to Defective Antibody Production in Aging. Cell Rep. **14**;12(2):163-71.

Sahin E, DePinho RA. (2012). Axis of ageing: telomeres, p53 and mitochondria. Nat Rev Mol Cell Biol. **16**;13(6):397-404.

Salminen A, Kaarniranta K, Kauppinen A. (2012). Inflammaging: disturbed interplay between autophagy and inflammasomes. Aging (Albany NY). **4**(3):166-75.

Sarg B, Koutzamani E, Helliger W, Rundquist I, Lindner HH. (2002). Postsynthetic trimethylation of histone H4 at lysine 20 in mammalian tissues is associated with aging. J Biol Chem. **18**;277(42):39195-201.

Sarode P, Zheng X, Giotopoulou GA, Weigert A, Kuenne C, Günther S, Friedrich A, Gattenlöhner S, Stiewe T, Brüne B, Grimminger F, Stathopoulos GT, Pullamsetti SS, Seeger W, Savai R. (2020). 'Reprogramming of tumor-associated macrophages by targeting β-catenin/FOSL2/ARID5A signaling: A potential treatment of lung cancer'. Sci Adv. **5**;6(23):eaaz6105.

Scaffidi P, Misteli T. (2006). Lamin A-dependent nuclear defects in human aging. Science. **19**;312(5776):1059-63.

Schafer MJ, White TA, Iijima K, Haak AJ, Ligresti G, Atkinson EJ, Oberg AL, Birch J, Salmonowicz H, Zhu Y, Mazula DL, Brooks RW, Fuhrmann-Stroissnigg H, Pirtskhalava T, Prakash YS, Tchkonia T, Robbins PD, Aubry MC, Passos JF, Kirkland JL, Tschumperlin DJ, Kita H, LeBrasseur NK. (2017). Cellular senescence mediates fibrotic pulmonary disease. Nat Commun. **23**;8:14532.

Schamberger AC, Mise N, Jia J, Genoyer E, Yildirim AÖ, Meiners S, Eickelberg O. (2014). Cigarette smoke-induced disruption of bronchial epithelial tight junctions is prevented by transforming growth factor-β. Am J Respir Cell Mol Biol. **50**(6):1040-52.

Schneider JL, Rowe JH, Garcia-de-Alba C, Kim CF, Sharpe AH, Haigis MC. (2021). The aging lung: Physiology, disease, and immunity. Cell. **15**;184(8):1990-2019.

Schneider JL, Sanchez CG. (2016). Autophagy and Metabolism. R. Bucala, P.J. Lee (Eds.), The Aging Lungs: Mechanisms and Clinical Sequelae, World Scientific, pp. 473-509.

Sebastian CL, Fontaine NM, Bird G, Blakemore SJ, Brito SA, McCrory EJ, Viding E. (2012). Neural processing associated with cognitive and affective Theory of Mind in adolescents and adults. Soc Cogn Affect Neurosci. **7**(1):53-63.

Seibold MA, Wise AL, Speer MC, Steele MP, Brown KK, Loyd JE, Fingerlin TE, Zhang W, Gudmundsson G, Groshong SD, Evans CM, Garantziotis S, Adler KB, Dickey BF, du Bois RM, Yang IV, Herron A, Kervitsky D, Talbert JL, Markin C, Park J, Crews AL, Slifer SH, Auerbach S, Roy MG, Lin J, Hennessy CE, Schwarz MI, Schwartz DA. (2011). A common MUC5B promoter polymorphism and pulmonary fibrosis. N Engl J Med. **21**;364(16):1503-12.

Signer RA, Morrison SJ. (2013). Mechanisms that regulate stem cell aging and life span. Cell Stem Cell. **7**;12(2):152-65.

Singh BN, Zhang G, Hwa YL, Li J, Dowdy SC, Jiang SW. (2010). Nonhistone protein acetylation as cancer therapy targets. Expert Rev Anticancer Ther. **10**(6):935-5.

Shaw AC, Goldstein DR, Montgomery RR. (2013). Age-dependent dysregulation of innate immunity. Nat Rev Immunol. **13**(12):875-87.

Shimi T, Butin-Israeli V, Adam SA, Hamanaka RB, Goldman AE, Lucas CA, Shumaker DK, Kosak ST, Chandel NS, Goldman RD. (2011). The role of nuclear lamin B1 in cell proliferation and senescence. Genes Dev. **15**;25(24):2579-93.

Shumaker DK, Dechat T, Kohlmaier A, Adam SA, Bozovsky MR, Erdos MR, Eriksson M, Goldman AE, Khuon S, Collins FS, Jenuwein T, Goldman RD. (2006). Mutant nuclear lamin A leads to progressive alterations of epigenetic control in premature aging. Proc Natl Acad Sci U S A. **6**;103(23):8703-8

Schumacker PT. (2011). Lung cell hypoxia: role of mitochondrial reactive oxygen species signaling in triggering responses. Proc Am Thorac Soc. **8**(6):477-84.

Snetselaar R, van Moorsel CHM, Kazemier KM, van der Vis JJ, Zanen P, van Oosterhout MFM, Grutters JC. (2015). Telomere length in interstitial lung diseases. Chest. **148**(4):1011-1018.

Snider SA, Margison KD, Ghorbani P, LeBlond ND, O'Dwyer C, Nunes JRC, Nguyen T, Xu H, Bennett SAL, Fullerton MD. (2018). 'Choline transport links macrophage phospholipid metabolism and inflammation'. J Biol Chem. **20**;293(29):11600-11611.

Sosulski ML, Gongora R, Danchuk S, Dong C, Luo F, Sanchez CG. (2015). Deregulation of selective autophagy during aging and pulmonary fibrosis: the role of TGFβ1. Aging Cell. **14**(5):774-83.

Sosulski ML, Gongora R, Feghali-Bostwick C, Lasky JA, Sanchez CG. (2017). Sirtuin 3 Deregulation Promotes Pulmonary Fibrosis. J Gerontol A Biol Sci Med Sci. **1**;72(5):595-602.

Stanley SE, Chen JJ, Podlevsky JD, Alder JK, Hansel NN, Mathias RA, Qi X, Rafaels NM, Wise RA, Silverman EK, Barnes KC, Armanios M. (2015). Telomerase mutations in smokers with severe emphysema. J Clin Invest. **125**(2):563-70.

Stripp BR, Reynolds SD. (2008). Maintenance and repair of the bronchiolar epithelium. Proc Am Thorac Soc. 15**;5(3):328-33.**

Sun F, Xiao G, Qu Z.(2017). 'Isolation of Murine Alveolar Type II Epithelial Cells'. Bio Protoc. **20**;7(10):e2288.

Summer R, Shaghaghi H, Schriner D, Roque W, Sales D, Cuevas-Mora K, Desai V, Bhushan A, Ramirez MI, Romero F. (2019). Activation of the mTORC1/PGC-1 axis promotes mitochondrial biogenesis and induces cellular senescence in the lung epithelium. Am J Physiol Lung Cell Mol Physiol. **1**;316(6):L1049-L1060.

Toledano E, Candelas G, Rosales Z, Martínez Prada C, León L, Abásolo L, Loza E, Carmona L, Tobías A, Jover JÁ. (2012). A meta-analysis of mortality in rheumatic diseases. Reumatol Clin. **8**(6):334-41.

Torres IO, Fujimori DG. (2015). Functional coupling between writers, erasers and readers of histone and DNA methylation. Curr Opin Struct Biol. **35**:68-75.

Tranah GJ, Katzman SM, Lauterjung K, Yaffe K, Manini TM, Kritchevsky S, Newman AB, Harris TB, Cummings SR. (2018). Mitochondrial DNA m.3243A > G heteroplasmy affects multiple aging phenotypes and risk of mortality. Sci Rep. **8**;8(1):11887.

Trucco C, Oliver FJ, de Murcia G, Ménissier-de Murcia J. (1998). DNA repair defect in poly(ADP-ribose) polymerase-deficient cell lines. Nucleic Acids Res. **1**;26(11):2644-9.

Tsukamoto H, Clise-Dwyer K, Huston GE, Duso DK, Buck AL, Johnson LL, Haynes L, Swain SL. (2009). Age-associated increase in lifespan of naive CD4 T cells contributes to T-cell homeostasis but facilitates development of functional defects. Proc Natl Acad Sci U S A. **27**;106(43):18333-8.

Ugalde AP, Ramsay AJ, de la Rosa J, Varela I, Mariño G, Cadiñanos J, Lu J, Freije JM, López-Otín C. (2011). Aging and chronic DNA damage response activate a regulatory pathway involving miR-29 and p53. EMBO J. **1**;30(11):2219-32

Van Deursen JM. (2014). The role of senescent cells in ageing. Nature. 2014 May 22;509(7501):439-46.

Van Deursen JM. (2019). Senolytic therapies for healthy longevity. Science. **17**;364(6441):636-637.

Van der Put E, Frasca D, King AM, Blomberg BB, Riley RL. (2004). Decreased E47 in senescent B cell precursors is stage specific and regulated posttranslationally by protein turnover. J Immunol. **15**;173(2):818-27.

Varela I, Cadiñanos J, Pendás AM, Gutiérrez-Fernández A, Folgueras AR, Sánchez LM, Zhou Z, Rodríguez FJ, Stewart CL, Vega JA, Tryggvason K, Freije JM, López-Otín C. (2005). Accelerated ageing in mice deficient in Zmpste24 protease is linked to p53 signalling activation. Nature. **22**;437(7058):564-8.

Vulliamy T, Marrone A, Goldman F, Dearlove A, Bessler M, Mason PJ, Dokal I. (2001). The RNA component of telomerase is mutated in autosomal dominant dyskeratosis congenita. Nature. **27**;413(6854):432-5

Vij N, Chandramani-Shivalingappa P, Van Westphal C, Hole R, Bodas M. (2018). Cigarette smoke-induced autophagy impairment accelerates lung aging, COPD-emphysema exacerbations and pathogenesis. Am J Physiol Cell Physiol. **1**;314(1):C73-C87.

Wang Y, Michikawa Y, Mallidis C, Bai Y, Woodhouse L, Yarasheski KE, Miller CA, Askanas V, Engel WK, Bhasin S, Attardi G. (2001). Muscle-specific mutations accumulate with aging in critical human mtDNA control sites for replication. Proc Natl Acad Sci U S A. **27**;98(7):4022-7.

Wang Z, Man MQ, Li T, Elias PM, Mauro TM. (2020). Aging-associated alterations in epidermal function and their clinical significance. Aging (Albany NY). **27**;12(6):5551-5565.

Warnon C, Bouhjar K, Ninane N, Verhoyen M, Fattaccioli A, Fransolet M, Lambert de Rouvroit C, Poumay Y, Piel G, Mottet D, Debacq-Chainiaux F.(2021). 'HDAC2 and 7 down-regulation induces senescence in dermal fibroblasts'. Aging (Albany NY). **12**;13(14):17978-18005.

Waters LR, Ahsan FM, Wolf DM, Shirihai O, Teitell MA. (2018). Initial B Cell Activation Induces Metabolic Reprogramming and Mitochondrial Remodeling. iScience. **27**;5:99-109.

Weintraub, Neal Lee. 'HDAC9, Aging and Alzheimer's Disease'. Project of August University. https://augusta.pure.elsevier.com/en/projects/hdac9-aging-and-alzheimers-disease-2.

Whittemore K, Vera E, Martínez-Nevado E, Sanpera C, Blasco MA. (2019). Telomere shortening rate predicts species life span. Proc Natl Acad Sci U S A. **23**;116(30):15122-15127.

Woldhuis RR, de Vries M, Timens W, van den Berge M, Demaria M, Oliver BGG, Heijink IH, Brandsma CA. (2020). Link between increased cellular senescence and extracellular matrix changes in COPD. Am J Physiol Lung Cell Mol Physiol. **1**;319(1):L48-L60.

Wu S, Ge Y, Huang L, Liu H, Xue Y, Zhao Y. (2014). BRG1, the ATPase subunit of SWI/SNF chromatin remodeling complex, interacts with HDAC2 to modulate telomerase expression in human cancer cells. Cell Cycle. **13**(18):2869-78.

Wu S, Ge Y, Li X, Yang Y, Zhou H, Lin K, Zhang Z, Zhao Y. (2020). BRM-SWI/SNF chromatin remodeling complex enables functional telomeres by promoting co-expression of TRF2 and TRF1. PLoS Genet. **5**;16(6):e1008799.

Xu HH, Su T, Xue Y. (2016). Histone H3 N-terminal acetylation sites especially K14 are important for rDNA silencing and aging. Sci Rep. **24**;6:21900.

Xu M, Pirtskhalava T, Farr JN, Weigand BM, Palmer AK, Weivoda MM, Inman CL, Ogrodnik MB, Hachfeld CM, Fraser DG, Onken JL, Johnson KO, Verzosa GC, Langhi LGP, Weigl M, Giorgadze N, LeBrasseur NK, Miller JD, Jurk D, Singh RJ, Allison DB, Ejima K, Hubbard GB, Ikeno Y, Cubro H, Garovic VD, Hou X, Weroha SJ, Robbins PD, Niedernhofer LJ, Khosla S, Tchkonia T, Kirkland JL. (2018). Senolytics improve physical function and increase lifespan in old age. Nat Med. **24**(8):1246-1256.

Yao H, Chung S, Hwang JW, Rajendrasozhan S, Sundar IK, Dean DA, McBurney MW, Guarente L, Gu W, Rönty M, Kinnula VL, Rahman I. (2012). SIRT1 protects against emphysema via FOXO3-mediated reduction of premature senescence in mice. J Clin Invest. **122**(6):2032-45.

Yang XJ, Seto E. (2008). The Rpd3/Hda1 family of lysine deacetylases: from bacteria and yeast to mice and men. Nat Rev Mol Cell Biol. **9**(3):206-18.

Yang W, Nagasawa K, Münch C, Xu Y, Satterstrom K, Jeong S, Hayes SD, Jedrychowski MP, Vyas FS, Zaganjor E, Guarani V, Ringel AE, Gygi SP, Harper JW, Haigis MC. (2016). Mitochondrial Sirtuin Network Reveals Dynamic SIRT3-Dependent Deacetylation in Response to Membrane Depolarization. Cell. **3**;167(4):985-1000.e21.

Yang SH, Meta M, Qiao X, Frost D, Bauch J, Coffinier C, Majumdar S, Bergo MO, Young SG, Fong LG. (2006). A farnesyltransferase inhibitor improves disease phenotypes in mice with a Hutchinson-Gilford progeria syndrome mutation. J Clin Invest. **116**(8):2115-21.

Yang L, Ma Z, Wang H, Niu K, Cao Y, Sun L, Geng Y, Yang B, Gao F, Chen Z, Wu Z, Li Q, Shen Y, Zhang X, Jiang H, Chen Y, Liu R, Liu N, Zhang Y. (2019). Ubiquitylome study identifies increased histone 2A ubiquitylation as an evolutionarily conserved aging biomarker. Nat Commun. **21**;10(1):2191.

Yousefzadeh M, Henpita C, Vyas R, Soto-Palma C, Robbins P, Niedernhofer L. (2021). DNA damage-how and why we age? Elife**. 29**;10:e62852.

Yuan YM, Luo L, Guo Z, Yang M, Lin YF, Luo C. (2015). Smoking, aging, and expression of proteins related to the FOXO3 signaling pathway in lung tissues. Genet Mol Res. **31**;14(3):8547-54

Zhang CL, McKinsey TA, Chang S, Antos CL, Hill JA, Olson EN.(2002). 'Class II histone deacetylases act as signal-responsive repressors of cardiac hypertrophy'. Cell. **23**;110(4):479-88.

Zhang Y, Liu T, Meyer CA, Eeckhoute J, Johnson DS, Bernstein BE, Nusbaum C, Myers RM, Brown M, Li W, Liu XS. (2008). 'Model-based analysis of ChIP-Seq (MACS)'. Genome Biol. **9(**9):R137.

Zhang R, Wang Y, Ye K, Picard M, Gu Z. (2017). Independent impacts of aging on mitochondrial DNA quantity and quality in humans. BMC Genomics. 21;18(1):890.

Zhao J, Zhao J, Legge K, Perlman S. (2011). Age-related increases in PGD(2) expression impair respiratory DC migration, resulting in diminished T cell responses upon respiratory virus infection in mice. J Clin Invest. **121**(12):4921-30.

Zhong L, D'Urso A, Toiber D, Sebastian C, Henry RE, Vadysirisack DD, Guimaraes A, Marinelli B, Wikstrom JD, Nir T, Clish CB, Vaitheesvaran B, Iliopoulos O, Kurland I, Dor Y, Weissleder R, Shirihai OS, Ellisen LW, Espinosa JM, Mostoslavsky R. (2010). The histone deacetylase Sirt6 regulates glucose homeostasis via Hif1alpha. Cell. **22**;140(2):280-93.

Zhu Y, Tchkonia T, Pirtskhalava T, Gower AC, Ding H, Giorgadze N, Palmer AK, Ikeno Y, Hubbard GB, Lenburg M, O'Hara SP, LaRusso NF, Miller JD, Roos CM, Verzosa GC, LeBrasseur NK, Wren JD, Farr JN, Khosla S, Stout MB, McGowan SJ, Fuhrmann-Stroissnigg H, Gurkar AU, Zhao J, Colangelo D, Dorronsoro A, Ling YY, Barghouthy AS, Navarro DC, Sano T, Robbins PD, Niedernhofer LJ, Kirkland JL. (2015). The Achilles' heel of senescent cells: from transcriptome to senolytic drugs. Aging Cell. **14**(4):644-58.

12. DECLARATION

I declare that I have completed this dissertation single-handedly without the unauthorized help of a second party and only with the assistance acknowledged therein. I have appropriately acknowledged and referenced all text passages that are derived literally from or are based on the content of published or unpublished work of others, and all information that relates to verbal communications. I have abided by the principles of good scientific conduct laid down in the charter of the Justus Liebig University of Giessen in carrying out the investigations described in the dissertation.

_____ _____

Place, Date Signature

13. ACKNOWLEDGEMENT

I firstly would like to thank my mentor, my role model and my advisor **Prof. Dr. Soni Savai Pullamsetti** for her brain stimulating scientific contribution, guidance, motivation, moral support and patience towards me. I am forever grateful to her for giving me a chance to grow as a freethinking scientist and to find my scientific voice. Her guidance helped me to reshape my personality as a scientist and enhanced my skills. This journey was mentally difficult to me but she was there for me, not only as an advisor but also as emotional support in every step. I appreciate her for the all support she provided.

Besides my mentor, I also would like to thank **Prof. Dr. Werner Seeger, PD Dr. Rajkumar Savai, Prof. Dr. Andreas Weigert, Prof. Serge Adnot, Dr. Stephan Klatt, Dr. Sven Zukunft, Prof. Ingrid Fleming, Prof. Dr. Miguel A. Alejandre Alcazar, Dr. Stefan Günther, Prof. Dr. Mario Looso, Siavash Mansouri, Dr. Giovanni Maroli, Rene Wiegandt, Dr. Anoop Cherian, Solmaz Khaghani, Dr. Katrin Ahlbrecht,** and **Elisabeth Marcos** for the collaborations, data generation, insightful comments and all scientific contributions into my thesis.

Special thanks to **Natascha Wilker, Jana Rostkovius, Uta Eule, Yanina Knepper, Ewa Bienek,** and **Daniel Grella** for all their technical support through my thesis. Especially, **Daniel** was literally my left hand at the later stages of the project and he supported me as both a colleague and a true friend, which I am ever grateful.

I sincerely thank my former fellow labmates **Dr. Swati Dabral, Dr. Elisabeth Gamen, Dr. Dijana Iloska-Leyer**, and **Dr. Pouya Sarvari** for teaching me all the techniques during my initial days in the lab. I would like to thank **Dr. Claudio Nardiello, Solmaz Khaghani** and **Dr. Alberto Rodriguez-Castillo** from AG Morty group for helping me for the all stages of AT2 cell isolation optimization and confocal microscopy.

I wholeheartedly thank **Dr. Prakash Chelladurai** for supporting me emotionally, especially for the last 8 months before his leaving by uplifting my mood and hope towards the life. He gave the ugliest yet funniest daddy jokes along with the deeper talks about the meaning of the life, history and time-space. I thank **Dr. Gabriela Diaz, Dr. Chanil Valasarajan, Dr. Swathi Veeroju, Dr. Anoop Cherian, Leili Jafari, Golnaz Hesami, Fatemeh Khassafi, Samuel Olapaju, Nassima Mordjana,** and **Sai Aravind Mandava** for all laughters, inside jokes, endless talks, memorable dinner and movie nights, and all enjoyable moments. All of them paved the way and moved me to reach this final point.

I wholeheartedly thank my closest friends **Oguzhan Yasarkan, Neslihan Sevinc, Dogan Ucar, Duygu Gülcan, Pinar Akyol, Zeynep Tavukcuoglu, Burak Uzay, Zahraa Msheik,** and **Despina Myti.** They say the friends are the brothers and sisters from other parents that you can get through the life journey if you are lucky enough. All of you are my biggest luck and comfort in this lifetime. Million times thanks for being always there for me, no matter what. Especially, I am ever grateful for **Oguzhan, Nesli, Dogan** and **Zahraa** for accepting me as who I am, supporting me in good and bad days, seeing a better side of me even if I cannot see, believing in me and my choices unconditionally and being partners in crime.

Lastly, I would like to thank my precious parents **Sükran** and **Semir Avci** sincerely**.** I firstly dedicated my entire thesis to my ever-loving mom. No doubt, many people contributed to this thesis but you are the only person who carried all the stress and difficulty along with me. **Mommy**, you are the strongest woman I have ever met. I truly understand and appreciate your nature, your quality and your sacrifices better with my age. You inspired and nurtured my passionate inner fire with your elegant and sophisticated personality, your endless love and compassion towards me. I am nobody without you. I tattooed your heart over mine. I would always choose you as my mom in every possible universe and dimension. **Daddy**, you are the best father, a daughter could ask for! Million times thanks for coloring my inner world, being my inner core and strength, biggest supporter and driving force ever. Thanks for letting me being wild, unpredictable, and authentic version of mine. I am forever grateful to you for giving me ultimate freedom and putting trust in me. You are truly my biggest confidence. You taught me that everything is possible in this world, there is no limit and I always should stay true to myself. I wholeheartedly thank you for being my playmate in art, music, books, and traveling. I am fully proud to be a mixed-mini copy of both of you. Finally, I thank my big-hearted sister **Zeynep Avci.** If I am black, you are white yet perfect combination as ying-yang. My precious baby, no word is enough to describe the love that I hold for you. Despite the 2 age-difference, you balance me with your maturity and you direct me to a better version of me. Thanks for accepting me, loving me with my all flaws, letting me being foolish and lively like a small kid, and being my best friend at the end of the day. Million times thanks for sharing this caring and loving sisterhood bond with me. I love you so much.